THESIS ON POWER ENGINEERING,
ELECTRICAL ENGINEERING, MINING ENGINEERING D59

New Converter Topologies for Integration of Hydrogen Based Long-Term Energy Storages to Renewable Energy Systems

ANNA ANDRIJANOVITŠ

TUT
PRESS

TALLINN UNIVERSITY OF TECHNOLOGY
Faculty of Power Engineering
Department of Electrical Engineering

Dissertation was accepted for the defence of the degree of Doctor of Philosophy in Engineering on 12.03.2013.

Supervisor: Dr. Dmitri Vinnikov, Department of Electrical Engineering, Tallinn University of Technology

Advisor: Dr. Oleksandr Husev, Chernihiv State Technological University, Ukraine

Opponents: Dr. Hannes Agabus, Marble Invest OÜ, Estonia

Dr. Sergii Ivanets, Dean of the Faculty of Electronic and Information Technology, Chernihiv State Technological University, Ukraine

Defence of the thesis: April 12, 2013

Declaration:
Hereby I declare that this doctoral thesis, my original investigation and achievement, submitted for the doctoral degree at Tallinn University of Technology has not been submitted for any academic degree.

Anna Andrijanovitš.....

ISSN 1406-474X
978-9949-23-446-2 (publication)
978-9949-23-447-9 (PDF)

ENERGEETIKA. ELEKTROTEHNIKA. MÄENDUS D59

Uued muundurite topoloogiad vesinikul põhinevate energiasalvestite integreerimiseks taastuvenergiasüsteemidesse

ANNA ANDRIJANOVITŠ

TTÜ
KIRJASTUS

Contents

Acknowledgement

The research presented in this PhD thesis was carried out at the Department of Electrical Drives and Power Electronics (Department of Electrical Engineering from 01.01.2013) of Tallinn University of Technology. First of all, I would like to thank my supervisor Dr. Dmitri Vinnikov for his guidance, motivation, patience and persistence, which made this thesis possible.

Next, my gratitude is due to the advisor of my thesis Dr. Oleksandr Husev for his invaluable help, advice and constructive criticism of the thesis.

I am also grateful to Mikhail Egorov for his support and useful cooperation at the early stage of my PhD research.

My special deep thanks go to my colleagues Andrei Blinov and Janis Zakis for providing a pleasant working atmosphere and all-round help during my research. I am grateful to you for your support during critical moments and for the time we spent together. Also, I am grateful to Anton Rassylkin for his useful advice in the formatting of the thesis and providing valuable recommendations.

My sincere thanks are due to Mare-Anne Laane for her text revision and advice regarding to my English writing throughout my PhD study.

I would also like to thank other colleagues and associates for their support, advice and friendship. Thanks to you I was able to broaden my vision and look at many things in a different way.

Doctoral School of Energy and Geotechnology II and Department of Electrical Engineering are gratefully acknowledged for their financial support. Funding from the Archimedes Foundation is also much appreciated.

Finally, I would like to express my greatest thanks to my family for their support, patience and love throughout the years of my study.

Thank you all. It was not easy but turned out an exciting time.

Anna Andrijanovitš

Abbreviations

2L-HB	two-level half-bridge
3L-NPCHB	three-level neutral point clamped half-bridge
AC	alternating current
CCM	continuous conduction mode
CD	current doubler
DC	direct current
DES	distributed energy storage
EEGI	European Electricity Grid Initiative
EL	electrolyzer
EMI	electromagnetic interference
EPDN	electronic power distribution network
EU	European Union
FB	full-bridge
FC	fuel cell
HB	half-bridge
LED	light emitting diode
LTES	long-term energy storage
PEC	power electronic converter
PSAFB	phase-shifted active full-bridge
PSM	phase-shift modulation
PV	photovoltaic
PWM	pulse-width modulation
qZS	quasi-Z-source
RB	reverse blocking
RMS	root mean square
SMES	superconducting magnetic energy storage
SOC	state-of-charge
STES	short-term energy storage
TUT	Tallinn University of Technology
VD	voltage doubler
VSI	voltage-source inverter
WT	wind turbine
ZCS	zero current switching
ZVS	zero voltage switching

Symbols

C_f	capacitance of the output filter
D	duty cycle
D_s	shoot-through duty cycle
E	constant related to the core material and dimensions of the inductor
E_{offT}	turn-off energy of the transistor
E_{offD}	turn-off energy of the diode
E_{onD}	turn-on energy of the diode
E_{onT}	turn-on energy of the transistor
f_{sw}	switching frequency
f_{qZS}	operation frequency of the qZS-network
i_B	battery current
i_L	current through the coil
$i_{Tr,2}$	current of the transformer secondary winding
I_{Cav}	average collector current
I_{Crms}	RMS collector current
I_{Dav}	diode average current
I_{Drms}	diode RMS current
k	coupling coefficient
k_L	relative current ripple of the filter inductor
k_U	relative ripple of the output voltage
L	inductance of the coil
L_f	output filter inductance
L_x	inductance of one inductor in qZS-network
N	number of turns of the coil
N_p	number of turns of the transformer primary winding
N_s	number of turns of the transformer secondary winding
P	rated power of the converter
P_B	power provided by the battery
P_{CD}	conduction losses of a diode
P_{CT}	conduction losses of a transistor
$P_{DC\text{-}bus}$	power of the supported system
P_{FC}	power of the fuel cell
P_{sw}	switching losses of the transistor module
r_B	battery internal resistance
r_C	collector-emitter on-state resistance
r_D	diode on-state resistance
t_a	active state time
t_{rev}	interval of energy return
T_{sw}	duration of the switching period
U_B	battery voltage
$\bar{u}_{C4}$	instantaneous voltage of the battery
U_{CEO}	collector-emitter saturation voltage
U_{DC}	intermediate DC-link voltage of the qZS converter

$U_{DC\text{-}bus}$	DC-bus voltage of the supported system
U_{DO}	forward voltage drop of the diode
U_{EL}	electrolyzer voltage
U_{FC}	fuel cell voltage
U_{SOC}	state of charge of the battery
U_{Tr}	amplitude voltage across transformer winding
ΔI_{ripple}	peak-to-peak current ripple
ΔU_{ripple}	peak-to-peak voltage ripple
φ	flux through magnetic core

List of author's publications directly connected to the topic of the PhD thesis (copies shown in the Appendix)

[PAPER-I] **Andrijanovits, A.**; Hoimoja, H.; Vinnikov, D. Comparative Review of Long-Term Energy Storage Technologies for Renewable Energy Systems. Electronics and Electrical Engineering, 2(118), pp. 21 – 26, 2012.

[PAPER-II] **Andrijanovitš, A.**; Egorov, M.; Lehtla, M.; Vinnikov, D. New Method for Stabilization of Wind Power Generation Using an Energy Storage Technology. Agronomy Research, 8(S1), pp. 12 – 24, 2010.

[PAPER-III] **Andrijanovitsh, A.**; Steiks, I.; Zakis, J.; Vinnikov, D. Analysis of State of the Art Converter Topologies for Interfacing of Hydrogen Buffer with Renewable Energy Systems. Scientific Journal of Riga Technical University. Power and Electrical Engineering, 29, pp. 87 – 94, 2011.

[PAPER-IV] **Andrijanovits, A.;** Beldjajev, V. Techno-Economic Analysis of Hydrogen Buffers for Distributed Energy Systems. Power Electronics, Electrical Drives, Automation and Motion (SPEEDAM), pp. 1401 – 1406, 2012.

[PAPER-V] Blinov, A.; **Andrijanovits, A.** New DC/DC Converter for Electrolyzer Interfacing with Stand-Alone Renewable Energy System. Electrical, Control and Communication Engineering, Vol. 1, Issue 1, pp. 24 – 29, 2013.

[PAPER-VI] **Andrijanovitš, A.**; Vinnikov, D.; Roasto, I.; Blinov, A. Three-Level Half-Bridge ZVS DC/DC Converter for Electrolyzer Integration with Renewable Energy Systems. 10th International Conference on Environment and Electrical Engineering (EEEIC´11), Rome (Italy), IEEE, pp. 683 – 686, 2011.

[PAPER-VII] Vinnikov, D.; Husev, O.; **Andrijanovitš, A.**; Roasto, I. New High-Gain Step-up DC/DC Converter for a Fuel Cell Interfacing in Hydrogen Buffer. Технічна електродинаміка, pp. 93 – 100, 2011.

[PAPER-VIII] Vinnikov, D.; **Andrijanovitš, A.;** Roasto, I.; Jalakas, T. Experimental Study of New Integrated DC/DC Converter for Hydrogen-Based Energy Storage. 10th International Conference on Environment and Electrical Engineering (EEEIC´11), Rome (Italy), IEEE, pp. 542 – 545, 2011.

[PAPER-IX] **Andrijanovits, A.**; Blinov, A.; Vinnikov, D.; Martins, J. Magnetically Coupled Multiport Converter with Integrated Energy Storage. Przeglad Elektrotechniczny, Vol. 88(7b), pp. 171 – 176, 2012.

Author's own contribution

The contribution by the author to the papers included in the thesis is as follows:

[PAPER I] Anna Andrijanovitš is the main author of the paper. She is responsible for literature overview, data collection and analyses. She had a major role in writing.

[PAPER II] Anna Andrijanovitš is the main author of the paper. She is responsible for literature overview, data collection and analyses. She had a major role in writing. She made the presentation of the paper at the International Scientific Conference "Biosystems Engineering 2010" (Tartu, Estonia).

[PAPER III] Anna Andrijanovitš is the main author of the paper. She is responsible for literature overview, data collection and analyses. She had a major role in writing. She made the presentation of the paper at Riga Technical University 52rd International Scientific Conference (Riga, Latvia).

[PAPER IV] Anna Andrijanovitš is the main author of the paper. She is responsible for literature overview, data collection, calculations and analyses. She had a major role in writing.

[PAPER V] Anna Andrijanovitš co-authored the paper. She is responsible for literature overview, data collection and analyses. She made the presentation of the paper at Riga Technical University 53rd International Scientific Conference (Riga, Latvia).

[PAPER VI] Anna Andrijanovitš is the main author of the paper. She is responsible for literature overview, data collection, modeling and analyses. She had a major role in writing. She made the presentation of the paper at the 10th International Conference on Environment and Electrical Engineering EEEIC´2011 (Rome, Italy).

[PAPER VII] Anna Andrijanovitš co-authored the paper. She is responsible for literature overview, data collection, modeling and analyzes.

[PAPER VIII] Anna Andrijanovitš co-authored the paper. She is responsible for literature overview, data collection and analyses. She made the presentation of the paper at the 10th International Conference on Environment and Electrical Engineering EEEIC´2011 (Rome, Italy).

[PAPER IX] Anna Andrijanovitš is the main author of the paper. She is responsible for literature overview, data collection, modeling and analyses. She had a major role in writing.

1 INTRODUCTION

1.1.1 General background

As is widely known, a power electronic converter (PEC) can sufficiently improve system controllability, reliability, size and efficiency in a majority of applications – beginning from high megawatt electrical drives up to ultra-compact power supplies for the telecom and aerospace industry. Thanks to recent rapid advances in semiconductor and packaging technologies as well as to the development of new converter topologies, engineering scientists are introducing new applications based on power electronics, such as *Electronic Power Distribution Networks* (EPDNs) [1][2], also known as *Smart Grids* [3][4] or *Active Distribution Networks* [3]. EPDN is an aggregation of multiple primary and secondary energy sources, several levels of energy storage and back-up and numerous active loads, all interfaced through PECs. To achieve the highest flexibility and energy efficiency, the EPDN should have a multilevel control: the lower (unit) level responsible for the separate control of secondary energy sources, storage systems and loads, while the higher (system) level performs a combined regulation of the whole system. Regardless of functions, control system philosophy and structure, the power flow control on the physical level could be most efficiently performed by using PECs. This is especially topical in EPDNs with renewable (i.e. solar panels or wind turbines) or alternative (i.e. fuel cells) energy sources, where the PEC is the only way to control the power source.

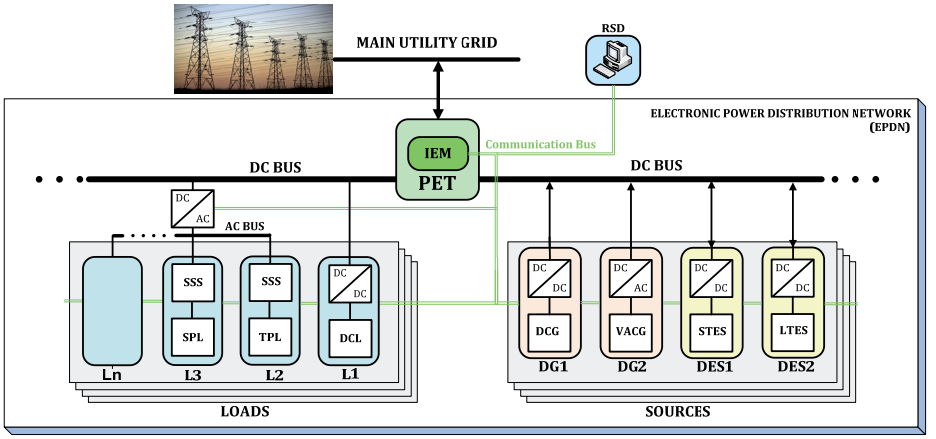

PET – Power electronic transformer (*solid-state* or *intelligent transformer*)
IEM – Intelligent energy management
RSD – Remote supervision and diagnostics
SSS – Solid-state switch
DG – Distributed generator
DES – Distributed energy storage
DCG – DC generator (photovoltaics, fuel cells)
VACG – Variable AC generator (wind- or microturbines)
STES – Short-term energy storage (batteries, supercapacitors, flywheels)
LTES – Long-term energy storage (hydrogen, pumped hydro, compressed air)
L – Load
SPL – Single-phase loads
TPL – Three-phase loads
DCL – DC loads

Figure 1.1 General structure of the EPDN

The conceptual solution of the future EPDN is presented in Figure 1.1. EPDN is shown to have two power supply buses: main DC and auxiliary AC. The DC bus is meant for interconnection and interaction of distributed generators (DGs), distributed energy storages (DES) and DC loads. To ensure maximal interoperability with currently widespread AC loads, the EPDN has an auxiliary AC bus, which could be fully eliminated with the introduction of a DC supply standard for consumer loads in the future (consumer electronics, LED lighting, motor drives, etc. could be more conveniently powered by DC [2]). One of the main advantages of the EPDN shown in Figure 1.1 is that the power flow of subsystems is controlled through a DC bus. Compared to traditional AC bus based solutions [5]-[8], its benefits are: fewer power conversion stages, higher efficiency and easier integration of renewable energy sources and storages.

1.1.2 Role of energy storages in an EPDN with renewable energy sources

Sustainability and efficient use of energy resources is an urgent issue today. The reasons are not only in the growth of demand and production, but also in the present level of resource exploitation, leading to exhaustion of energy resources and related environmental impacts. A sustainable use of energy requires applications and methods that could increase efficiency. This is especially important in an EPDN with renewable energy sources. The most widespread renewable energy sources used in EPDNs are the wind turbines (WTs) and photovoltaic (PV) plants.

An extensive penetration of renewable energy sources is a global growing trend. The European Union (EU) is working to reduce the effects of climate change and establish a common energy policy. As part of this policy, the unity of the Heads of State or Government of the European Union agreed in the directive 2009/28/EC, implemented by December 2010, on binding targets to increase the share of renewable energy. By 2020 renewable energy should account for 20% of the EU's final energy consumption. To meet this common target, each Member State needs to increase its production and use the renewable energy in electricity, heating, cooling and transport [9]. Main advantages of renewable energy are zero fuel costs and lower impact on the environment. However, one of the most significant challenges is the intermittent nature of many renewable energy resources. Figure 1.2 shows an example of unpredictable energy production by Estonian wind farms. Due to unforecastable wind and difficulty in precise forecasting, periods of excess energy, as well as lack of energy occur. It is often easier to lump the behaviour of these resources within the load and treat them as a load variation instead of using them as generators. To compensate unstable operation of renewable energy sources, an energy storage system needs to be introduced. Increasing the amount of storage (power and energy) associated with a renewable energy will gradually make the output more controllable and predictable.

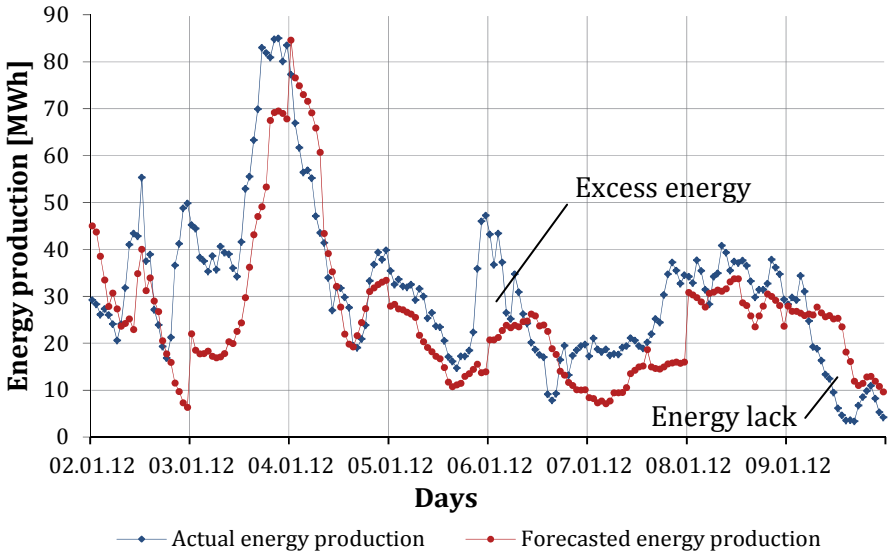

Figure 1.2 An example of unpredictable energy production by Estonian wind farms [10]

A variety of technologies are available for energy storage in the power systems. To identify the most feasible solutions, it is necessary to consider many parameters, such as cost, lifetime, reliability, size, storage capacity, and environmental impact. Energy storage technologies can be generally divided into three main groups: mechanical, electromagnetic and electrochemical storage [11]-[15].

Mechanical storage includes pumped hydro storage, compressed air energy storage and flywheels. Electromagnetic storage includes inductors or superconducting magnetic energy storage (SMES). Electrochemical storage includes all types of batteries, supercapacitors (ultracapacitors) as well as hydrogen based energy storage. Hydrogen is one of the promising alternatives that can be used as an energy carrier. Implementation of hydrogen based long-term energy storages (LTES), also known as hydrogen buffers, in EPDNs with renewable energy sources has attracted much attention [16]-[18]. Essential elements of a hydrogen buffer is an electrolyzer (EL), which converts electrical energy into hydrogen by splitting water into hydrogen and oxygen and a fuel cell (FC), which transforms the chemical energy in the hydrogen form back to electrical energy [19]. The energy flows in the hydrogen buffers are controlled by a PEC. PECs are needed to match the different voltage levels in the hydrogen buffer system and to control the power flow between the EPDN and the hydrogen buffer.

1.1.3 Motivation of the Thesis

This PhD research reviews the existing PEC topologies for hydrogen buffer interfacing with an EPDN and proposes a variety of new approaches with main attention to energy efficiency, size-weight characteristics, modularity and integrity.

The *energy efficiency* is the most important parameter of the hydrogen buffer. The diagram in Figure 1.3 shows the generalized loss distribution between the main components of the hydrogen buffer [20]-[25]. As can be seen, the majority of losses occur during the electrochemical processes of hydrogen conversion into electrical energy by using the FC and energy conversion into hydrogen by using the EL. Losses in the PEC stage constitute about 12% of the total losses [PAPER-IV]. The PECs used in hydrogen buffers today have an average efficiency of 82-86%. Therefore, increasing the average efficiency of the PEC stage, the overall energy efficiency of the hydrogen buffer could also be improved.

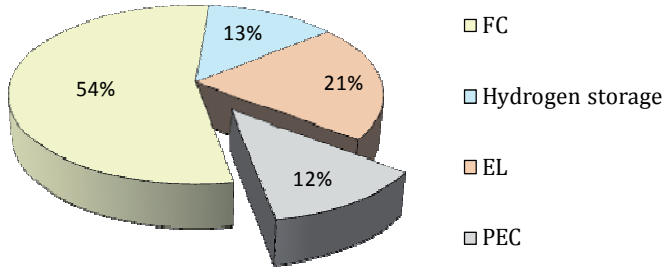

Figure 1.3 Typical loss distribution in the hydrogen buffer

Besides efficiency, the *size-weight optimization* is also a priority aim for the hydrogen-based LTES. In several wind-hydrogen systems, the PEC stage of the hydrogen buffer could be installed inside the nacelle close to the main PEC of the WT to achieve a more compact integrated system. In that case, the WT tower could be used to store hydrogen, as shown in Figure 1.4 [26][27]. For a cost-effective system, the volume of the WT tower should be used as much as possible for hydrogen storage and accommodation of the EL and the FC. The power transmission cables are placed in a pipe, which is installed in the middle of the tower. This concept eliminates the need for the high-flex cable and the conduit required for the exterior power transmission design. Such integrated design could help to eliminate long interconnection wires and therefore reduce the power losses. However, the size and weight of the PEC will have direct influence on the size and weight of the nacelle. It is well known that the reduced nacelle weight and size significantly optimize transportation and installation of the WT. Therefore, the development of compact and lightweight PECs for the hydrogen buffer is another challenge, which can be solved by optimization of the components and reduction of power conversion stages in PECs.

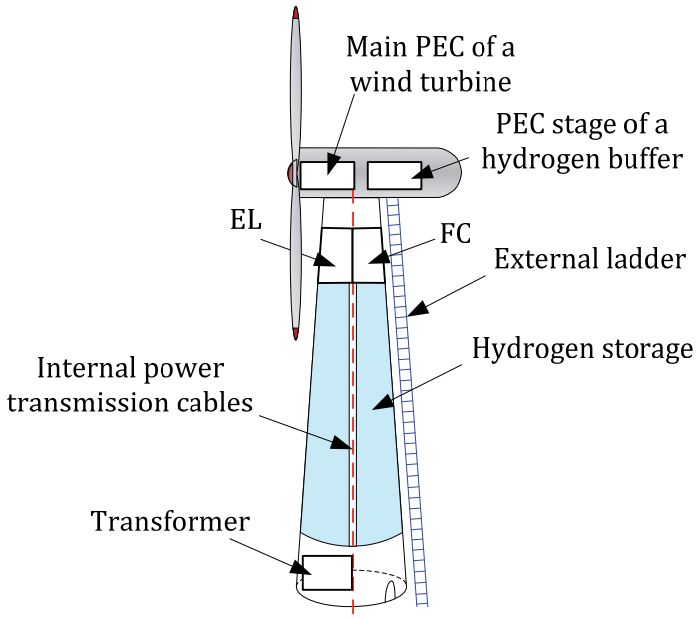

Figure 1.4 General principle of an integrated wind-hydrogen system

Finally, *integrity* is also an important issue. The stochastic nature of the renewable energy requires that the source of energy be able to respond to fast changing loads. Typically, the hydrogen based LTES has a slow transient response because of the natural electrochemical reactions. To solve this problem, an additional short-term energy storages (STES) (battery, supercapacitor) is required, which can respond to the increased load instantly in order to improve the power quality of the hydrogen buffer. A STES is commonly used due to its high round-trip efficiency and convenience for charging/discharging. In addition, it takes care of the effects caused by instantaneous load ripples/spikes and renewable energy peaks. However, STES is not appropriate for long-term energy storage because of its low energy density, self-discharge and leakage. The combination of STES with hydrogen-based LTES can significantly improve the performance of the EPDN with renewable energy sources [28]-[33].

1.1.4 The main hypotheses and objectives of the PhD research

Hydrogen based LTES is a promising technology. Thanks to its specific properties (zero fuel cost, lower environmental impact, high responsiveness, high energy density, flexibility in storage and release rates), it could have clear benefits in the stabilization of energy production by renewable energy sources in EPDNs. A hydrogen buffer needs to be introduced to maintain energy balance of the EPDN during the periods of unstable work of renewable energy resources and to keep the stable and predictable energy production. The implementation of the new improved PEC topologies could enhance technical and economic

feasibility of the hydrogen based LTES in the EPDN with renewable energy sources.

The main goal of the thesis is to develop and experimentally validate new methods, topologies and solutions, which will substantially contribute to the further improvement of the hydrogen based LTES technology without increasing their complexity or reducing the reliability significantly.

Main objectives of the research:

- analysis and classification of state-of-the-art and technology trends of the hydrogen based LTES;
- analysis of the implementation challenges of the hydrogen based LTES in the EPDN with renewable energy sources;
- synthesis, analysis and experimental verification of new DC/DC converter topologies for the hydrogen based LTES with special attention to energy efficiency and integrity;
- analysis of implementation possibilities and benefits of the multiport DC/DC converters in the hydrogen based LTES.

In order to achieve the above objectives and to verify the hypotheses set forth here, comprehensive research and development tasks were solved. The research methods applied are based on the mathematical analysis, computer simulations and prototyping. To estimate performance, the power losses and operating frequency of the proposed solutions were compared. Computer simulations were performed in PSIM9, MATHCAD14, PSpice9.2 and MATLAB/Simulink simulation packages. In addition, for the experimental validation of new proposed topologies and methods, the small-scale experimental setups were assembled and tested in the Power Electronics Laboratory of TUT.

1.1.5 Contributions of the thesis

This thesis presents extended knowledge and new solutions for future development of the hydrogen based LTES technology. The originality of research is contained in theoretical and practical findings.

Theoretical originality includes the classification of technology trends of the hydrogen based LTES and comparison of their properties with those of traditional LTES. The implementation challenges of the hydrogen based LTES for the stabilization of energy production in the EPDN with renewable energy sources are highlighted. As a case study, the possibility of using hydrogen for compensating the instability of the energy production by Estonian wind farms is discussed. The techno-economic analysis of the hydrogen based LTES was performed in order to indicate the weaknesses of the technology and to help to increase the efficiency of the hydrogen production in the EPDN with renewable energy sources.

Practical originality includes the variety of new energy efficient DC/DC converter topologies proposed by the author for the electrical interfacing of the electrochemical stage of the hydrogen based LTES with EPDN. All the proposed topologies have been experimentally verified and demonstrated an outstanding performance in row with high efficiency (90...93%). By help of elaborated design guidelines, these topologies could be also implemented in other application fields, such as telecom, rolling stock, aerospace, marine etc. where the efficiency, reliability and integrity play a major role. Moreover, the number of new modulation methods (improved modulation method for a half-bridge step-down DC/DC converter with a phase-shifted active full-bridge rectifier, output voltage programmed control for the qZS-based step-up DC/DC converters, etc.) were proposed and experimentally validated. As one of important results of this PhD research, the idea of magnetic integration of the developed two-port converters resulted in a new multiport converter technology for the interfacing of a hydrogen buffer with the DC-bus of an EPDN. Finally, the new method of a STES (battery) integration to the FC-side port of the proposed multiport converters was analysed and experimentally validated.

The current relevance of the thesis is related to faster development of sustainable power engineering. Given research was initiated and motivated by the European Electricity Grid Initiative (EEGI) Roadmap 2010-18 and Implementation Plan 2010-12, which is driving strategies for European-wide research in the field. Furthermore, the research corresponds to the main objectives of the Estonian Energy Technology Program (development and optimization of energy transmission and distribution networks, development of energy balancing and storage technologies for wind parks).

The research activities within the thesis were supported by targeted financing research project SF0140016s11 and two grants (G8538 and G8020).

1.1.6 Dissemination of results and publications

The results obtained during the PhD research were reported at 11 International conferences and workshops and published in 13 papers. Seven of them have appeared in the International peer-reviewed journals and five are available through the IEEExplore database. The most important papers directly connected to the topic of the dissertation are listed in the Appendix.

2 HYDROGEN BASED LONG-TERM ENERGY STORAGE: STRUCTURE, OPERATION PRINCIPLE, LIMITATIONS

2.1 Hydrogen buffer as a long-term energy storage

Each energy storage technology has certain properties with regard to storage capacity, power, response time and cost. Grouping storage technologies with regard to storage capacity is relevant because it can be used to exclude those sizes not relevant in relation to renewable energy systems [33]-[38]. More detailed description of the energy storage technologies is given by the author in publication [PAPER-I].

Based on their storage capacity, energy storages can be categorized as STES and LTES, as shown in Figure 2.1. STES includes the supercapacitors, flywheels, inductors or SMES and batteries. LTES could be subdivided into pumped hydro storage, compressed air energy storage and hydrogen based energy storage. Different energy storage technologies have a wide range of energy release rates (discharge rates) that extend from seconds to many hours and days (Figure 2.2) [38]. Renewable energy sources cannot be easily regulated or dispatched. Peak levels generated by them may not coincide with the peak demand. In the case of instability of renewable energy production, LTES could be used. It allows alternative energy sources to be used as a base load or enables an increase of predictability to nearly 100 % for a certain period of time. The time horizon could be days or weeks, depending on the storage size and variations allowed.

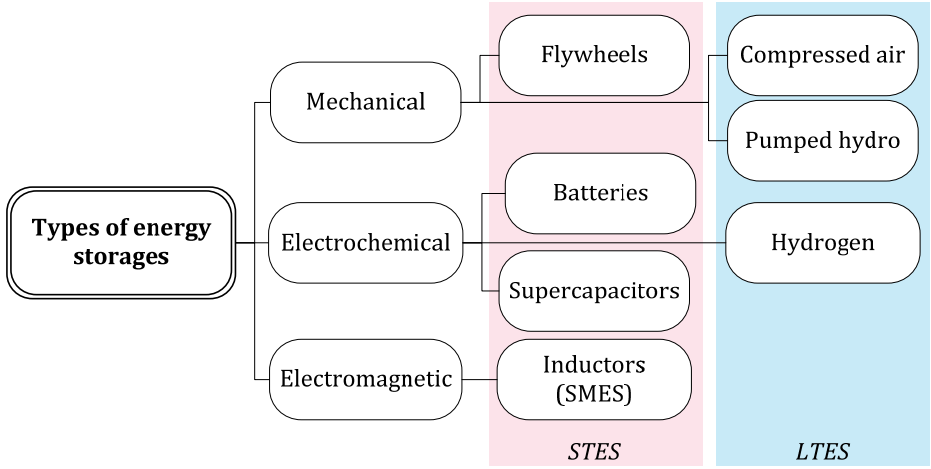

Figure 2.1 General classification of energy storage technologies

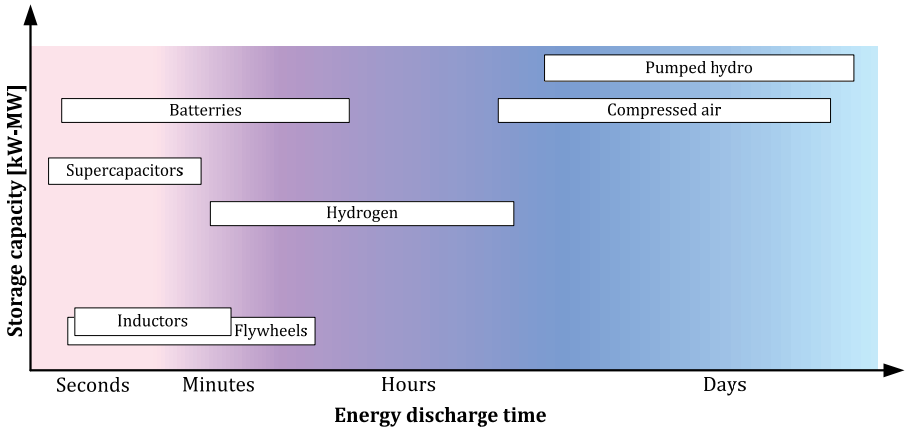

Figure 2.2 Typical energy storage capacities and discharge times of different energy storage technologies [38]

General technical parameters of LTES in the wind power context are summarized in Table 2.1 [37][39]. The universality of hydrogen implies that it can replace other fuels for stationary generating units for power generation in various industries. Having all the advantages of fossil fuels, hydrogen is free of harmful emissions when used with dosed amount of oxygen, thus reducing the greenhouse effect. Combination of an energy storage system and a renewable energy source allows controllable power production.

Table 2.1 Comparison of LTES

Storage system	Capacity, MW	Efficiency, %	Technology
Pumped hydro	100…1000	70 – 80	Mechanical
Compressed air	0.1…1000	75 – 85	Mechanical
Hydrogen	0.1 – 1	20 – 40	Electrochemical

2.2 General components and operating principle of a hydrogen buffer

In the publication [PAPER-II] a hydrogen-based LTES for the stabilization of wind power generation was presented and discussed. The general operating principle of a hydrogen-based LTES is shown in Figure 2.3. The system consists of three main stages: hydrogen production by the EL, hydrogen storage and electricity production by the FC. The operating voltages of the EL and the FC are matched with the voltage of the DC bus of an EPDN by help of a PEC.

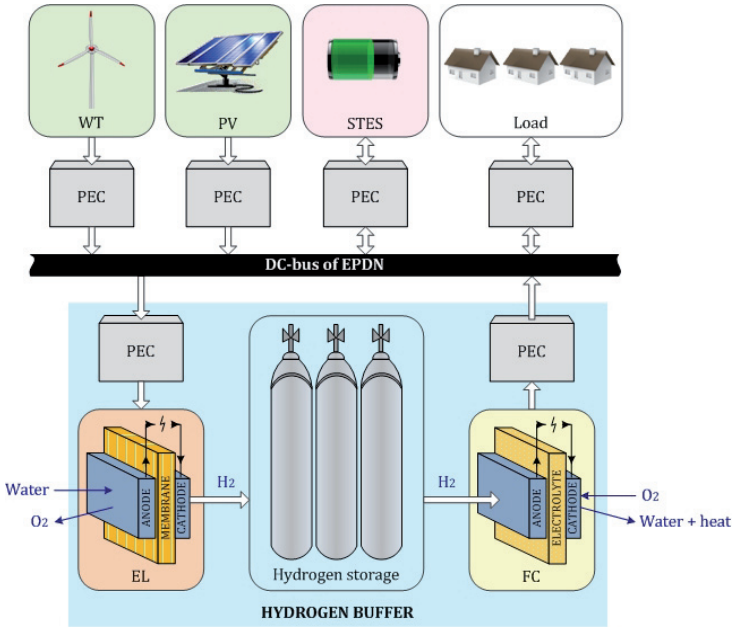

Figure 2.3 Energy exchange processes in the hydrogen buffer

In the excess energy periods, the EL converts the excess electrical energy from the renewable energy source into chemical energy by using water electrolysis. There are three basic types of the EL: alkaline, proton exchange membrane and high-temperature solid oxide. Today's most widespread industrial ELs are alkaline and proton exchange membrane. These two EL types allow higher operating pressures, higher current density and low applied voltage to the cell. Moreover, proton exchange membrane EL is easier to operate and provides fast start-up. The total EL efficiency varies between 75% and 90% [40].

The second stage is the hydrogen storage. Typically, the produced hydrogen is accumulated in a tank. There are four basic methods for hydrogen storage [41]:

- compressed and stored in a pressure tank;
- cooled to a liquid state and kept cold in an insulated tank;
- activated carbon;
- metal hydrides.

In order to select the optimal integration method of hydrogen based energy storage in the EPDN, the hydrogen storage capacity of each method was compared. Table 2.2 shows that the compressed gas method has a very low leakage rate compared to the other methods, high hydrogen capacity and dynamic energy efficiency. Activated carbon also has a high efficiency; however, a very low temperature is required during the process. Because the required energy storage time could be long, a low leakage rate is critical to preventing an additional dynamic energy loss.

Table 2.2 Comparison of hydrogen storage methods

Hydrogen storage methods		Energy intensity, MJ/kg	Efficiency	Leakage rate/day, %
Compressed gas	300 bar	0.915	0.92	0.000024
	700 bar	0.905	0.91	0.000033
Liquid		28-45	0.63-0.77	1
Activated carbon		8-10	0.92-0.93	0.2
Hydrides	Low temperature (<100˚C)	0.9-0.93	0.9-0.93	-
	High temperature (>300˚C)	0.79-0.83	0.79-0.83	-

The last stage is the electricity production stage. In order to stabilize energy production during the absence of the renewable energy, stored hydrogen could be re-used by help of a FC, which converts chemical energy into electrical energy by oxidizing hydrogen. The FC takes the hydrogen from the tanks to generate electricity, plus water and heat as by-products. Having considered all the FC types, we can conclude that an alkaline FC is a more perspective type that can be used for hydrogen based LTES because of high efficiency and low reaction losses of oxygen reduction. This type is technically most feasible also because of its operating flexibility regarding start-up and shut-down procedures as well as intermittent operation [42][43].

2.3 State-of-the-art PEC topologies for electrical interfacing of a hydrogen buffer with an EPDN

Typically, the EL and the FC are connected to the EPDN via individual (dedicated) PECs. The operating voltage of a DC-bus of an EPDN is higher than that of the main components of the hydrogen buffer. Therefore, the EL is connected to the DC-bus of the EPDN through the step-down DC/DC converter, while the FC should be interfaced by the step-up DC/DC converter. In principle, many basic power converter topologies can be used for the EL and the FC interconnections with the DC-bus of the EPDN. Because of comparatively high input and output voltage differences (in several cases the voltages could differ by more than 10 times), the DC/DC converters with a high-frequency voltage matching transformer are preferred. For safety reasons this transformer should also perform the function of galvanic isolation of the primary and the secondary side. In the analysis of the state-of-the-art converters for the hydrogen buffer application [PAPER-III] it was stated that the majority of presented topologies concentrate on the FC integration to the EPDN and only minor publications focus on the PEC for an EL.

The EL and the FC perform opposite functions. Instead of generating electrical energy as the FC does, the EL consumes it. The EL is a low DC voltage sensitive load and it cannot be directly connected to the uncontrolled high DC voltages [44]. To connect the EL to the DC-bus of DES, it is required to buck the voltage of the DC-bus to the level of the EL [45]. As a result of the analysis of the references according to the DC/DC converter applications of the ELs [46]-[54], inverter side topologies can be classified into FB and HB. Moreover, in the inverter side the switching losses must be kept as low as possible. Thus, zero voltage switching (ZVS) and zero current switching (ZCS) topologies are preferred. In the case of a rectifier side, a low component count is preferred, as the current is relatively high. Thus, the current doubler rectifier with coupled inductors is the most convenient choice.

The FC is a power source with low unregulated DC output voltage. To connect the FC to the load, it is necessary to step-up and to stabilize the relatively low output voltage of the FC to a certain operating voltage level. As a result of the analysis of the references according to the DC/DC converter applications of the FCs [55]-[78], these converters can be classified as converters for small or medium power systems. In a power range about 1-3 kW, converters like half-bridge or push-pull are suitable topologies. For a power range higher than 3 kW, the single-phase full-bridge converter is an appropriate solution for the FC applications. The three-phase full-bridge DC/DC converter topology can be also used to improve the losses distribution in the converter and to increase the power density of the PEC. However, due to the increased number of components in the three-phase configuration, the reliability of the PEC could become an issue.

2.4 Economic issues of a hydrogen buffer

The global energy challenges of today are huge: about 78% of the global energy demand is satisfied through coal, oil and gas. At the same time, oil resources are expected to deplete between 2020 and 2030. Limited availability of fossil energy resources urge to make use of renewable sources for electric energy generation.

Table 2.3 shows the breakdown of the renewable energy technologies in the European Union Member States [79].

Table 2.3 Total renewable energy capacity for all European Union Member States

	2005	**2010**	**2015**	**2020**
Hydropower, GW	119.4	122.4	130.0	139.7
Geothermal, GW	0.7	0.8	1.0	1.6
Solar, GW	2.2	26.1	58.0	91.4
Wave, GW	0.2	0.2	0.4	2.3
Wind, GW	40.4	84.9	143.2	213.6
Biomass, GW	15.7	22.6	32.4	43.6

Regarding the mix of renewable energy technologies for the year 2020, the most important contribution is expected from the wind power. Renewables play an increasing part in the energy equation in the EU. Overall, the prices of support mechanisms are decreasing, especially for the "established" technologies, such as solar, wind and biomass. The average prices per renewable technologies shown in Figure 2.4 are based on the sum of the different available tariffs [80].

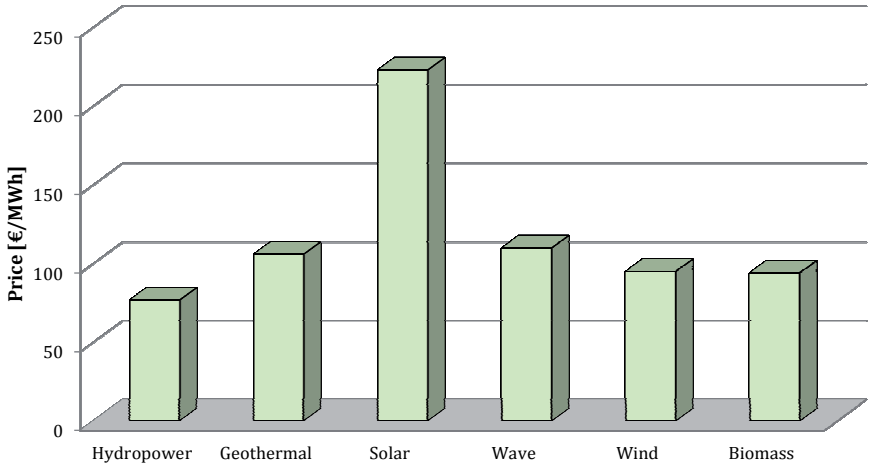

Figure 2.4 Energy costs for different renewable energy resources

Due to the increasing use of renewable energy sources, the issue of the stabilization of the renewable energy generation is gaining in importance. Interest in hydrogen as a long-term energy storage is continuously growing. The hydrogen based long-term energy storage system costs vary widely, mostly as a function of a system size. System utilization (i.e. capacity factor) has the most significant impact on hydrogen price. The hydrogen buffer produces electricity for stationary uses and has the potential for low-cost hydrogen due to increased equipment utilization. The financial data of the hydrogen buffer components are compared in Figure 2.5. Since the prices are confidential, a price value of the EL was chosen from the prices reported in [81], assuming a large-scale economy and medium-sized units. The PEC price is typically included in the EL price. The financial parameters of the hydrogen compression and storage system were taken from [82]. In this chapter, a moderate price value of the FC, including the PEC price, is assumed to be based on [81][83].

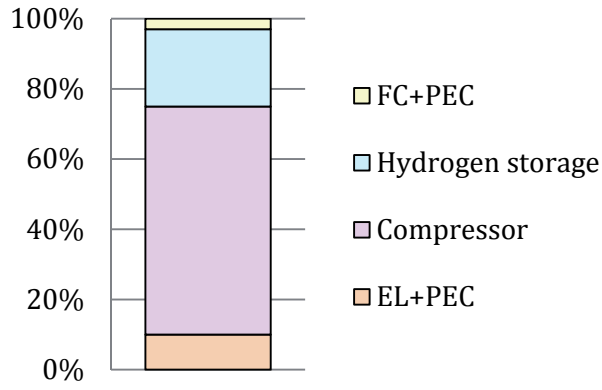

Figure 2.5 Capital cost distribution for the hydrogen buffer

2.5 Generalizations

Hydrogen is already widely produced and used, but it is now being considered for use as an energy carrier for stationary power. Challenges to an expanded use of hydrogen for stationary power production include improvements in scientific processes and technologies for producing hydrogen with low to zero emissions of greenhouse gases and costs that can ultimately be competitive in the energy marketplace. Non-polluting hydrogen, energy-dense and the most abundant element in nature, is a renewable and environmentally clean energy source. But whether it can be produced and used inexpensively is the crux of a large and growing effort in research. Today, the production of hydrogen is expensive and energy intensive. Hydrogen production is a large and growing industry. The development of efficient and affordable PEC technologies can improve the cost and energy efficiency of the hydrogen based LTES, but not significantly. Centralized hydrogen production will become more economical and feasible when the hydrogen fueling market has grown large enough.

3 NEW PEC TOPOLOGIES FOR THE HYDROGEN BUFFER INTEGRATION TO AN EPDN

As mentioned above, synchronization between the main components of the hydrogen based LTES and the EPDN occurs at the power electronic stage. This is achieved by using the PEC. The development of the PEC can improve the conversion efficiency that reduces the cost and improves the energy source utilization. This PhD research was mostly dedicated to the synthesis and experimental validation of new DC/DC converter topologies for the hydrogen buffer interfacing with the DC-bus of an EPDN. The new proposed topologies could be classified as follows:

- Two-port (individual) DC/DC converters
  - Step-down DC/DC converters for EL interfacing with the DC-bus of an EPDN
    - Two-level half-bridge step-down DC/DC converter with a phase-shifted active full-bridge rectifier
    - Three-level half-bridge step-down DC/DC converter with a current doubler rectifier
  - Step-up DC/DC converters for FC interfacing with the DC-bus of an EPDN
    - qZS-based full-bridge step-up DC/DC converter with a voltage doubler rectifier
- Multiport (integrated) DC/DC converters

In the case study, the EPDN with 560 V DC-bus voltage was selected (which is a typical rectified voltage of a 3x400 V AC transmission line). The general operating voltages of the EL and FC considered here are specified in Table 3.1.

Table 3.1 General operating parameters of the hydrogen buffer considered for the case study

Parameter	Symbol	Value
DC-bus voltage of the EPDN (input/output voltage of the hydrogen buffer), V	$U_{DC\text{-}bus}$	560±20%
Rated voltage of the EL, V	U_{EL}	70
Minimal voltage of the FC, V	$U_{FC,min}$	32
Maximal voltage of the FC, V	$U_{FC,max}$	60
Rated power of the hydrogen buffer, kW	P	2

3.1 Interfacing of a hydrogen buffer by two-port converters

As stated above, the most traditional way of the connection of the hydrogen buffer to the DC-bus of an EPDN is the two-port (individual) DC/DC converters. As shown by Table 3.1, the voltage must be stepped-down by 8 times and stepped-up by more 30 times during the DC-bus of an EPDN interfacing with the EL and the FC, correspondingly.

3.1.1 Two-level half-bridge step-down DC/DC converter with a phase-shifted active full-bridge rectifier

The improved galvanically isolated step-down DC/DC converter for the EL integration with the EPDN was presented and analysed in [PAPER-V]. The converter has a two-level half-bridge (2L-HB) inverter on its primary side, a high-frequency step-down transformer and a phase-shifted active full-bridge (PSAFB) rectifier based on reverse blocking (RB) switches (MOSFETs with series diodes were used in this case study) on the secondary side (Figure 3.1).

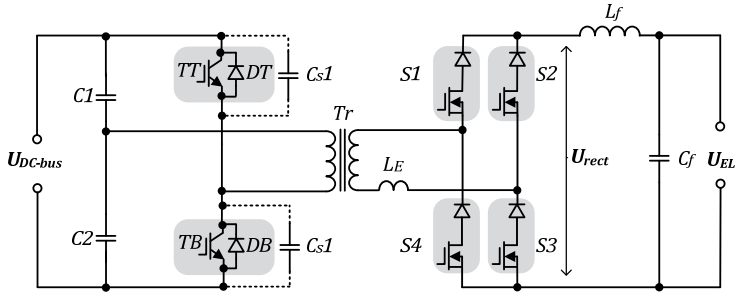

Figure 3.1 Proposed 2L-HB step-down DC/DC converter with a PSAFB rectifier

Operation principle

In the converters with a synchronous rectifier, the output voltage is generally controlled by the varying delay time between the turn-on of the switches in the rectifier and the turn-on of the switches in the inverter. The disadvantage of such traditional modulation algorithms is the presence of the intervals of energy return from the load to the power supply. If the energy return is not possible, there will be an increase of the input voltage of the inverter and a deviation of the midpoint potential of the capacitor input voltage divider. Moreover, energy circulation corresponds to the generation of the reactive power, resulting in the reduction of the converter efficiency due to increased conduction losses.

To overcome this disadvantages, the modulation algorithm of the rectifier switches was modified, as shown in Figure 3.2. The proposed algorithm provides phase-shifted control whereas practically no energy is returned into the power supply. This is achieved by introducing two additional switching states of the rectifier switches. The control of the output voltage can be achieved by varying the current freewheeling duration (time interval t_3-t_6). The energy return interval (time interval t_2-t_3) could be constant and should be kept as short as possible in order to maintain high power factor and reduce conduction losses.

The phase-shifted synchronous rectifier concept is a well-known method to reduce the ringing, increase the efficiency and achieve the ZVS of converter switches. The other advantages are the possibility of using non-dissipative capacitive snubbers in the inverter and constant frequency operation, allowing for simple control of the converter.

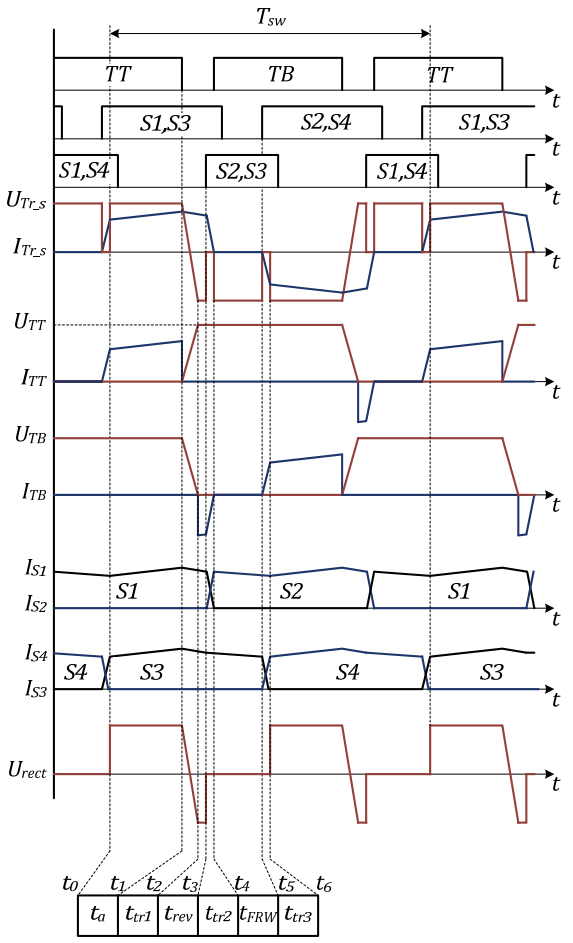

Figure 3.2 General operation principle of the proposed 2L-HB step-down DC/DC converter with a PSAFB rectifier

Key equations

Some guidelines are provided how to select the parameters for the experimental converter with the PSAFB rectifier. In order to simplify the calculations, it is assumed that the opponents are lossless, the input capacitors and the transformer magnetizing inductance are large enough and therefore the input voltage ripple and the magnetizing current are negligible.

The output voltage can be expressed by the following equation:

$$U_{EL} = \frac{U_{DC\text{-}bus} \cdot (t_a - t_{rev})}{T_{sw}} \cdot \frac{N_s}{N_p}, \qquad (3.1)$$

where $U_{DC\text{-}bus}$ is the DC-bus voltage of the EPDN (input voltage of the converter) and N_s/N_p is the transformer turns ratio.

To estimate the parameters of the output filter inductor, it is assumed that the current of the inductor is continuous:

$$L_f = \frac{(U_{Tr-s} - U_{EL}) \cdot t_a}{\Delta I_{ripple}} = \frac{t_a \cdot U_{EL}^2}{P \cdot k_L} \cdot \left[\frac{1}{2 \cdot f_{sw} \cdot (t_a - t_{rev})} - 1 \right], \qquad (3.2)$$

where $U_{Tr\text{-}s}$ is the amplitude voltage across transformer secondary, ΔI_{ripple} is the inductor ripple current, k_L is the relative inductor ripple current, P is the rated power of the converter and f_{sw} is the switching frequency.

The capacitance of the output filter capacitor can be approximated as:

$$C_f = \frac{\Delta I_{ripple} \cdot t_a}{\Delta U_{ripple}} = \frac{t_a \cdot k_L \cdot P}{k_U \cdot U_{EL}^2}, \qquad (3.3)$$

where ΔU_{ripple} is the output ripple voltage and k_U is the relative voltage ripple.

Experimental verification

To experimentally validate the theoretical background a 2 kW prototype was assembled (Figure 3.3). Six independent pulse width modulation (PWM) channels were used. Two channels with small dead time were used to drive IGBTs in the inverter and four channels were used to control the rectifier. As mentioned, rectifier switches should have RB capability. In the prototype, MOSFETs with series connected diodes were used. In practical applications these switches could be replaced by RB IGBTs or fast thyristors for reduced power dissipation during the on-state.

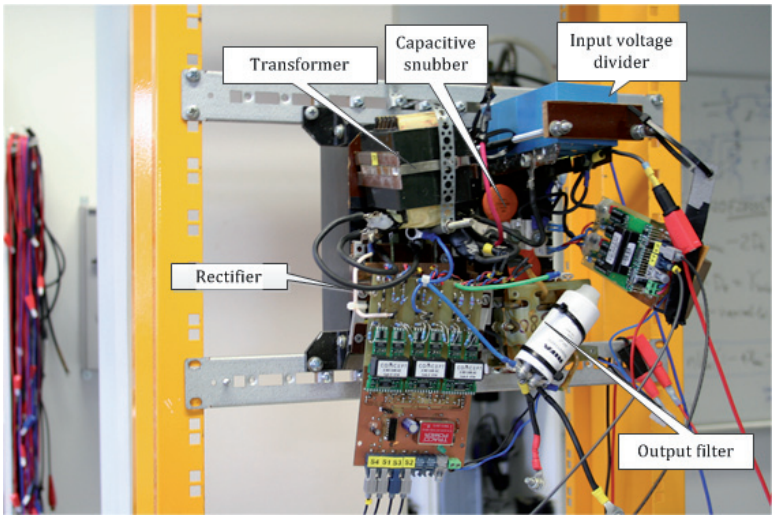

Figure 3.3 Experimental prototype of the 2L-HB step-down DC/DC converter with a PSAFB rectifier

The experimental waveforms are presented in Figure 3.4. The test results completely correspond to the theoretically predicted waveforms. The proposed converter provides ZVS in the inverter side and ZCS in the rectifier side.

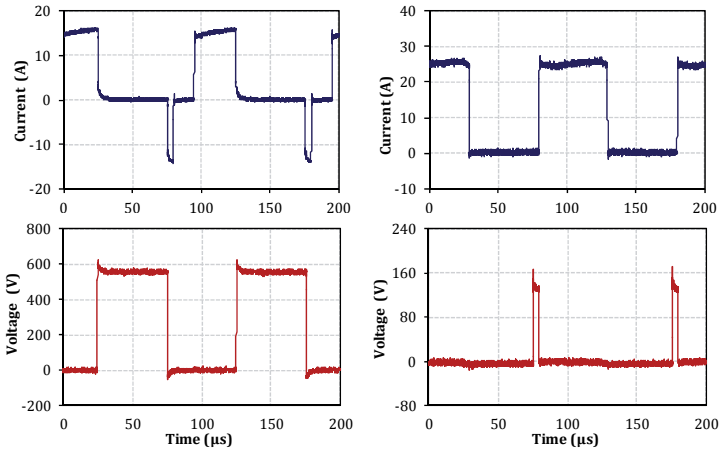

Figure 3.4 Experimental voltage and current waveforms of the TT transistor module (a); S1 transistor (b) (U_{in}=560 V; f_{sw}=10 kHz)

The reduction in the IGBT turn-off power loss has been achieved by help of capacitive snubbers. The total turn-off losses with a snubber were significantly reduced (by 30-35%) as compared to turn-off without a snubber.

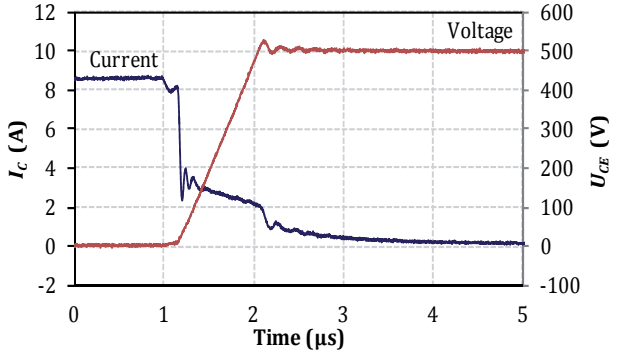

Figure 3.5 Experimental turn-off waveforms of the TT transistor module with a snubber

Estimation of efficiency

A basis for the design of the PEC is the determination of the expected power dissipation in the semiconductors. The estimation of the semiconductor losses is based on the calculation of the average and RMS currents and the datasheet information. The losses in the semiconductors are divided into conduction and switching losses. Conduction losses of a transistor:

$$P_{CT} = U_{CEO} \cdot I_{Cav} + r_C \cdot I_{Crms}{}^2, \tag{3.4}$$

where U_{CEO} is the collector-emitter saturation voltage, I_{Cav} is the average collector current, r_C is the collector-emitter on-state resistance and I_{Crms} is the RMS current of the transistor.

Conduction losses of the diode:

$$P_{CD} = U_{DO} \cdot I_{Dav} + r_D \cdot I_{Drms}{}^2, \tag{3.5}$$

where U_{DO} is the forward voltage drop of the diode, I_{Dav} is the average current of the diode, r_D is the diode on-state resistance and I_{Drms} is RMS current of the diode.

Switching losses are defined by E_{onT} – turn-on energy of the transistor; E_{onD} – turn-on energy of the diode; E_{offT} – turn-off energy of the transistor; E_{offD} – *turn*-off energy of the diode. Typically, the turn-on energy of the diode is neglectable. As a result, the total switching losses of the transistor module (transistor with freewheeling diode) can be estimated by

$$P_{sw} = \left(E_{onT} + E_{offT} + E_{offD}\right) \cdot f_{sw}, \tag{3.6}$$

where f_{sw} is the switching frequency.

In order to simplify the calculations, the magnetic and wire conduction losses were neglected. As a result, the estimated converter efficiency as a function of the input voltage and output power is presented in Figure 3.6. In its nominal operating point (input voltage 560 V DC at the rated power), the converter demonstrated an efficiency near 92% (Figure 3.6a). The decreased current gives a reduction in the semiconductor losses, thus, for the same power the increase of the input voltage will lead to the efficiency rise. At 50% load the nominal input voltage will result in the efficiency drop of 1% (Figure 3.6b).

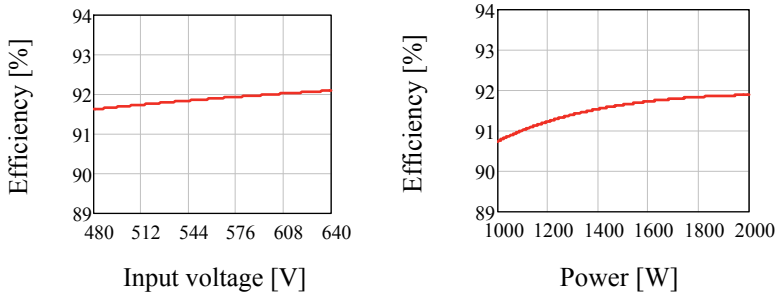

(a) *(b)*

Figure 3.6 Efficiency of the proposed 2L-HB step-down DC/DC converter with a PSAFB rectifier as a function of the input voltage (a) and the output power (b)

3.1.2 Three-level half-bridge step-down DC/DC converter with a current doubler rectifier

As an alternative to the two-level topologies, the multilevel topologies with lower voltage devices that have increased switching performance could be implemented. The three-level neutral point clamped half-bridge (3L-NPCHB) step-down DC/DC converter with a current doubler (CD) rectifier proposed in article [PAPER-VI] is shown in Figure 3.7.

In contrast to the 2L-HB step-down DC/DC converter with a PSAFB rectifier, the 3L-NPCHB inverter utilized in the primary part features inherent ZVS, thus increasing the efficiency of the PEC. The CD rectifier used in the secondary part of the proposed converter was derived from the full-bridge rectifier (FB) by the replacement of bottom diodes in both legs by inductors (*L1* and *L2*) with equal inductances. In contrast to the FB rectifier, the CD topology inhibits several advantages: the total volume of the two filter inductors might be equal or even smaller than the inductor of the FB due to their lower operating frequency and lower current ratings. Additionally, the CD rectifier offers a potential benefit of better-distributed power dissipation, which might be advantageous in a PEC with improved power density.

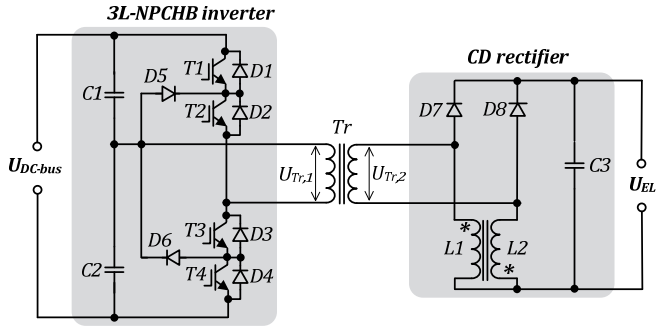

Figure 3.7 Proposed 3L-NPCHB step-down DC/DC converter with a CD rectifier

Operation principle

The operation of a 3L-NPCHB inverter can be generally divided into four operating modes: two conduction and two freewheeling modes. An explanatory timing diagram of the inverter switches, the resulting primary winding voltage of the isolation transformer and main waveforms of the DC rectifier are presented in Figure 3.8. Since the 3L-NPCHB inverter has four transistors, four independent PWM channels are also required, which increase the complexity of the control program and load the controller. A new concept that uses hardware based signal multiplication circuit was proposed in the current research project. By use of this method, only two independent PWM channels are needed. The control is made very easy: outer transistors *T1* and *T4* are controlled directly from the PWM generators of a microcontroller, while inner switches *T3* and *T2* are driven by the inversions of the corresponding control PWM signals.

The PWM algorithm permits all transistors to be operated under ZVS without additional components merely utilizing parasitic elements of the circuit, such as junction and freewheeling diode capacitances across each IGBT, and leakage inductance of the isolation transformer. Moreover, the CD rectifier introduced offers loss reduction in the secondary side of the converter in contrast to the traditional FB rectifier due to the twice reduced operation current of the rectifier diodes and the secondary winding of the transformer.

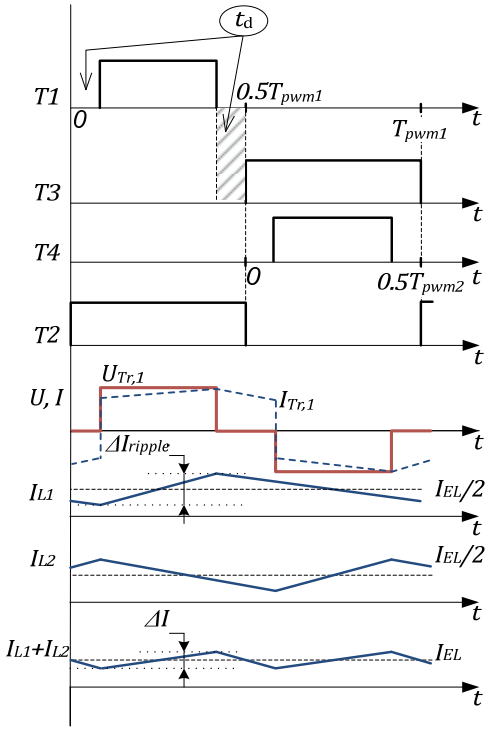

Figure 3.8 General operational principle of the proposed 3L-NPCHB step-down DC/DC converter with a CD rectifier

Key equations

The proposed converter is very simple in design and operation. The terminal voltage of the EL could be simply regulated by the duty cycle variation of the transistors *T1…T4*. Neglecting losses in components, the output voltage could be estimated as:

$$U_{EL} = \frac{U_{DC-bus}}{2} \cdot D \cdot \frac{N_s}{N_p}, \tag{3.7}$$

where $U_{DC\text{-}bus}$ is the DC-bus voltage of the EPDN (input voltage of the converter), D is the duty cycle of the inverter switches and N_s/N_p is the transformer turns ratio.

The values of inductances of the CD rectifier can be estimated by

$$L_1 = L_2 = \frac{U_{EL} \cdot (1-D)}{\Delta I_{ripple} \cdot f_{sw}}, \tag{3.8}$$

where ΔI_{ripple} is the inductor ripple current and f_{sw} is the switching frequency.

With electrolytic capacitors, capacitance could be evaluated as:

$$C_3 = \frac{80 \cdot 10^{-6} \cdot \Delta I_{ripple}}{\Delta U_{ripple}}, \tag{3.9}$$

where ΔU_{ripple} is the output ripple voltage.

Experimental verification

To validate the proposed topology, the experimental setup with the power rating of 2 kW was assembled. The experimental converter was comprehensively tested in different operation conditions and has shown excellent performance despite its simple structure and control principle.

The proposed PWM method [PAPER-VI] provides the 3L-NPCHB inverter with the ZVS of all transistors without any additional components (Figure 3.9). The sufficient condition for ZVS is that the isolation transformer should have relatively high leakage inductance of windings and the dead time implemented should be smaller than the time needed to utilize the leakage energy. Also, Figure 3.9 shows that all the transistors have a hard turn-off, which results in remarkable turn-off losses. However, reducing the leakage inductance of the isolation transformer together with the 20-40% decrease of the duty cycle will result in ZVS/ZCS of the inner transistors *T2* and *T3*.

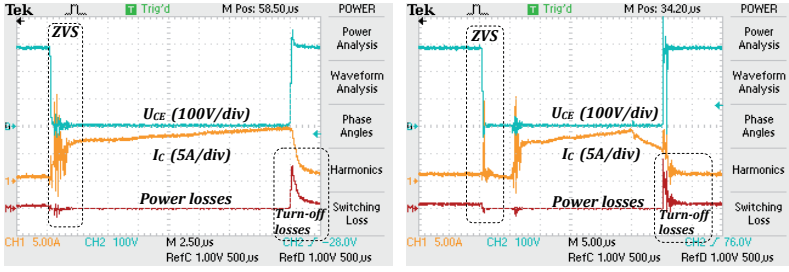

(a) *(b)*

Figure 3.9 ZVS operation of outer transistors T1 and T4 (a) and inner transistors T2 and T3 (b) in the 3L-NPCHB inverter with the proposed modulation method (duty cycle D=0.4)

In order to match the 25% peak-to-peak output current ripple requirement and achieve a 20% better power density of the rectifier stage, two single inductors of the CD rectifier were replaced by a specially designed coupled inductor. The measured current waveforms of both windings of the coupled inductor and the resulting output current of the converter are shown

in Figure 3.10. Thanks to the high coupling coefficient used in the current design (k>0.94), the operating currents of windings have significantly reduced ripple, which finally features at around 1.14 and 1.3 times decreased RMS current values in both windings of the inductor as well as in the secondary winding of the isolation transformer, respectively. As a consequence, the winding losses of the isolation transformer and the coupled inductor were proportionally reduced. Moreover, thanks to the ripple cancellation effect of the CD rectifier, the output current of the converter (sum of the two winding currents) has a twice reduced ripple as compared to that of each winding of the coupled inductor.

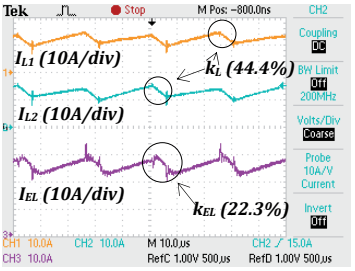

Figure 3.10 Measured current waveforms of coupled inductor windings (I_{L1} and I_{L2}) and the resulting output current (I_{EL}) of the CD rectifier with a coupled inductor

The estimated converter efficiency as a function of the input voltage and output power is presented in Figure 3.11. As in the HB converter with controlled RB switches at the secondary side case, for the same power, the increase of the input voltage will improve the efficiency of the converter because of the reduced semiconductor losses (Figure 3.11a). The Figure 3.11b shows that with the increasing power, the semiconductor losses grow linearly. It allows keeping the almost constant efficiency within the whole operating power range.

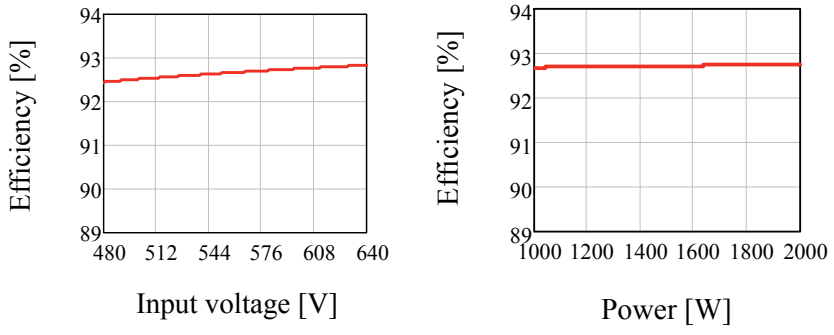

Figure 3.11 Efficiency of the proposed 3L-NPCHB step-down DC/DC converter with a CD rectifier as a function of the input voltage (a) and the output power (b)

3.1.3 qZS-based full-bridge step-up DC/DC converter with a voltage doubler rectifier

During this research a brand new type of galvanically isolated high step-up DC/DC converter was introduced: the qZS-based full-bridge (qZS-FB) step-up DC/DC converter with a voltage doubler (VD) rectifier (Figure 3.12) [PAPER-VII]. The new converter for FC interfacing in a hydrogen buffer provides such advantages as increased reliability, an isolation transformer with a reduced turns ratio and reduced impact on the FC due to continuous input current.

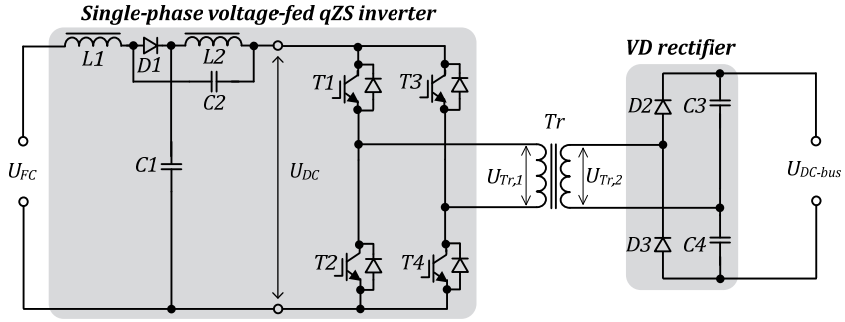

Figure 3.12 Proposed qZS-FB step-up DC/DC converter with a VD rectifier

The most important part of the proposed converter is a voltage-fed qZS inverter. The qZS inverter is a combination of a traditional full-bridge inverter with a special quasi-impedance (qZS) network, which consists of two capacitors *C1* and *C2*, two inductors *L1* and *L2* and a diode *D1*. If necessary, the qZS inverter can boost the input voltage by introducing a special shoot-through switching state, which is the simultaneous conduction (cross conduction) of both switches of the same inverter's phase leg. This switching state is forbidden for the traditional voltage-source inverters (VSI) because it causes the short circuit of the DC-link capacitors. In the qZS inverter, the shoot-through states are used to boost the magnetic energy stored in the DC-side inductors *L1* and *L2* without short circuiting the DC capacitors *C1* and *C2*. This increase in magnetic energy, in turn, provides the boost of the voltage seen on the inverter output during traditional operating states.

The VD rectifier used in the secondary part of the proposed converter was derived from the full-bridge rectifier (FB) by the replacement of diodes in one leg by the capacitors (*C3* and *C4*) with equal capacitance. The resulting advantages of the VD rectifier over the traditional FB scheme are the doubling effect of the secondary winding voltage of the isolation transformer and reduced power dissipation due to the smaller number of rectifying diodes and full elimination of the smoothing inductor. Moreover, thanks to VDR the dynamic performance and stability of the PEC could be increased.

Operation principle

The central idea implemented in the proposed converter is to keep the intermediate DC-bus voltage (U_{DC}) constant despite variations in the FC voltage U_{FC}. By keeping the U_{DC} constant, the PWM inverter could be operated with a fixed duty cycle, thus ensuring constant volt-second and flux swing of the isolation transformer [90]. In accordance with the U_{FC}, the operating modes of the proposed DC/DC converter could be broadly categorized as non-shoot-through and shoot-through operating modes.

If the U_{FC} is equal or higher than the desired U_{DC} level, the converter starts to operate in the non-shoot-through mode. In this mode the qZS inverter operates as a traditional voltage source full-bridge inverter performing only the buck function of the input voltage. If the U_{FC} drops below the predefined U_{DC} level, the converter begins to operate in the shoot-through mode. The varying output voltage of the FC is first preregulated to a desired U_{DC} level by adjusting the shoot-through duty cycle. Afterwards the isolation transformer is being supplied from the inverter with a voltage of constant amplitude.

The proposed phase shift modulation (PSM) principle of the qZS inverter is presented in Figure 3.13. In this method the shoot-through states are generated during the zero states. To reduce switching losses of the transistors, the number of shoot-through states per period was limited by two. Moreover, in order to equalize the conduction losses of the transistors, shoot-through current is distributed between both inverter legs [91].

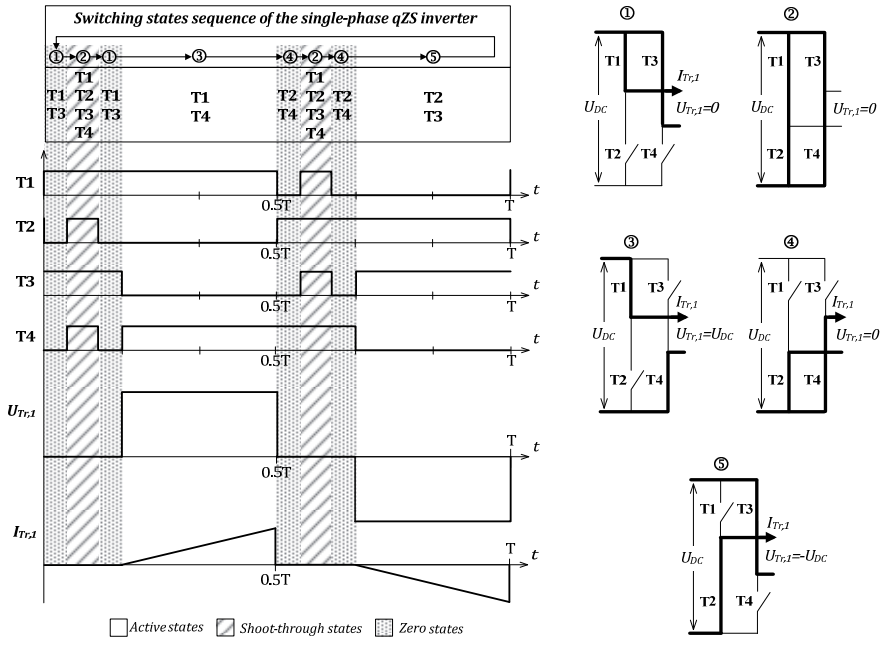

Figure 3.13 General operational principle of the single-phase qZS inverter with the proposed PSM method

Key equations

Neglecting losses in the components, the intermediate DC-link voltage of the qZS-FB step-up DC/DC converter could be regulated simply by the variation of a shoot-through duty cycle D_s:

$$U_{DC} = U_{FC} \cdot \frac{1}{1-2 \cdot D_s}, \tag{3.10}$$

where U_{FC} is the operating voltage of the FC (input voltage of the converter).

The output voltage of the converter operating in the shoot-through mode could be estimated as:

$$U_{DC-bus} = 2 \cdot U_{DC} \cdot \frac{N_s}{N_p}, \tag{3.11}$$

where N_s/N_p is the transformer turns ratio.

The capacitance of qZS inductors needed to limit the peak-to-peak DC-link voltage ripple by $k_{U,DC}$ could be calculated as:

$$C_x = \frac{2 \cdot P \cdot D_S}{U_{FC} \cdot U_{DC} \cdot f_{qZS} \cdot k_{U,DC}}, \tag{3.12}$$

where C_x is the capacitance of one capacitor, P is the power rating of the converter, D_S is the duty cycle of shoot-through states and f_{qZS} is the operation frequency of the qZS-network.

The inductor in the qZS-network will limit the current ripple through the switches during the shoot-through states. Choosing an acceptable peak-to-peak current ripple k_L, the inductance can be calculated by

$$L_x = \frac{D_S \cdot U_{FC}^2}{P \cdot f_{qZS} \cdot k_L} \cdot \frac{1-D_S}{1-2D_S}, \tag{3.13}$$

where L_x is the inductance of one inductor and P is the power rating of the converter.

To minimize the size and weight of the inductors, it was decided to build two inductors of the qZS-network on the common core, thus forming the coupled inductor (Figure 3.14). For a single coil on one core, the flux through the core is

$$\phi = E \cdot N \cdot i_L, \tag{3.14}$$

where E is the constant related to the core material and dimensions, N is the number of turns of the coil and i_L is the current through the coil.

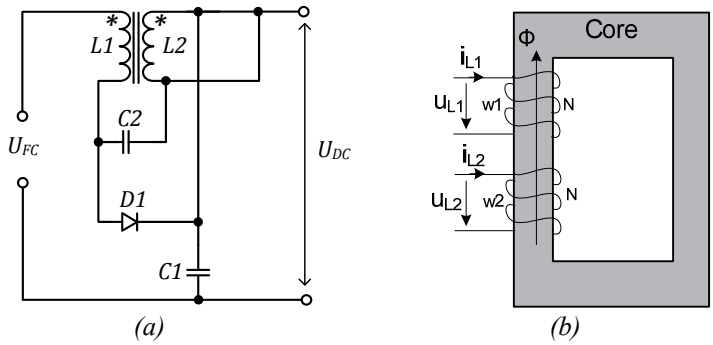

Figure 3.14 qZS network with a coupled inductor (a) and operation principle of the coupled inductor (b)

The inductance of the coil is

$$L = \frac{N \cdot \phi}{i_L} = E \cdot N^2 \cdot \tag{3.15}$$

In the voltage-fed qZS inverter, the currents through inductors *L1* and *L2* are always exactly the same in terms of waveform and magnitude. For two coils on one core with exactly the same current, the flux through the core is:

$$\phi = 2 \cdot E \cdot N \cdot i_L . \tag{3.16}$$

The resulting inductance of each winding when supplying exactly the same current to the two windings is:

$$L = \frac{N \cdot \phi}{i_L} = 2 \cdot E \cdot N^2 . \tag{3.17}$$

It is seen from Eq. 3.17 that the inductance of each winding is doubled. Therefore, for the same operating conditions, we need to build two windings with twice smaller inductance than in the case of separate inductors. In our case it finally resulted in a 35% decrease of the overall volume of a coupled inductor in comparison with a standard approach with two separate inductors.

Experimental verification

To validate the proposed topology, the experimental setup with the power rating of 2 kW was assembled (Figure 3.15).

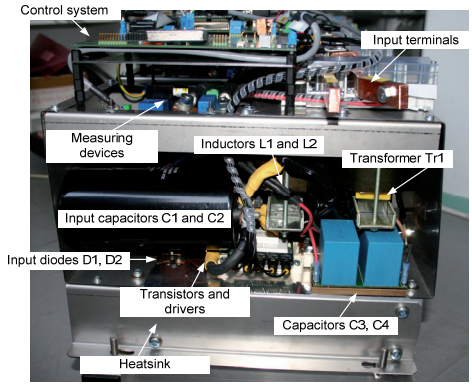

Figure 3.15 Experimental prototype of the qZS-FB step-up DC/DC converter with a VD rectifier

The converter was first tested with a low FC voltage, at the terminal voltage of 40 V. To boost the FC voltage to the desired voltage level of the intermediate DC-link (60 V), the shoot-through duty cycle D_s was set to 0.19. The active state duty cycle was 0.4. Figure 3.16a shows that the qZS inverter with the proposed modulation algorithm ensures the demanded gain of the FC voltage (U_{FC} = 40 V and U_{DC} = 60 V, as expected). Moreover, the VD rectifier provides the demanded voltage doubling effect of the peak voltage of the secondary winding of the isolation transformer, thus ensuring the ripple-free voltage of 560 V DC at the output (Figure 3.16b). For the second operating point, when the FC voltage equals the desired intermediate DC-bus voltage, the shoot-through states are eliminated and the converter operates as a traditional VSI.

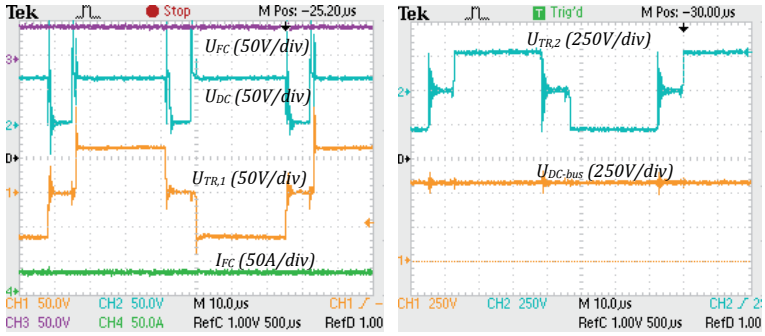

(a) *(b)*

Figure 3.16 Experimental waveforms of the input, intermediate DC and primary winding voltages (a) and output and secondary winding voltages (b)

Since the operation of all transistors in the PSM method is identical (Figure 3.13), only the switching transients of the transistor *T1* were examined and analysed. Figure 3.17 shows the experimental waveforms of the collector-emitter voltage U_{CE}, collector current I_C and power loss P_{Loss} of transistor *T1*. All the turn-on/off and conduction intervals are separated by the dashed lines.

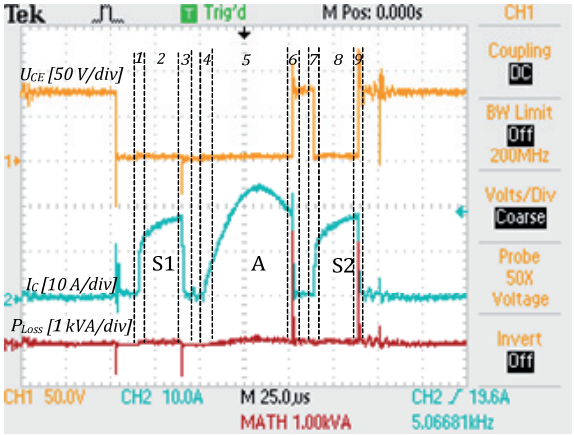

Figure 3.17 Experimental waveforms of one switching period of top transistors in the PSM shoot-through modulation method

It is seen from Figure 3.17 that due to the inherent properties of the proposed PSM algorithm, the transistor is fully soft switched during the first shoot-through state *S1* (Figure 3.18). However, during *S2* (7 and 9) the transistor is partially soft switched and the turn-on/off transients are presented in Figure 3.19. Figure 3.20a and Figure 3.20b show the turn-on and turn-off intervals (4 and 6) of the active state according to Figure 3.17. During turn-on, the transistor is soft switched but during turn-off it is hard switched.

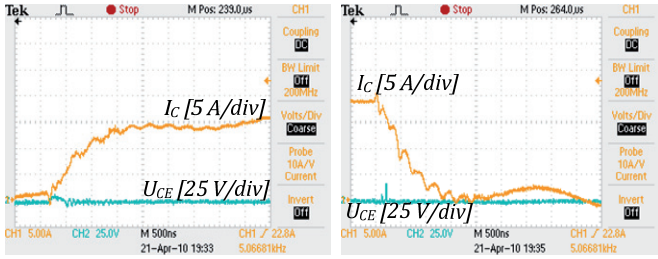

(a) *(b)*

Figure 3.18 Shoot-through state S1 turn-on (a) and turn-off (b) intervals of top transistors

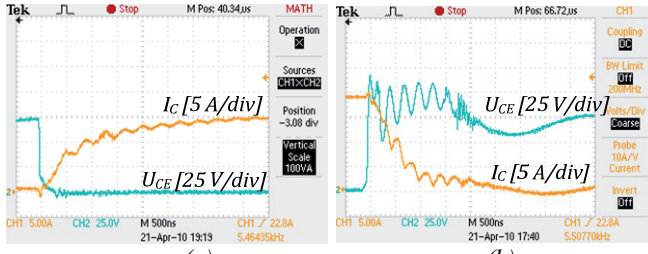

(a) *(b)*

Figure 3.19 Shoot-through state S2 turn-on (a) and turn-off (b) intervals in the PWM shoot-through modulation method

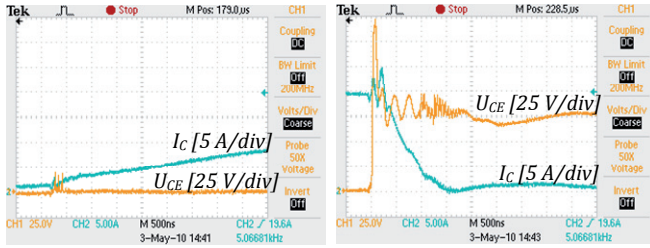

(a) *(b)*

Figure 3.20 Active state A turn-on (a) and turn-off (b) intervals of transistors in the PSM shoot-through modulation method

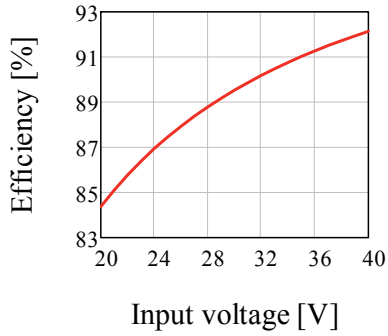

Figure 3.21 Estimated efficiency as a function of the input voltage of the proposed qZS-based step-up DC/DC converter

The estimated converter efficiency as a function of the input voltage is presented in Figure 3.21. It is seen that the converter achieves its maximum efficiency (92%) at the maximal input voltage, which corresponds to the light load conditions of the FC. By increasing the power, the efficiency is decreasing almost linearly to 84%. The efficiency drop is mostly caused by the high circulation currents of the qZS-network and high power dissipation in qZS diode *D1* as well as inverter switches during the shoot-through states.

3.2 Interfacing of hydrogen buffer by a multiport converter

In previous chapters a variety of new DC/DC converter topologies for the interfacing of a hydrogen buffer with the DC-bus of an EPDN were presented. These converters are the two-port converters since they all have two power ports, one connecting the source for power input and another connecting the load for power output. The stochastic nature of the renewable energy requires that the energy source should be able to respond to fast changing loads. Since the FC has a slow response time and prefers to be operated under constant power, a battery is often used as additional energy storage in the hydrogen buffer [92]-[94]. The battery should have a special charger circuit that integrates it to the DC-bus of the EPDN. It leads to a complex multiconverter system

(individual PECs for EL, FC and battery, as seen from Figure 2.3) with a high number of energy conversion stages, complex control and reduced efficiency.

The multiport converter is an emerging technology for complex power electronic systems with multiple power sources and loads. Having the single power processing stage, the multiport converter cannot only interface all power sources and loads and modify the electric energy form but also manage the power flow between the sources and loads.

As an important result of this PhD research, an idea was proposed to implement the multiport converter technology for the interfacing of a hydrogen buffer with the DC-bus of an EPDN [PAPER-VIII]. For hydrogen buffer applications, the multiport concept can provide a reduced parts-count solution compared with the conventional structure that uses multiple converters. A multiport converter will best satisfy integrated power conversion, efficient thermal management, compact packaging, and centralized control requirements [95][96]. These advantages can potentially improve the overall cost, efficiency and flexibility of the hydrogen buffers used in the EPDN.

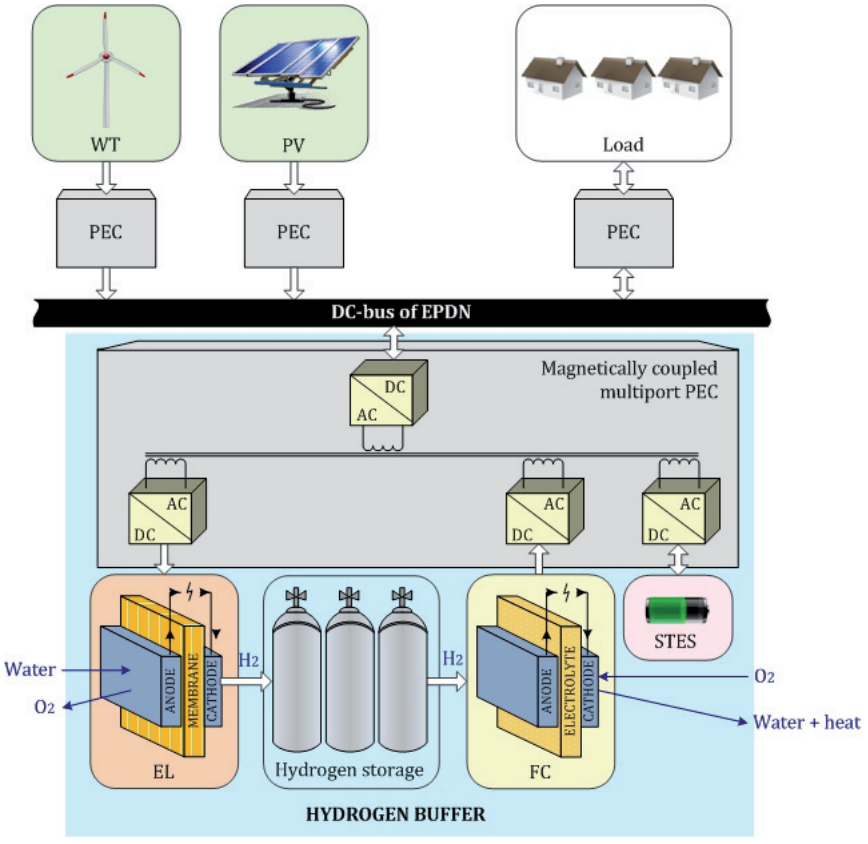

Figure 3.22 General idea of a magnetically coupled multiport converter in a hydrogen based LTES

In the proposed approach (Figure 3.22), the multiport converter has four ports: two unidirectional ports for connection of the FC and EL and two bidirectional ports for connection of the STES (battery) and for the connection to the DC-bus of an EPDN. All the ports are galvanically coupled by help of the multiwinding isolation transformer. This allows easy matching of the different voltage levels of the ports and provides galvanical isolation demanded for safety reasons in several cases.

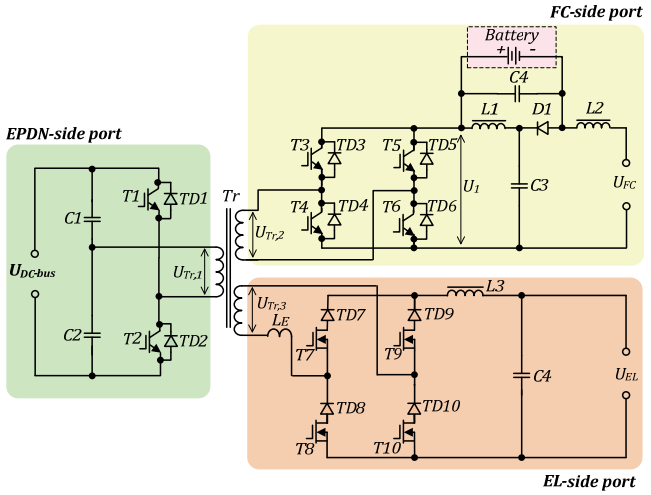

(a)

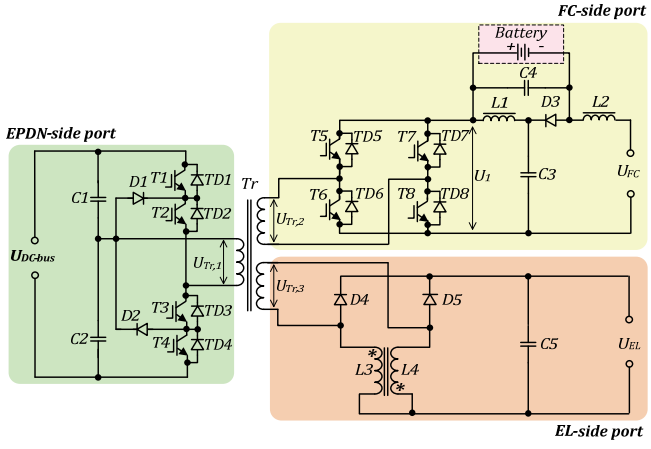

(b)

Figure 3.23 New proposed multiport DC/DC converter topologies for hydrogen buffer integration with the DC-bus of the EPDN: 2L-HB inverter magnetically coupled with a PSAFB rectifier and qZS-FB inverter (a) and 3L-HB inverter magnetically coupled with a CD rectifier and a qZS-FB inverter (b)

Generally, the multiport converter can be constructed from the basic switching cells including the buck/boost, half-bridge, full-bridge, boost half-bridge, and boost full-bridge cells [96]. In our case study we have analysed the magnetic integration of the new converter topologies presented in Section 3.1. As a result, two novel magnetically coupled multiport DC/DC converters for the hydrogen buffer integration with the DC-bus of the EPDN were synthesized (Figure 3.23). In accordance with the operation principle of the hydrogen buffer, the proposed multiport converters could have two distinct operation modes: hydrogen generation from surplus energy of an EPDN (i.e. EL operation mode when the energy is transferred from the EPDN-side port to the EL-side port) and a power back-up mode with the electricity generation by a FC (i.e. FC operation mode when the energy is transferred from the FC-side port to the EPDN-side port). The control of energy flows in both operating modes is similar to that of individual converters described in previous chapters. It must be noted here that in a FC operation mode the EPDN-side port could operate either in the uncontrolled mode (i.e. rectification through the freewheeling diodes of the transistor modules) or in the controlled mode (synchronous rectification).

During the research the new method of STES (battery) integration to the FC-side port of the proposed multiport converters was proposed and experimentally validated [PAPER-IX]. Typically, to apply a battery, an additional charging circuit is required, leading to increased complexity of the converter. However, by utilizing the property of the qZS inverter, the battery could be connected without any additional circuits, as shown in Figure 3.23. The average voltage across the battery terminals equals the average voltage of the capacitor *C4*:

$$U_B = U_{C4,avr} = \frac{D_S}{1-2\cdot D_S}\cdot U_{FC}\cdot \tag{3.18}$$

In addition to the general FC operation mode described in Section 3.1.3, several submodes could also be distinguished in the topology with an integrated battery:

- battery assisted mode: the FC and the battery provide both the power to the DC-bus to manage the peak power demand;
- battery charging mode: the FC power is higher than the load demanded power, the battery being charged from the FC;
- battery stand-by mode: the battery is fully charged and the FC provides full power only to the DC-bus.

The state-of-charge (SOC) of the battery is controlled by varying the shoot-through duty cycle D_s of the qZS inverter switches. The battery current depends on the voltage U_B and instantaneous voltage $\bar{u}_{C4}$ as well as on its internal resistance r_B:

$$i_B = \frac{U_B - \overline{u}_{C4}}{r_B}. \tag{3.19}$$

Hence, the state-of-charge (SOC) of the battery is controlled by varying the shoot-through duty cycle D_S of the qZS inverter switches. The battery current depends on the voltages U_{C4} and U_B as well as on its internal resistance r_B (Figure 3.24):

$$i_B = \frac{U_B - U_{C4}}{r_B}, \tag{3.20}$$

where U_B is the voltage rating of the battery. Hence, the state of the charge of the battery depends on the voltage:

$$U_{SOC} = U_B - U_{C4}. \tag{3.21}$$

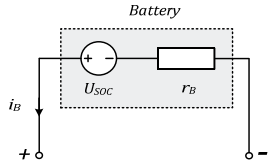

Figure 3.24 Simplified equivalent circuit of a battery

In order to keep the system in continuous conduction mode (CCM), the current of the qZS diode should never reach zero during the non-shoot-through state and the following expression should be satisfied:

$$i_B < i_{Tr,2}. \tag{3.22}$$

where $i_{Tr,2}$ is the current of the transformer secondary winding.

Next, the power equations for particular submodes of the FC operation mode are justified:

1) Battery assisted mode: $P_{FC}<P_{DC\text{-}bus}$

The FC and the battery provide the power to the DC-bus; the power equation is

$$P_{FC} - P_{DC-bus} + P_B = 0, \tag{3.23}$$

where P_{FC} is the power of the fuel cell, $P_{DC\text{-}BUS}$ is the power flowing into the DC-bus and P_B is the power provided by the battery. In this case $i_{L1}>i_{L2}$

2) Battery charging mode: $P_{FC}>P_{DC\text{-}bus}$

The FC supplies both the battery and the DC-bus in this case $i_{L1}>i_{L2}$ and the power equation is

$$P_{FC} - P_{DC-bus} - P_B = 0. \tag{3.24}$$

3) Battery stand-by mode: $P_{FC}=P_{DC\text{-}bus}$

The fuel cell provides full power to the DC-bus and the battery is fully charged. In this case $i_{L1}=i_{L2}$ and the power equation is

$$P_{FC} - P_{DC-bus} = 0 . \qquad (3.25)$$

To validate the proposed topology, the experimental setup with the power rating of 2 kW was assembled (Figure 3.25).

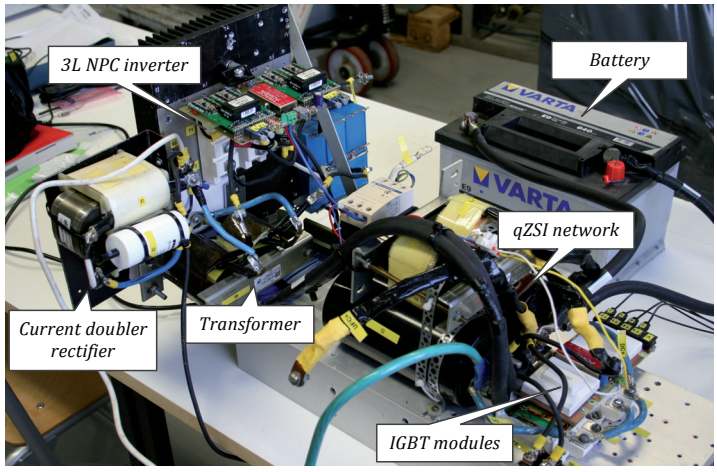

Figure 3.25 Experimental prototype of the multiport converter

It was experimentally verified that the system without a battery (Figure 3.26a) had an appreciable voltage drop at the DC-bus, while the system with the battery was able to correspond to the increased load current and provided considerably more stable output voltage (Figure 3.26b).

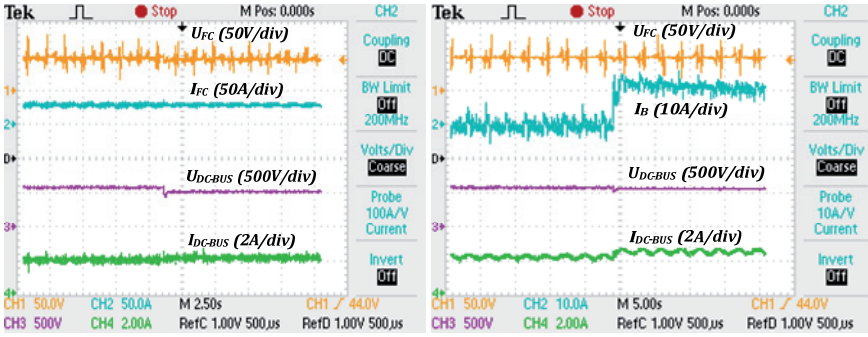

(a) *(b)*

Figure 3.26 Experimental waveforms of the FC operating mode of the proposed multiport DC/DC converter without the battery (a) and with the battery connected in parallel with C4 (b)

Figure 3.27 shows the battery state changing from charging to discharging during the operation with limited FC current when the load suddenly increases. As estimated, during charging $i_{L1}>i_{L2}$ and when the battery supplies the load $i_{L1}>i_{L2}$. Since the battery voltage remains relatively constant during the operation, the intermediate DC-link voltage of the qZS inverter is stable.

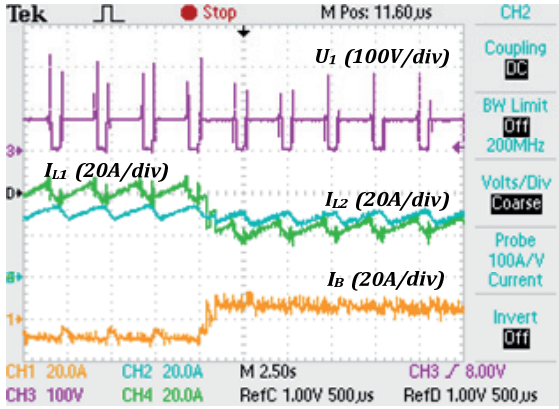

Figure 3.27 Intermediate DC-link voltage, current of the inductors L1 and L2 and battery current during the operation with limited current when the load suddenly increases

3.3 Generalizations

In this chapter, a variety of brand new DC/DC converter topologies for the hydrogen buffer interfacing with an EPDN were proposed and experimentally validated. Below, the main advantages and challenges of the proposed topologies are summarized.

2L-HB step-down DC/DC converter with a PSAFB rectifier. Due to the possibility to reduce switching losses, the implementation of a PSAFB rectifier in high-power HB DC/DC converters could be a highly promising alternative to traditional diode rectifiers. The new proposed modulation algorithm for the converter with a PSAFB rectifier allows the ZVS of the inverter switches and the ZCS of the rectifier switches over the whole range of operation conditions. At the same time, the parasitic oscillations after the turn-off of the inverter's IGBTs are completely avoided. The leakage inductance of the transformer acts as the turn-on snubber for rectifier transistors and turn-off losses of the inverter transistors could be reduced using lossless capacitive snubbers. The proposed solution has only minor modifications on the inverter side, it requires no additional bulky passive components or a frequency modulation algorithm, it features reduced energy circulation during the operation and provides significant power loss reduction in the inverter. As a downside, the topology requires reverse-blocking switches in the rectifier. This capability is often achieved by series connection of a transistor and a diode, which results in increased conduction losses.

3L-NPCHB step-down DC/DC converter with a CD rectifier. This topology features the three-level inverter on the primary side, which provides an excellent opportunity of using transistors with twice reduced blocking voltage in comparison with the two-level counterpart. The proposed PWM method provides the 3L-NPCHB inverter with the ZVS of all transistors without any additional components only by utilizing the leakage inductance of the isolation transformer. The specificity of the CD rectifier related to the isolation transformer is that the secondary winding's amplitude voltage is twice as high as that of the full-bridge rectifier. As a result, the turns number of the secondary winding of the isolation transformer will be reduced by 50%. On the other hand, the secondary current of the isolation transformer is half the output current in case of a CD rectifier. Thus, the cross-section of a wire required for the secondary winding could be twice reduced in contrast to the full-bridge transformer. Each inductor of the CD topology conducts only half the output current, which in turn gives a possibility of reduced copper loss and power dissipation distributed better than with the full-bridge design. All these advantages finally resulted in high efficiency (92-93%) in all operating points and modes of the experimental converter. A specific drawback of the three-level inverter is that the conduction losses increased by 30% due to series connection of two transistors (sum of voltage drops) during the conduction period. However, it cannot affect the overall feasibility of this topology in any load conditions.

qZS-FB step-up DC/DC converter with a VD rectifier. This topology represents a new approach to the high step-up DC/DC converters where the voltage gain is performed at every voltage conversion stage. First, the voltage is boosted in the qZS inverter by help of the special shoot-through operating state. Afterwards the voltage is stepped up in the isolation transformer proportionally to its turns ratio and finally doubled in the voltage doubler rectifier. Presence of the qZS-network at the inverter stage ensures the inherent "shoot-through proof" feature – the converter will not be destroyed by the simultaneous conduction of the top and bottom switches, which could be caused by the misgating due to the EMI. The utilization of leakage inductance of the isolation transformer in combination with a proper modulation method will result in the decreased dynamic losses of the inverter due to the presence of ZVS and ZCS. The converter demonstrated the efficiency near 92% at the maximal input voltage, which could be further improved to 97% by the introduction of the LC resonance network. However, the efficiency drop at the maximal power point caused by the increased power dissipation in the semiconductors during the shoot-through stages could become an issue.

Magnetically coupled multiport DC/DC converters. The multiport topology provides significant advantages over the traditional multiconverter approach, such as integrated power conversion, efficient thermal management, compact packaging, and centralized control. By magnetic integration of two-port converters of the hydrogen buffer, the number of stages of the conventional

structure can be reduced. For example, in the proposed multiport DC/DC converter topologies by sharing the conversion devices (transistors and diodes) of the DC-bus side port, the redundancy was reduced. Finally, it resulted in 20% better power density than with the traditional multiconverter approach as well as in reduced component count, lower cost, and control simplicity. For further improvement of integrity and reduction of redundancy, the converterless integration of a STES (battery) into the qZS-based FC side port was considered. The integrated battery will help to balance the power difference between the FC and the EPDN and finally improve the dynamic response of the hydrogen buffer.

4 FUTURE RESEARCH DIRECTIONS

The future work could continue with the analysis of implementation possibilities of the hydrogen based LTES in the Estonian energy sector. Estonia has a long coastal line and islands, which is a large part in the Baltic region. Wind power appears to be one of the most perspective and widespread among alternative energy sources in Estonia. New local wind power stations are being developed in compliance with the requirements of the EU and the latest PEC technologies. Introducing a huge amount of wind power in the energy systems might imply a lower capacity value of the wind generated electricity. However, a system with a high penetration of wind power needs more reserve capacity as backup to deal with short-run fluctuations in the level of wind output. Unforecastable winds make it difficult to plan production (Figure 1.2), complicating parallel operation with other power plants intended for compensating the instability of wind production. The fluctuating level of demand on the conventional power stations can make the market price of electricity very volatile, which brings challenges to the companies which need to trade it. Thus, the hydrogen based LTES is needed for the stabilization of wind power generation. Results show that combining controllable hydrogen production with wind power can cost-effectively reduce a substantial share of the power imbalances resulting from wind forecast uncertainties.

In the future research special attention should be paid to a feasibility study of distributed energy generation in the conditions of open electricity market. The idea of an open electricity market is to create competition in as many links of the power supply chain as possible. After the market opening new business opportunities for market participants will evolve, there will be competition in electricity generation and retail. For producers, the electricity market will provide an opportunity to sell what they generate. A functioning market, along with transparent pricing, will in turn give investors and producers a basis for making long-term investment decisions. In the conditions of an open electricity market the hydrogen produced can be also used for transport, for combined heat and power, or simply to generate electricity at a time when prices are higher. Interest in hydrogen as a transportation fuel is growing. This implies a considerable need for hydrogen transport and delivery infrastructure. Between the two ends of the economic chain, hydrogen has to be packaged by compression or liquefaction to become a commodity. In the transportation, hydrogen has to be produced, packaged, transported, stored, transferred to cars, then stored and transported again before it is finally admitted to fuel cells. There are two possibilities of hydrogen delivery: road and pipeline delivery. Surface transportation of hydrogen gas is expensive, especially over long distances, because of the amount of pressure required to store the hydrogen. Liquefied hydrogen is denser, but liquefaction is extremely costly and energy inefficient. Nevertheless, transport using cryogenic tankers is currently the most common method because of the lack of underground pipelines. Hydrogen has a very small amount of energy by volume as compared to other fuels. As a result, distribution

and delivery are costly and result in inefficiencies associated with it. Most of the analyses show that gaseous hydrogen pipelining costs approximately 1.3 to 1.8 times more per unit energy distance than natural gas. Pipelines are very expensive to design and construct and must have high utilization to justify the initial capital cost. Thus, the interactions between the hydrogen production and the electricity market require further research and development.

References

[1] Boroyevich, D.; Burgos, R.; Arnedo, L.; Fei Wang. Synthesis and Integration of Future Electronic Power Distribution Systems. Power Conversion Conference (PCC'07), pp. K-1-K-8, 2-5 April 2007.

[2] Boroyevich, D.; Cvetkovic, I.; Dong Dong; Burgos, R.; Fei Wang; Lee, F. Future Electronic Power Distribution Systems a Contemplative View. 12th International Conference on Optimization of Electrical and Electronic Equipment (OPTIM'2010), pp. 1369-1380, 20-22 May 2010.

[3] Ajaja, A. Reinventing Electric Distribution. IEEE Potentials, Vol.29, no. 1, pp. 29-31, Jan.-Feb. 2010.

[4] Chowdhury, S; Chowdhury S. P.; Crossley, P. Microgrids and Active Distribution Networks. Institution of Engineering and Technology (IET), 320 pp, 2009.

[5] Peng, F.Z.; Yun Wei Li; Tolbert, L.M. Control and Protection of Power Electronics Interfaced Distributed Generation Systems in a Customer-Driven Microgrid. IEEE Power & Energy Society General Meeting PES'2009, pp.1-8, 26-30 July 2009.

[6] Yun Wei Li; Ching-Nan Kao. An Accurate Power Control Strategy for Power-Electronics-Interfaced Distributed Generation Units Operating in a Low-Voltage Multibus Microgrid. IEEE Transactions on Power Electronics, Vol. 24, no. 12, pp. 2977-2988, Dec. 2009.

[7] Zhenhua Jiang; Xunwei Yu. Hybrid DC- and AC-Linked Microgrids: Towards Integration of Distributed Energy Resources. IEEE Energy 2030 Conference ENERGY 2008, pp.1-8, 17-18 Nov. 2008.

[8] Zhenhua Jiang; Xunwei Yu. Power Electronics Interfaces for Hybrid DC and AC-linked Microgrids. IEEE 6th International Power Electronics and Motion Control Conference IPEMC '2009, pp. 730-736, 17-20 May 2009.

[9] Implementation of the Renewable-Energy-Directive by the EU Member States http://www.ecologic.eu/4164

[10] Elering Company http://www.elering.ee

[11] Nguyen, T. D; Tseng, K. J; Zhang, S; Zhang, C. A Flywheel Cell for Energy Storage System. Proceedings of the IEEE, pp. 214-219, 2008.

[12] Boyes, J. D; Clark, N. H. Technologies for Energy Storage. Flywheels and Super Conducting Magnetic Energy Storage. Proceedings of the IEEE, pp. 1548-1550, 2000.

[13] Rausmussen, C. N. Improving Wind Power Quality with Energy Storage. Proceedings of the IEEE, pp. 1-7, 2009.

[14] Smith, S. C; Sen, P. K; Kroposki, B. Advancement of Energy Storage Devices and Applications in Electrical Power System. Proceedings of the IEEE, 2008.

[15] Nigim, K; Reiser, H. Energy Storage for Renewable Energy Combined Heat, Power and Hydrogen Fuel (CHPH2) Infrastructure. Proceedings of the Electrical Power and Energy Conference, 2009.

[16] Cavallaro, C.; Chimento, F.; Musumeci, S.; Sapuppo, C.; Santonocito, C. Electrolyser in H2 Self-Producing Systems Connected to DC Link with Dedicated Phase Shift Converter. International Conference on Clean Electrical Power (ICCEP'07), pp. 632-638, 21-23 May 2007.

[17] Cavallaro, C.; Cecconi, V.; Chimento, F.; Musumeci, S.; Santonocito, C.; Sapuppo, C. A Phase-Shift Full Bridge Converter for the Energy Management of

Electrolyzer Systems. IEEE International Symposium on Industrial Electronics, (ISIE'07), pp. 2649-2654, 4-7 June 2007.

[18] Ugartemendia, J.J.; Ostolaza, X.; Moreno, V.; Molina, J.J.; Zubia; I. Wind Generation Stabilization of Fixed Speed Wind Turbine Farms with Hydrogen Buffer. 11th Spanish-Portuguese Conference on Electrical Engineering (11CHLIE), pp. 1-5, 1-4 July 2009.

[19] Faias S.; Santos P.; Sousa J.; Castro R. An Overview on Short and Long–Term Response Energy Storage Devices for Power Systems Applications. Proceedings of the International Conference On Renewable Energies and Power Quality (ICREPQ'08), pp.1-6, 2008.

[20] Korpas, M.; Holen, A. T. Operation Planning of Hydrogen Storage Connected to Wind Power Operating in a Power Market. IEEE Transaction on Energy Conversion, vol. 21, no. 3, pp. 742-749, September 2006.

[21] Agbossou, K.; Kolhe, M.; Hamelin, J.; Bose, T. K. Performance of a Stand-Alone Renewable Energy System Based on Energy Storage as Hydrogen. IEEE Transaction on Energy Conversion, vol. 19, no. 3, pp. 633-640, September 2004.

[22] Agbossou, K.; Doumbia, M. L.; Anouar, A. Optimal Hydrogen Production in a Stand-Alone Renewable Energy System. IEEE, pp. 2932-2936, 2005.

[23] Wang, C.; Nehrir, M. H. Power Management of Standalone Wind/Photovoltaic/Fuel Cell Energy System. IEEE Transaction on Energy Conversion, vol. 23, no. 3, pp. 1-11, 2008.

[24] Ellis, M. W.; Von Spakovsky, M. R.; Nelson, D. J. Fuel Cell Systems: Efficient, Flexible Energy Conversion for the 21st Century. IEEE, vol. 89, no. 12, pp. 1808-1818, December 2001.

[25] Yu, S.; Mays, T. J.; Dunn, R. W. A New Methodology for Designing Hydrogen Energy Storage in Wind Power Systems to Balance Generation and Demand. IEEE, pp. 1-2, 2009.

[26] Kottenstette, R.; Cortell, J. Hydrogen Storage in Wind Turbine Towers. NREL/TP-500-34656. Technical Report. National Renewable Energy Laboratory, September 2003.

[27] Poore, R.; Lettenmaier, T. Alternative Design Study Report: WindPACT Advanced Wind Turbine Drive Train Designs Study. NREL/SR-500-33196. Subcontractor Report. National Renewable Energy Laboratory, August 2003.

[28] Korpaas, M.; Hildrum, R.; Holen, A. T. Optimal Operation of Hydrogen Storage for Energy Sources with Stochastic Input. IEEE Bologna PowerTech Conference, pp. 1-8, 2003.

[29] Bapu, B. R. R.; Karthikeyan, J.; Reddy, K. V. K. Hydrogen Storage in Wind Turbine Tower – a Review. IEEE, pp. 308-312, 2010.

[30] Iannuzzi, D.; Pagano, M. Efficiency of Hydrogen Based Storage Systems for Stand-Alone PV Applications: Numerical and Experimental Results. IEEE, pp. 555-561, 2009.

[31] Gao, W.; Zheglov, V.; Wang, G.; Mahajan, S. M. PV-Wind-Fuel Cell-Electrolyzer Micro-Grid Modeling and Control in Real Time Digital Simulator. IEEE, pp. 29-34, 2008.

[32] Chedid, R.; Chaaban, F. B.; Shihab, R. A Simplified Electric Circuit Model for the Analysis of Hybrid Wind-Fuel Cell Systems. IEEE, pp. 1-6, 2007.

[33] Doumbia, M. L.; Agbossou, K.; Granger, E. Modelling and Simulations of a Hydrogen Based Photovoltaic/Wind Energy System. IEEE, pp. 2601-2606, 2007.

[34] Andrijanovitš, A.; Vinnikov, D. Multiport DC/DC Converters for Interfacing of Hydrogen Buffer with Wind Turbine. 9th International Symposium "Topical Problems in the Field of Electrical and Power Engineering", Doctoral School of Energy and Geotechnology. Tallinn: Elektriajam, pp.95-99, 2010.
[35] Nguyen, T. D.; Tseng, K. J.; Zhang, S.; Zhang, C. A Flywheel Cell for Energy Storage System. Proceedings IEEE, pp. 214-219, 2008.
[36] Boyes, J. D.; Clark, N. H. Technologies for Energy Storage. Flywheels and Super Conducting Magnetic Energy Storage. Proceedings IEEE, pp.1548-1550, 2000.
[37] Rausmussen, C. N. Improving Wind Power Quality with Energy Storage. Proceedings IEEE.
[38] Smith, S. C.; Sen, P. K.; Kroposki, B. Advancement of Energy Storage Devices and Applications in Electrical Power System. Proceedings IEEE, 2008.
[39] Nigim, K.; Reiser, H. Energy Storage for Renewable Energy Combined Heat, Power and Hydrogen Fuel (CHPH2) Infrastructure. Proceedings IEEE Electrical Power and Energy Conference, 2009.
[40] Kroposki, B.; Levene, J.; Harrison, K.; Sen, P. K.; Novachek, F. Electrolysis: Opportunities for Electric Power Utilities in a Hydrogen Economy. 38th North American Power Symposium. NAPS, pp. 567-576, 2006.
[41] Yu, S.; Mays, T. J.; Dunn, R. W. A New Methodology for Designing Hydrogen Energy Storage in Wind Power Systems to Balance Generation and Demand. Proceedings of the IEEE, 2009.
[42] Fuel Cell Handbook. Eg & G Technical Services, Inc. 2004.
[43] Matthew, M. Fuel Cell Engines. John Wiley & Sons, Inc. 2008.
[44] Srinivasan, S. Fuel Cells: from Fundamentals to Applications. Springer, USA, 2006.
[45] Wang, C.; Nehrir, M. H. Power Management of a Stand-Alone Wind/Photovoltaic/Fuel Cell Energy System. IEEE Transactions on Energy Conversion, 2008.
[46] Gautam, D. S.; Bhat, A. K. S. A Comparison of Soft-Switched DC to DC Converters for Electrolyser Application. Proceedings of India International Conference on Power Electronics, pp. 274-279, 2006.
[47] Gautam, D. S.; Bhat, A. K. S. A Two-Stage Soft-Switched Converter for Electrolyser Application. Fifteenth National Power Systems Conference (NPSC). IIT Bombay, 2008.
[48] Jang, Y.; Jovanović, M. M. A New Family of Full-Bridge ZVS Converters. IEEE, pp. 622-628, 2003.
[49] Nayak, D. K.; Reddy, S. R. Simulation of Soft Switched PWM ZVS Full-Bridge Converter. International Journal of Computer and Electrical Engineering, vol. 2, no. 3, 2010.
[50] Borage, M.; Tiwari, S.; Bhardwaj, S.; Kotaiah, S. A Full-Bridge DC/DC Converter with Zero-Voltage-Switching over the Entire Conversion Range. IEEE Transactions on Power Electronics, vol. 23, no. 4, 2008.
[51] Chandrasekhar, P.; Rama Reddy, S. Design of LCL Resonant Converter for Electrolyser. International Journal of Electronic Engineering Research, vol. 2, no. 3, 2010.
[52] Dudrik, J.; Oetter, J. High-Frequency Soft-Switching DC/DC Converters for Voltage and Current DC Power Sources. Acta Polytechnica Hungarica, vol. 4, no. 2, 2007.

[53] Bhat, A. K. S. Analysis and Design of LCL-Type Series Resonant Converter. IEEE, pp.172-178, 1990.
[54] Steigerwald, R. L. A Comparison of Half-Bridge Resonant Converter Topologies. IEEE Transactions on Power Electronics, vol. 3, no. 2, 1988.
[55] Shen, Z. B.; El-Saadany, E. F. Novel Interfacing for Fuel Cell Based Distributed Generation. IEEE Power Engineering Society General Meeting, June 2007.
[56] Sharma, R.; Gao, H. A New DC/DC Converter for Fuel Cell Powered Distributed Residential Power Generation Systems. IEEE, pp. 1014-1018, 2006.
[57] Younis, M. A. A.; Rahim, N. A.; Mekhilef, S. Dynamic and Control of Fuel Cell System", IEEE Industrial Electronics and Applications, pp. 2063-2067, June 2008.
[58] Xu, H.; Kong, L.; Wen, X. Fuel Cell Power System and High Power DC/DC Converter. IEEE Transaction on Power Electronics, vol. 19, no. 5, pp. 1250-1255, September 2004.
[59] Narjiss, A.; Depernet, D.; Gustin, F.; Hissel, D.; Berthon, A. Design and Control of a Fuel Cell DC/DC Converter for Embedded Applications. IEEE, 2008.
[60] Larico, H. R. E.; Barbi, I. Voltage-Fed Three-Phase Push-Pull DC/DC Converter. IECON´09, 35th Annual Conference of IEEE, pp. 956-961, November 2009.
[61] Mohr, M.; Fuchs, F. Voltage-Fed and Current-Fed Full-Bridge Converter for the Use in Three-Phase Grid Connected Fuel Cell Systems. IEEE Power Electronics and Motion Control Conference, August 2006.
[62] Mohr, M.; Fuchs, F. Current-Fed Full-Bridge Converters for Fuel Cell Systems Connected to the Three Phase Grid. IEEE, pp. 4313-4318, 2006.
[63] Zhu, X.; Xu, D.; Shen, G.; Xi, D.; Mino, K.; Umida, H. Current-Fed DC/DC Converter with Reverse Block IGBT for Fuel Cell Distributing Power System. Industry Applications Conference, pp. 2043-2048, October 2005.
[64] Rathore, A. K.; Mazumder, S. K. Novel Zero-Current Switching Current-Fed Half-Bridge Isolated DC/DC Converter for Fuel Cell Based Applications. Energy Conversion Congress and Exposition, pp. 3523-3529, September 2010.
[65] Meo, S.; Perfetto, A.; Piegari, L.; Esposito, F. A ZVS Current-Fed DC/DC Converter Oriented for Applications Fuel Cell Based. The 30th Annual Conference of the IEEE Industrial Electronics Society, pp. 932-937, November 2004.
[66] Andersen, G. K.; Klumpner, C.; Kjaer, S. B.; Blaabjerg, F. A New Green Power Inverter for Fuel Cells. IEEE Power Electronics Specialists Conference, pp. 727-733, 2002.
[67] Bojoi, R.; Pica, C.; Tenconi, A. New DC/DC Converter with Reduced Low-Frequency Current Ripple for Fuel Cell in Single-Phase Distributed Generation. IEEE Industrial Technology (ICIT), pp. 1213-1218, March 2010.
[68] Larico, H. R. E.; Barbi, I. Double-Coupled Current-Fed Push-Pull DC/DC Converter: Analysis and Experimentation. IEEE Power Electronics Conference, COBEP´09, pp. 305-312, October 2009.
[69] Cha, H.; Enjeti, P. A Novel Three-Phase High Power Current-Fed DC/DC Converter with Active Clamp for Fuel Cells. IEEE Power Electronics Specialists Conference, pp. 2485-2489, June 2007.
[70] Andersen, R. L.; Barbi, I. A Three-Phase Current-Fed Push-Pull DC/DC Converter. IEEE Transaction on Power Electronics, vol. 24, no. 2, pp. 358-368, February 2009.

[71] Lee, S.; Park, J.; Choi, S. A Three-Phase Current-Fed Push-Pull DC/DC Converter with Active Clamp for Fuel Cell Applications. IEEE.
[72] Vinnikov, D.; Roasto, I.; Jalakas, T. New Step-Up DC/DC Converter with High-Frequency Isolation. IEEE, pp. 670-675, 2009.
[73] Peng, F. Z. Z-Source Inverter. IEEE Transactions on Industry Applications, vol. 39, no. 2, pp. 504-510, April 2003.
[74] Shen, M.; Joseph, A.; Wang, J.; Peng, F. Z.; Adams, D. J. Comparison of Traditional Inverters and Z-Source Inverter for Fuel Cell Vehicles. IEEE Transactions on Power Electronics, vol. 22, no. 4, pp. 1453-1463, July 2007.
[75] Vinnikov, D.; Roasto, I.; Zakis, J.; Strzelecki, R. New Step-Up DC/DC Converter for Fuel Cell Powered Distributed Generation Systems: Some Design Guidelines. Journal of Electrical Review, vol. 86, no. 8, pp. 245-252, 2010.
[76] Li, Y.; Anderson, J.; Peng, F. Z.; Liu, D. Quasi-Z-Source Inverter for Photovoltaic Power Generation Systems. IEEE Applied Power Electronics Conference and Exposition, pp. 918-924, February 2009.
[77] Yao, Z.; Xiao, L.; Huang, Y.; Gong, C. Push-Pull Forward Three-Level Converter with Reduced Rectifier Voltage Stress. IEEE, pp. 1654-1660, 2009.
[78] Jin, K.; Ruan, X.; Yang, M.; Xu, M. A Hybrid Fuel Cell Power System. IEEE Transactions of Industrial Electronics, Vol. 56, No. 4, pp. 1212-1222, April 2009.
[79] Beurskens, L. W. M.; Hekkenberg, M.; Vethman, P. Renewable Energy Projections as Published in the National Renewable Energy Action Plans of the European Member States. 2011.
[80] Prices for Renewable Energies in Europe: Report 2011-2012. European Renewable Energies Federation (EREF), 2012.
[81] Weinert, J. X.; Lipman, T. E. An Assesment of the Near-Term Costs of Hydrogen Refueling Stations and Station Components. Institute of Transportation Studies, University of California, 2006.
[82] Amos, W. A. Costs of Storing and Transporting Hydrogen. NREL, 1998.
[83] Doty, F. A Realistic Look at Hydrogen Price Projections. Doty Scientific, Inc. Columbia, 2004.
[84] Blinov, A. Research of Switching Properties and Performance Improvement Methods of High-Voltage IGBT based DC/DC Converters. PhD. Thesis, Tallinn University of Technology, TUT Press, 2012.
[85] Martins, J. F.; Joyce, A.; Rangel, C.; Sotomayor, J.; Castro, R.; Pires, A.; Carvalheiro, J.; Silva, R. A.; Viana, S. RenH2 - Stand-Alone Energy System Supported by Totally Renewable Hydrogen Production. Proc. of International Conference on Power Engineering, Energy and Electrical Drives (POWERENG'07), pp. 566-570, 2007.
[86] Prasad, A. R.; Ziogas, P. D.; Manias, S. Analysis and Design of a Three-Phase Offline DC/DC Converter with High-Frequency Isolation. IEEE Transactions on Industry Applications, vol. 28, no. 4, pp. 824-832, 1992.
[87] Rabinovici, R. Three-Phase High Frequency DC/DC Converter. Electronics Letters, vol. 26, issue 13, pp. 829-830, 1990.
[88] Vinnikov, D. Isolated DC/DC Converter Topology with a Three-Phase Intermediate AC-Link. Proc. of 2006 International Baltic Electronics Conference, pp. 1-4, 2006.

[89] Prasad, A .R.; Ziogas, P. D.; Manias, S. Analysis and Design of a Three-Phase Offline DC-DC Converter with High-Frequency Isolation. IEEE Transactions on Industry Applications, vol. 28, no. 4, pp. 824-832, Jul/Aug 1992.

[90] Vinnikov, D.; Roasto, I. Quasi-Z-Source-Based Isolated DC/DC Converters for Distributed Power Generation. IEEE Transactions on Industrial Electronics, vol. 58, no.1, pp. 192-201, 2011.

[91] Roasto, I.; Vinnikov, D. Analysis and Evaluation of PWM and PSM Shoot-Through Control Methods for Voltage-Fed qZSI Based DC/DC Converters. 14th International Power Electronics and Motion Control Conference (EPE-PEMC'10), pp.T3-100-T3-105, 2010.

[92] Gao, W.; Zheglov, V.; Wang, G.; Mahajan, S. M. PV-Wind-Fuel Cell-Electrolyzer Micro-Grid Modeling and Control in Real Time Digital Simulator. IEEE, pp. 29-34, 2008.

[93] Thounthong, P.; Sethakul, P.; Rael, S.; Davat, B. Performance Investigation of Fuel Cell/Battery and Fuel Cell/Supercapacitor Hybrid Sources for Electric Vehicle Applications. IEEE, pp. 455-459, 2009.

[94] Boscaino, V.; Capponi, G.; Livreri, P.; Marino, F. Fuel Cell Modeling for Power Supply Systems Design, IEEE, pp. 1-4, 2008.

[95] Tao, H.; Kotsopoulos, A.; Duarte, J. L.; Hendrix, M. A. M. Family of Multiport Bidirectional DC/DC Converters. IEE Proceedings on Electric Power Applications, vol. 153, no. 3, pp. 451- 458, 2006.

[96] Tao, H.; Duarte, J. L.; Hendrix, M. A. M. Multiport Converters for Hybrid Power Sources. IEEE Power Electronics Specialists Conference (PESC'08), pp. 3412-3418, 2008.

Abstract

New Converter Topologies for Integration of Hydrogen Based Long-Term Energy Storages to Renewable Energy Systems

Use of alternative energy sources is an urgent issue today. Main advantages of renewable energy are zero fuel costs and lower impact on the environment. However, renewable energy sources, such as solar and wind power, are difficult to use due to their stochastic variability. In order for renewable energy to be generally used for regular consumers, the concept of a hydrogen buffer was introduced to stabilize unregulated renewable energy generation.

Essential elements of the hydrogen based long-term energy storage (LTES), also known as a hydrogen buffer, are an electrolyzer, a hydrogen storage system and a fuel cell. To achieve proper voltage matching, the main components of the hydrogen buffer should be connected to the DC-bus of the supported renewable energy system via different power electronic converters: the electrolyzer is interfaced by help of a step-down DC/DC converter, while the fuel cell is connected by help of a step-up DC/DC converter.

The main goal of the thesis was to develop and experimentally validate new methods, topologies and solutions, which will substantially contribute to the further improvement of the hydrogen based LTES technology without increasing their complexity or reducing the reliability significantly. As a result of a comprehensive research and development work, a variety of new energy efficient DC/DC converter topologies for the electrical interfacing of electrochemical stage of the hydrogen based LTES with EPDN were proposed. All the topologies have been experimentally verified and demonstrated an outstanding performance in a row with high efficiency (90...93%). By help of elaborated design guidelines these topologies could be also implemented in other application fields, such as telecom, rolling stock, aerospace, marine etc. where the efficiency, reliability and integrity play a major role. Moreover, the number of new control methods (improved control method for half-bridge step-down DC/DC converter with a phase-shifted active full-bridge rectifier, output voltage programmed control for the qZS-based step-up DC/DC converters, etc.) were proposed and experimentally validated. As one of important results of this PhD research, the idea of magnetic integration of the developed two-port converters resulted in a new multiport converter technology for the interfacing of a hydrogen buffer with the DC-bus of an EPDN. Finally, the new method of a STES (battery) integration to the FC-side port of the proposed multiport converters was analysed and experimentally validated.

Kokkuvõte

Uudsed muundurite topoloogiad vesinikul põhinevate energiasalvestite integreerimiseks taastuvenergiasüsteemidesse

Alternatiivseid energiaallikaid kasutatakse tänapäeval üha rohkem, kuna nii on võimalik säästa fossiilseid kütuseid ja vähendada mõju keskkonnale. Samas on taastuvad energiaallikad nagu tuul ja päike raskestikasutatavad nende muutlikkuse tõttu. Nende energiaallikate laialdasemaks kasutamiseks tuleb kasutada energia salvestamist. Pikaajaliseks energiakandjaks sobib hästi vesinik.

Põhilised vesinikupõhise pikaajalise energiasalvesti osad on elektrolüüser, vesiniku hoidmiseks ja jaotamiseks vajalikud süsteemid ja kütuselement. Vesinikusalvesti erinevad plokid on läbi spetsiaalsete jõupooljuhtmuundurite ühendatud ühise alalispingesiiniga. Elektrolüüser ühendatakse läbi pinget madaldava muunduri, samas kui kütuselemet tuleb ühendada alalispingesiiniga läbi pinget tõstva muundusseadme.

Käesolevas doktoritöös uuritakse vesinikusalvestites kasutatavate jõupooljuhtmuundurite skeemilahendusi ja pakutakse välja skeemilahenduslikke uuendusi parandamaks vesinikusalvesteid teenindavate muundusseadmete parameetreid, tõstmata oluliselt nende keerukust või langetamata töökindlust.

Uudne skeemilahendus võimaldab omavahel siduda minimaalse arvu muundamisastmetega elektrolüüseri, päikesepaneeli või elektrituuliku kütuselemendi ja lühiajalised energiasalvestid.

Kõiki antud doktoritöös kirjeldatud skeemilahendusi on eksperimentaalselt katsetatud, mille käigus tuvastati nende suurepärased väljundparameetrid ja kõrge kasutegur (90...93%).

Doktoritöös väljatöötatud projekteerimisjuhiseid võib kasutada ka mitmetel teistel rakendusaladel nagu sides, elektriraudteel, lennunduses ja merenduses jõupooljuhtmuundurite töökindluse ja kasuteguri tõstmiseks.

Lisaks skeemilahendustele on välja pakutud ja katseliselt uuritud ka mitmeid uudseid juhtimisalgoritme (parandatud juhtimisalgoritm pinget langetavale poolsildvaheldiga ning faasinihkega juhitava täissildalaldiga alalispingemuundurile ning juhtimisalgoritm kvaasiimpedants-allikaga pinget tõstvale alalispingemuundurile). Käesoleva doktoritöö üks tähtsamaid ideesid on kaheviiguliste (sisend ja väljund) muundusseadmete integreerimine magnetahela abil ühte mitmikviikudega (*multiport converter*) muundurisse. Lisaks sellele on välja pakutud ka uudne meetod energiasalvesti (elektrokeemiline aku) lisamiseks kütuselementi teenindavasse muundurisse, mis on üks osa mitmikviikudega muundurist.

Elulookirjeldus

1. Isikuandmed

Ees- ja perekonnanimi	Anna Andrijanovitš
Sünniaeg ja -koht	21. juuli 1984, Kohtla-Järve, Eesti
Kodakondsus	eesti

2. Kontaktandmed

Aadress	Jõhvi, Ida-Virumaa
Telefon	+37255592568
E-posti aadress	anna.andrijanovits@gmail.com

3. Hariduskäik

Õppeasutus (nimetus lõpetamise ajal)	Lõpetamise aeg	Haridus (eriala/kraad)
Ahtme Gümnaasium	2003	Keskharidus
Tallinna Tehnikaülikool, Elektriajamite ja jõuelektroonika instituut	2006	Bakalaureusekraad
Tallinna Tehnikaülikool, Elektriajamite ja jõuelektroonika instituut	2008	Magistrikraad

4. Keelteoskus (alg-, kesk- või kõrgtase)

Keel	Tase
Vene	emakeel
Eesti	kesktase
Inglise	kesktase
Saksa	algtase

5. Teenistuskäik

Töötamise aeg	Tööandja nimetus	Ametikoht
08.05.2006 - 17.03.2008	Tehnogen OÜ	Ehitiste projekteerija
24.03.2008 - 19.11.2012	Eesti Energia Võrguehitus AS	Elektriprojekteerija
03.12.2012 - jätkub	Elektrilevi OÜ	Võrgu planeerija

7. Kaitstud lõputööd

   Anna Sergejeva, magistrikraad, 2008, (juhendaja) Dmitri Vinnikov, Elektrolüüsi kasutamine ületoodetud energia salvestamiseks tuuleenergeetikas, Tallinna Tehnikaülikool, Energeetikateaduskond, Elektriajamite ja jõuelektroonika instituut, Elektriajamite ja elektrivarustuse õppetool.

8. Teadustöö põhisuunad
   - Loodusteadused ja tehnika
   - Energeetikaalased uuringud

9. Uurimisprojektid
   - ETF8020 "Võimsate IGBT muundurite innovatiivsete juhtimis- ja diagnoostikasüsteemide uurimine"
   - ETF8538 "Kvaasi-impedantsallikaga alalis- ja vahelduvpingemuundurid"
   - SF0140016s11 "Aktiivsete elektrijaotusvõrkude muundurite topoloogiad ja juhtimismeetodid"

Curriculum vitae

1. Personal data

Name	Anna Andrijanovitš
Date and place of birth	21 July 1984, Kohtla-Järve, Estonia

2. Contact information

Address	Jõhvi, Ida-Virumaa
Phone	+37255592568
E-mail	anna.andrijanovits@gmail.com

3. Education

Educational institution	Graduation year	Education (field of study/degree)
Ahtme Gümnaasium	2003	Secondary education
Tallinn University of Technology, Department of Electrical Drives and Power Electronics	2006	Bachelor degree
Tallinn University of Technology, Department of Electrical Drives and Power Electronics	2008	Master of science degree

4. Language competence/skills (fluent, average, basic skills)

Language	Level
Russian	native
Estonian	average
English	average
German	beginner

5. Professional Employment

Period	Organisation	Position
08.05.2006 - 17.03.2008	Tehnogen OÜ	Construction designer
24.03.2008 - 19.11.2012	Eesti Energia Võrguehitus AS	Electrical designer
03.12.2012 - continuous	Elektrilevi OÜ	Network planner

7. Defended theses

   Anna Sergejeva, Master's Degree, 2008, (supervisor) Dmitri Vinnikov, Use of Electrolysis for Energy Storage in Wind Power, Tallinn University of Technology, Faculty of Power Engineering, Department of Electrical Drives and Power Electronics, Chair of Electrical Drivers and Electrical Supply.

8. Main areas of scientific work / Current research topics
   - Natural Sciences and Engineering
   - Research in the field of Power Engineering

9. Research projects
   - ETF8020 “Research of Advanced Control and Diagnostics Systems for the High-Power IGBT Converters”
   - G8538 “Quasi-Impedance Source DC/DC and AC/AC Converters”
   - SF0140016s11 “New Converter Topologies and Control Methods for Electronic Power Distribution Networks”

Appendix

[PAPER-I] **Andrijanovits, A.**; Hoimoja, H.; Vinnikov, D. Comparative Review of Long-Term Energy Storage Technologies for Renewable Energy Systems. Electronics and Electrical Engineering, 2(118), pp. 21 – 26, 2012.

ELECTRONICS AND ELECTRICAL ENGINEERING
ISSN 1392 – 1215 2012. No. 2(118)
ELEKTRONIKA IR ELEKTROTECHNIKA

ELECTRONICS
T 170
ELEKTRONIKA

Comparative Review of Long-Term Energy Storage Technologies for Renewable Energy Systems

A. Andrijanovits, H. Hoimoja, D. Vinnikov
Department of Electrical Drives and Power Electronics, Tallinn University of Technology, Ehitajate tee 5, 19086 Tallinn, Estonia, phone: +3726203705, e-mail: sergejeva84@hot.ee

crossref http://dx.doi.org/10.5755/j01.eee.118.2.1168

Introduction

Energy storage systems for a long time have been utilized in many forms and applications. Today's energy storage technologies are used to achieve electric power systems of higher reliability and to contribute to the broader use of renewable energy. Wind power appears to be one of the most perspective and widespread renewable energy sources. Because of unregulated energy generation of wind generators, with the wind speed fluctuating, the output too is fluctuating, i.e. at some instances energy overflow and deficiency will appear (Fig. 1) [1].

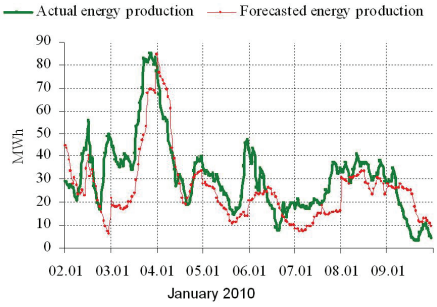

Fig. 1. An example of unpredictable energy generation by Estonian wind farms

An energy storage element introduced into a wind power plant will change the spectrum and statistical distribution of the output power. Increasing the amount of storage (power and energy) associated with a wind power plant will gradually make the output more controllable and predictable [2].

Energy storage technologies

A variety of technologies are available for energy storage in the power system. To identify the most relevant storage solutions it is necessary to include considerations of many relevant parameters, such as cost, lifetime, reliability, size, storage capacity, and environmental impact. All these parameters should be evaluated against the potential benefit of adding storage to reach a decision about the type of storage to be added. There may also be cases where the value of adding storage is not sufficient to justify such an investment.

Energy storage technologies can be generally divided into three main groups: mechanical, electrochemical and electromagnetic storage (Fig. 2). Mechanical storage includes pumped hydro storage, compressed air energy storage and flywheels. Electrochemical storage includes all types of batteries as well as a hydrogen based energy storage. Electromagnetic storage includes supercapacitors and superconducting magnetic energy storage.

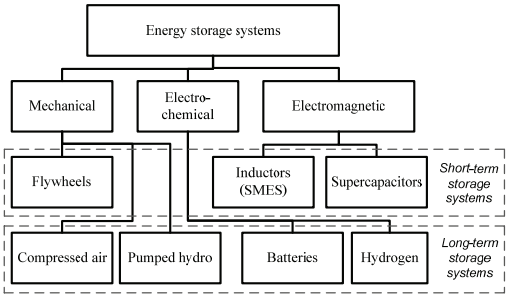

Fig. 2. Classification of energy storage technologies

Each technology has certain properties with regard to storage capacity, power, response time and cost. Grouping storage technologies with regard to storage capacity is relevant because it can be used to exclude those sizes not relevant in relation to renewable energy systems [3–7].

Different energy storage technologies have a wide range of energy release rates (discharge rates) that extend from seconds to many hours and days (Fig. 3) [7].

Based on their energy storage capacity, energy storages can be categorized as short-term and long-term

energy storages. Short-term storage systems include the supercapacitor energy storage (SCES), flywheel energy storage (FES) and superconducting magnetic energy storage (SMES) (Fig. 2). The long-term storage systems could be subdivided into pumped hydroelectric energy storage (PHES), compressed air energy storage (CAES), battery energy storage (BES), and hydrogen energy storage (HES) (Fig. 2).

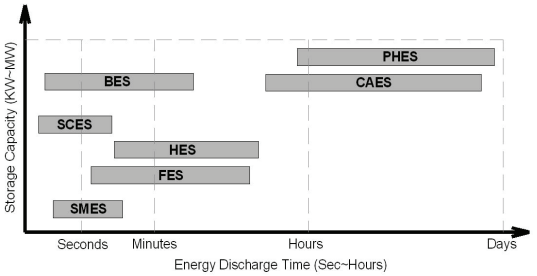

Fig. 3. Typical energy storage capacities and discharge times of different energy storage technologies

Renewable energy sources cannot be easily regulated or dispatched. Peak levels generated by a wind power plant may not coincide with the peak demand. In the case of instability of wind production, long-term storage technologies could be used. It allows wind farms to be used as a base load or enables an increase of predictability to nearly 100 % for a certain period of time. The time horizon could be days or weeks, depending on storage size and variations allowed.

General technical parameters of long-term energy storage technologies in the wind power context are summarized in Table 1 [6, 8].

Table 1. Comparison of long-term energy storages

Storage system	Capacity, MW	Efficiency, %	Technology
Pumped hydroelectric	100…1000	70 – 80	Mechanical
Compressed air	0.1…1000	75 – 85	Mechanical
Batteries	0.1 – 10	60 – 80	Electrochemical
Hydrogen	0.1 – 1	20 – 40	Electrochemical

Pumped hydroelectric energy storage

Pumped hydroelectric energy storage (PHES) has been in use worldwide for more than 70 years. These large-scale energy storage plants represent the most widespread energy storage technology in use today. Pumped hydro units operate on the principle of a hydro-electric power plant. However, their generator units serve also as motors. During off-peak hours surplus power is used to pump water from a lower reservoir to a higher level reservoir (Fig. 4) whilst pump/turbine (PT) operates as a pump and a motor/generator (MG) as a motor. At peak demand, water is released from the higher reservoir to turn the turbine and to produce electricity, and then the MG operates in the generating mode and the PT as a turbine [9].

PHS plants can produce a large amount of energy for sustained periods of time. In addition, these plants have round trip efficiencies in the range of 70 to 80 %. Their storage capacity is dependent only on the size of the reservoir. Thus, instead of having only a few hours of energy storage it could be days. The major drawback of this design is the significant area of land required to create the reservoirs and the elevation needed between them. Many of the desirable sites are already in use and other ones have encountered opposition from environmental groups. The environmental impact of large-scale PHS facilities is becoming more of an issue, especially where existing reservoirs are not available. Environmental considerations such as impacts on fisheries, recreation, water quality, aesthetics, and land use have sharply limited the further development of this technology [10]. There is, however, an alternative to avoid the environmental impacts of the large reservoirs by placing them underground. The use of underground PHS plants has proven to be technically feasible, but with the high costs associated with placing them underground none currently exist today [6, 11, 12].

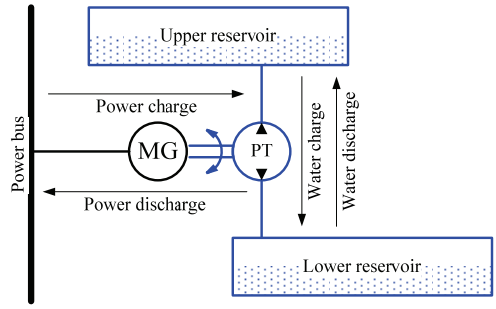

Fig. 4. Power and water flows in a PHS

Compressed air energy storage

Compressed air energy storage (CAES) systems use off peak electrical power generated from base load plants or renewable energy sources to compress air at high pressure (typically around 75 bar) into an underground reservoir or a surface vessel. Then, during times of high electrical demand this compressed air is combined with a fuel to drive a turbine generator set. The energy flow and air state changing of the CAES system is shown in Fig. 5 [9, 13].

With the CAES plant fuel consumption is reduced by two thirds as compared to the conventional units and the plant is capable of starting up within tens of minutes. It does not require a lengthy startup time like other spinning reserves, such as thermal units.

CAES plants require a large volume of compressed air to operate for extended periods of time. The principle of storing a gas underground is based on a proven method developed by the oil and gas industry. Typical ratings for a CAES system are in the range of 50–300 MW, with an efficiency of about 85 %.

The main key to a CAES system is that the reservoir has to be air tight and very large. Smaller units using above ground storage tanks are usually limited in their energy storage capacity to only a few hours [11]. In order to achieve a higher efficiency or remove the need for an

additional conventional fuel there are many new hybrid CAES technologies being developed. These new hybrid systems under development use supercapacitors, oil-hydraulics and pneumatics to increase the efficiency of the design [6, 12].

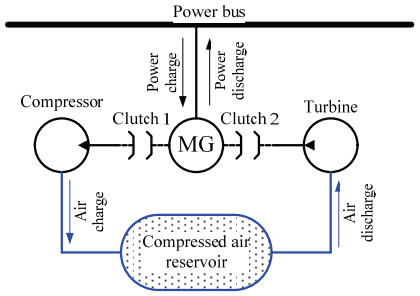

Fig. 5. CAES energy flow diagram

Battery energy storage

Batteries are one of the most cost-effective energy storage technologies available, with energy stored electrochemically [14]. Battery energy storage systems (BES) are modular, quiet, and non-polluting. They can be located almost anywhere and can be installed relatively quickly. Charging a battery causes reactions in the compounds, which then store the energy in a chemical form. Upon demand, reverse chemical reactions cause electricity to flow out of the battery and back to the grid, as shown in Fig. 6 [9]. Instead of two separate ac/dc converters for charging/discharging, a sole bidirectional converter may be utilized.

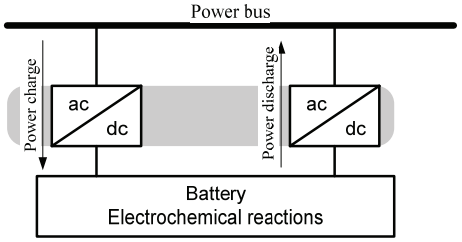

Fig. 6. Energy flows in a BESS

Fast response is one of the strong points of the battery technology: some batteries can respond to load changes in about 20 milliseconds. The efficiency of battery modules is in the range of 60–80 % [6, 11]. Batteries, however, have some very unique challenges. During an electrical charge and discharge cycle the temperature change in the battery must be controlled or it can affect the battery's life expectancy. The type of battery being used will determine how resistant it is to life degradation due to temperature.

Another major concern is the battery's life cycle. This is defined as the number of charge/discharge cycles that a battery can supply depending on the depth of discharge. The battery cycle application may require the BESS to charge and discharge multiple times a day. As long as the depth of discharge is relatively low the battery's cycle of life will remain unaffected. However, if the depth of discharge is large, then the battery's life cycle can be degraded. If the desired cycle of life of a battery is 20000 cycles, then the depth of discharge cannot be greater than approximately 15 % (Fig. 7) [6].

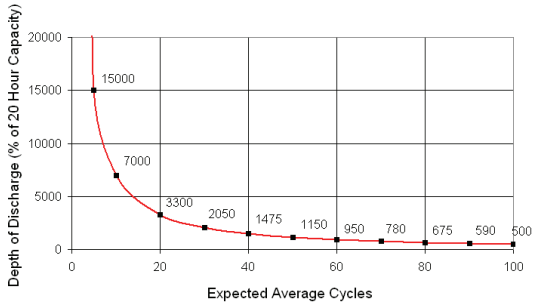

Fig. 7. Life cycle of batteries

The maximum discharge rate of the battery is also of concern because the battery can also be damaged by using too high discharge rates. Depending on the type of battery and its application, the discharge rate maybe its capacity divided by 4, 6 or even 10. This limits the available current in the battery for immediate use.

There are also environmental concerns related to battery storage due to toxic gas generation during battery charge/discharge. The disposal of hazardous materials presents some battery disposal problems [6, 14].

There are many new battery technologies that are being developed to store more energy, last longer, and cost less than the Lead-Acid battery. Some of these new battery technologies are lithium ion, Hydrogen Vanadium Redox, Regenesys Redox (both of the two also known as flow-through batteries), Sodium Sulfur, Nickel Metal Hydride, Nickel Cadmium, and Zinc Bromide.

Hydrogen energy storage

Hydrogen is one of the promising alternatives that can be used as an energy carrier. The universality of hydrogen implies that it can replace other fuels for stationary generating units for power generation in various industries. Having all the advantages of fossil fuels, hydrogen is free of harmful emissions when used with dosed amount of oxygen, thus reducing the greenhouse effect [15].

Essential elements of a hydrogen energy storage system comprise an electrolyzer unit which converts electrical energy input into hydrogen by decomposing water molecules, the hydrogen storage system itself and a hydrogen energy conversion system which converts the stored chemical energy in the hydrogen back to electrical energy (Fig. 8) [9]. The major application of the stored hydrogen is the electricity production by help of fuel cells. Water to hydrogen conversion efficiency is averaged at 65 % and fuel cell conversion efficiency is 65 – 70 % which ends up to 20 – 40 % overall system efficiency [6, 7, 11].

It must be kept in mind that in terms of storage, hydrogen is not used as a fuel, but as an energy carrier in a wider sense.

There are five basic methods for hydrogen storage:

- Compressed and stored in a pressure tank;
- Cooled to a liquid state and kept cold in an insulated tank;
- Physisorpted in carbon;
- Metal hydrides;
- Complex compounds.

In order to select the optimal integration method of hydrogen base energy storage in the wind power system the hydrogen storage capacity of each method has been compared. Fig. 9 [16] shows how much volume is needed to store a mass unit. As it can be seen, metal hydrides and complex compounds occupy a smaller volume to store the same amount of hydrogen; however, this method is not suitable for this application due to its high adsorption/absorption temperature. Both liquid hydrogen and compressed gas at high pressure were better candidates for suitable methods for this project, however, liquid hydrogen requires more expensive equipments and very low temperature.

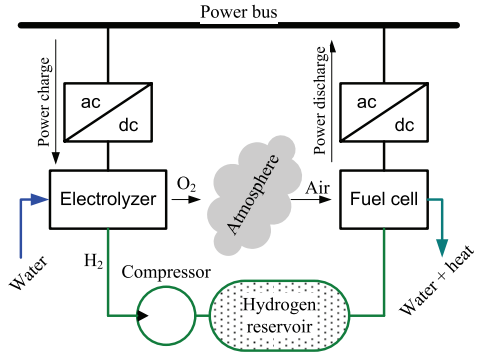

Fig. 8. Energy exchange processes of the hydrogen based energy storage

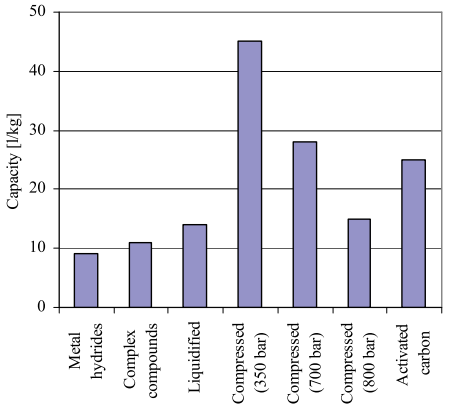

Fig. 9. Comparison of hydrogen storage capacity by different methods for the same occupied volume

There are various inefficiencies involved with storage and recovery of electrical energy via the use of hydrogen. Energy is consumed to place the hydrogen in storage. This varies with the different energy storage approaches, the efficiency of each method is summarised in Table 2 [16].

From Fig. 9 and Table 2 it can be seen that the energy lost to compress the gas is relatively low and therefore yields higher conversion efficiency. Activated carbon also has a high efficiency; however, a very low temperature is required during the process. Because the required energy storage time could be long due to the strong wind periods lasting extended periods of time, a low leak rate is critical to preventing additional dynamic energy loss.

It can be seen from Table 2 that the compressed gas method has a very low leakage rate compared to the other methods, high hydrogen capacity and dynamic energy efficiency [16].

Table 2. The energy required to place the hydrogen in storage varies between the various energy storage approaches and the corresponding efficiency

Hydrogen storage approaches		**Energy intensity (MJ/kg)**	**Efficiency**	**Leakage rate (/day), %**
Compressed gas	300 bar	0.915	0.92	0.000024
	700 bar	0.905	0.91	0.000033
Liquid		28-45	0.63-0.77	1
Activated carbon		8-10	0.92-0.93	0.2
Hydrides	Low temperature (<100˚C)	0.9-0.93	0.9-0.93	-
	High temperature (>300˚C)	0.79-0.83	0.79-0.83	-

Application example

Researchers at the Department of Electrical Drives and Power Electronics have introduced the concept of using hydrogen for compensating the instability of wind production. A typical configuration of a wind turbine connected to the transmission grid was formed by a set of wind generators electrically connected to a distribution grid, sharing one single infrastructure for access and control.

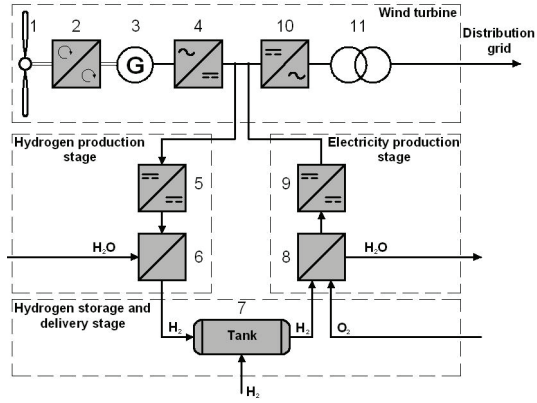

Fig. 10. Block diagram of the proposed hydrogen buffer for wind turbines: 1 – blades, 2 – gearbox, 3 – generator, 4 – rectifier, 5 – interface dc/dc converter for the electrolyzer, 6 – electrolyzer, 7 – hydrogen storage tank, 8 – fuel cell, 9 – interface dc/dc converter for the fuel cell, 10 – inverter, 11 – power transformer

As mentioned above, the hydrogen buffer used to stabilise unregulated energy production consists of hydrogen production, hydrogen storage and delivery as well as electricity production stages. In hydrogen production stage excess electrical energy from the wind generator is converted into chemical energy by using water electrolysis and stored in a tank. In electricity production stage during wind stills, hydrogen is converted into electrical energy by using a fuel cell. Combining energy storage and distributed generation results in a system which can produce controlled power [17].

A comparative SWOT analysis of storage technologies

In the analysis of the advantages and disadvantages of long-term energy storage possibilities, a SWOT (strengths, weaknesses, opportunities, threats) approach can be performed. Strengths and weaknesses are related to the present state-of-the-art, opportunities and threats with a view towards the possible future developments.

In Table 3 [7, 9, 11, 14, 18, 19] the storage technologies discussed are compared side by side. In terms of distributed storage it becomes clear that the main competitors to the hydrogen technology are the electrochemical batteries. The emerging technologies such as flow-through batteries may have characteristics similar to the hydrogen-based solutions; however, in the analysis of the material costs, the price and availability of the rare-earth metals and other resources to produce advanced batteries are to be discussed.

The future of hydrogen storage depends mostly on the improved efficiency of the energy conversion cycle, the storage media and advanced power electronic converters for grid interfacing. The recent developments in the converter design, especially regarding the implementation of the qZS topology make the hydrogen based energy storage systems attractive to many industrial applications [17]. Another advantage is the co-production of heat, which contributes to the popularity of the hydrogen based energy storages even in residential use.

Conclusions

The quality of wind energy may be improved by introducing energy storage. Ensuring availability and reducing variability are two strongly coupled ways of looking at improvements. Making energy more available means making it more predictable, reliable and controllable. The prospect of energy storage is to remove fluctuations on shorter timescales (seconds to hours). A good idea is to implement hybrid solutions, where long-term deviations are compensated by fuel cell systems and shorter fluctuations by supercapacitors [20].

Utilization of energy storage systems will be a major step in the solution to the use of renewable energy along with the current issues of reliability, stability, and power quality. A new wind power design methodology that identifies the optimal use of hydrogen energy storage in order to balance the electricity production to load demand has been proposed. Different hydrogen storage methods were carefully compared and the compressed gas approach was chosen as the best solution for this study due to its relatively high conversion efficiency, easy operation and low leakage rate.

Ultimately, the SWOT analysis revealed some advantages and disadvantages of hydrogen as compared to the other long-term storage possibilities. Though battery systems are preferred in the present situation, the hydrogen and fuel cells are likely to increase their share with a faster or at least equal pace.

Table 3. Comparative SWOT analysis of long-term storage possibilities

	Strengths	Weaknesses	Opportunities	Threats
CAES	High capacity. Low cost per kWh. Minor needs for power electronic converters.	Need for underground cavities. Need for fuel.	Can prospectively be adopted for distributed storage.	Popularity related to thermal power plants.
PHES	High capacity. Low cost per kWh. Minor needs for power electronic converters.	Centralised storage. Geographical restrictions.	Can be used for off-shore wind parks and with lower reservoir under seabed.	Can become obsolete when distributed storage preferred.
BES	Distributed storage. Good configurability.	High investment costs. Cycle life. Temperature dependent.	Emerging technologies.	Constant development phase complicates selection. Raw materials limited.
Hydrogen	Distributed storage. Other uses for produced hydrogen. Minor environmental issues.	Low efficiency. High investment costs. Need for power electronics and control. Need for stable load.	Market penetration. Perspective nanotube storage media. Dedicated converters.	Maturing battery technologies. EMI issues related to the use of power electronics converters.

Acknowledgements

This research work has been supported by Estonian Ministry of Education and Research (Project SF0140016s11), Estonian Science Foundation (Grant ETF8538) and Estonian Archimedes Foundation (project „Doctoral School of Energy and Geotechnology-II“).

References

1. **Andrijanovitš A., Egorov M., Lehtla M., Vinnikov D.** New Method for Stabilization of Wind Power Generation Using an Energy Storage Technology // Agronomy Research. – Biosystems Engineering. – Tartu, 2010. – Vol. 1. – No. 8. – P. 12–24.

2. **Andrijanovitš A., Vinnikov D.** Multiport DC/DC Converters for Interfacing of Hydrogen Buffer with Wind Turbine // 9th International Symposium "Topical Problems in the Field of Electrical and Power Engineering". – Doctoral School of Energy and Geotechnology. – Tallinn: Elektriajam, 2010. – P. 95–99.
3. **Nguyen T. D., Tseng K. J., Zhang S., Zhang C.** A Flywheel Cell for Energy Storage System // Proceedings of the IEEE, 2008. – P. 214–219.
4. **Boyes J. D., Clark N. H.** Technologies for Energy Storage. Flywheels and Super Conducting Magnetic Energy Storage // Proceedings of the IEEE, 2000. – P. 1548–1550.
5. **Rausmussen C. N.** Improving Wind Power Quality with Energy Storage // Proceedings of the IEEE, 2009. – P. 1–7.
6. **Smith S. C., Sen P. K., Kroposki B.** Advancement of Energy Storage Devices and Applications in Electrical Power System // Proceedings of the IEEE, 2008.
7. **Nigim K., Reiser H.** Energy Storage for Renewable Energy Combined Heat, Power and Hydrogen Fuel ($CHPH_2$) Infrastructure // Proceedings of the Electrical Power and Energy Conference. – IEEE, 2009.
8. **Lund P. D., Paatero J. V.** Energy Storage Options for Improving Wind Power Quality // Nordic Wind Power Conference. – Espoo, 2006.
9. **Faias S., Santos P., Sousa J., Castro R.** An Overview on Short and Long–Term Response Energy Storage Devices for Power Systems Applications // Proceedings of the International Conference On Renewable Energies and Power Quality (ICREPQ'08), 2008. – P. 1–6.
10. **Daneshi H., Srivastava A. K., Daneshi A.** Generation Scheduling with Integration of Wind Power and Compressed Air Energy Storage // Proceedings of the IEEE, 2010.
11. **Choi S. S., Tseng K. J., Vilathgamuwa D. M., Nguyen T. D.** Energy Storage Systems in Distributed Generation Schemes // Proceedings of the IEEE, 2008.
12. **Schainker R. B.** Executive Overview: Energy Storage Options for a Sustainable Energy Future // Proceedings of the IEEE.
13. **Vongmanee V., Monyakul V.** A New Concept of Small–compressed Air Energy Storage System Integrated with Induction Generator // Proceedings of the IEEE, 2008. – P. 866–871.
14. **Ribeiro P. F., Johnson B. K., Crow M. L., Arsoy A., Liu Y.** Energy Storage Systems for Advanced Power Applications // Proceedings of the IEEE, 2001. – Vol. 89. – No. 12. – P. 1744–1756.
15. **Andrijanovitš A., Egorov M., Lehtla M., Vinnikov D.** A Hydrogen Technology as Buffer for Stabilization of Wind Power Generation // 8th International Symposium "Topical Problems in the Field of Electrical and Power Engineering". – Tallinn: Elektriajam, 2010. – P. 62–70.
16. **Yu S., Mays T. J., Dunn R. W.** A New Methodology for Designing Hydrogen Energy Storage in Wind Power Systems to Balance Generation and Demand // Proceedings of the IEEE, 2009.
17. **Andrijanovitš A., Vinnikov D.** New Bidirectional Multiport DC/DC Converter for Interfacing of Hydrogen Buffer with Wind Turbines // 10th International Symposium "Topical Problems in the Field of Electrical and Power Engineering". – Tallinn: Elektriajam, 2011. – P. 85–90.
18. **Andriukaitis D., Anilionis R.** Thermal Oxidation Process Influence to the Three–Dimensional Integrated Structures // Electronics and Electrical Engineering. – Kaunas: Technologija, 2009. – No. 8(96). – P. 81–84.
19. **Balaišis P., Eidukas D., Gužauskas R., Valinevičius A.** Modeling of Efficiency of Dynamic Electronic Systems // Electronics and Electrical Engineering. – Kaunas: Technologija, 2008. – No. 6(86). – P. 55–59.
20. **Onar O. C., Uzunoglu M., Alam M. S.** Modeling, control and simulation of an autonomous wind turbine/photovoltaic/fuel cell/ultra–capacitor hybrid power system // Journal of Power Sources, 2008. – Vol. 185. – P. 1273–1283.

Received 2011 02 06
Accepted after revision 2011 11 17

A. Andrijanovits, H. Hoimoja, D. Vinnikov. Comparative Review of Long-Term Energy Storage Technologies for Renewable Energy Systems // Electronics and Electrical Engineering. – Kaunas: Technologija, 2012. – No. 2(118). – P. 21–26.

Sustainability of electric power systems will involve very large use of renewable energy sources for power production. Wind power is one of the cleanest and safest of all the renewable methods of generating electricity. However, wind power fluctuations have adverse impacts on power quality, such as local voltage and system frequency. Energy storage devices will be needed at different locations in the power system, to store the surplus of power from renewable sources for later use during non-generation time periods or low power generation time periods. This paper will give an overview of different storage technologies. Ill. 10, bibl. 20, tabl. 3 (in English; abstracts in English and Lithuanian).

A. Andrijanovits, H. Hoimoja, D. Vinnikov. Ilgalaikio energijos kaupimo technologijų taikymo atsinaujinančioms energijos sistemoms lyginamoji analizė // Elektronika ir elektrotechnika. – Kaunas: Technologija, 2012. – Nr. 2(118). – P. 21–26.

Energetikos sistemų išsilaikomumui užtikrinti gaminant energiją reikės naudoti daug atsinaujinančių energijos šaltinių. Vėjo energija yra vienas iš švariausių ir saugiausių atsinaujinančių elektros energijos šaltinių. Tačiau vėjo energijos fliuktuacijos turi neigiamą poveikį energijos kokybei (įtampai ir sistemos dažniui). Energijos kaupimo įtaisai bus reikalingi skirtingose energijos sistemos vietose perteklinei energijai iš atsinaujinančių šaltinių kaupti ir vėliau jai panaudoti. Pateikiama skirtingų kaupimo technologijų apžvalga. Il. 10, bibl. 20, lent. 3 (anglų kalba; santraukos anglų ir lietuvių k.).

[PAPER-II] **Andrijanovitš, A.**; Egorov, M.; Lehtla, M.; Vinnikov, D. New Method for Stabilization of Wind Power Generation Using an Energy Storage Technology. Agronomy Research, 8(S1), pp. 12 – 24, 2010.

New Method for Stabilization of Wind Power Generation Using Energy Storage Technology

A. Andrijanovitš, M. Egorov, M. Lehtla and D. Vinnikov

Department of Electrical Drives and Power Electronics,
Tallinn University of Technology, Ehitajate tee 5, EE19086 Tallinn, Estonia;
e-mail: sergejeva84@hot.ee; mikhail.egorov@ttu.ee; mlehtla@cc.ttu.ee; dm.vin@mail.ee

Abstract. Wind power appears to be one of the most perspective and widespread renewable energy sources in Estonia. However, wind is difficult to forecast. This complicates production planning and parallel operation with compensating power plants, allowing periods of excess energy and lack of energy to occur. This paper proposes a new energy storage technology to compensate unstable operation of windmills. This is based on a hydrogen buffer, which accumulates excess energy from windmills and transfers it to the DC-link of windmills converter. As all components of the hydrogen buffer are electrically connected to the DC-link, there are three main stages. The first stage is hydrogen production, which is realized with the help of water electrolysis in periods of excess energy. Interfacing is carried out with electrical components, such as DC/DC converter with a step-down isolation transformer. The second stage is hydrogen storage and delivery. The produced hydrogen is accumulated in a tank locally or in industrial gas storage. Hydrogen may be mixed with natural gas and distributed to natural gas pipelines. The third stage is electricity production. The stored energy is used to produce electrical energy during the absence of wind or in conditions of a weak wind. Hydrogen is converted into electricity by a fuel cell. Interfacing is carried out using electrical components with the help of DC/DC converter with a step-up isolation transformer. The paper represents the structure of the proposed hydrogen-based energy buffer and reviews its main elements.

Key words: Renewable energy storage, electrolysis, hydrogen buffer, fuel cell

INTRODUCTION

Sustainability and efficient use of energy resources is an urgent issue today. Reasons lie not only in the growth of demand and production, but also in the present level of resource exploitation leading to exhaustion of energy resources and related environmental impacts. The sustainable use of energy requires applications and methods that could increase efficiency. This is especially important in converter applications.

Traditional methods of energy conversion in power plants have some disadvantages, such as impact on the environment. Some new unconventional methods of energy generation have less impact on the environment. The cost of power generation is one of the main criteria when choosing a method for its production. Today, traditional technologies seem to be cheaper than the alternative

ones. Energy produced from renewable sources lacks the cost of fuel, however, it has higher capital costs.

The predicted costs and cost price of electricity production based on renewable sources have been given in Table 1 (Solovjev, 2006). The use of renewable energy and storage offers prospects of significant decrease in fossil fuel extraction and accompanying environmental pollution (Andrijanovitš, 2009).

Table 1. Prediction costs and cost price of electricity production

Renewable source	Specific capital cost, $ kW^{-1}			Cost of production, cent kWh^{-1}		
	2005	2030	2050	2005	2030	2050
Onshore wind farm	900–1,100	800–900	750–900	4.2–2.2	3.6–2.1	3.5–2.1
Offshore wind farm	1,500–2,500	1,500–,1900	1,400–1,800	6.6–21.7	6.2–18.4	6–18
Solar power	3750–3850	1,400–1,500	1,000–1,100	17.8–54.2	7–32.5	6–29
Fuel cell	3,000–10,000	500–1,000	300–500	2–3	2–3	2–3

The use of wind energy can be considered technically and economically feasible only at average wind speed 4.5 m s^{-1} (Risthein, 2007). Average annual wind speed and large wind parks in Estonia, (Fig. 1), (Risthein, 2007).

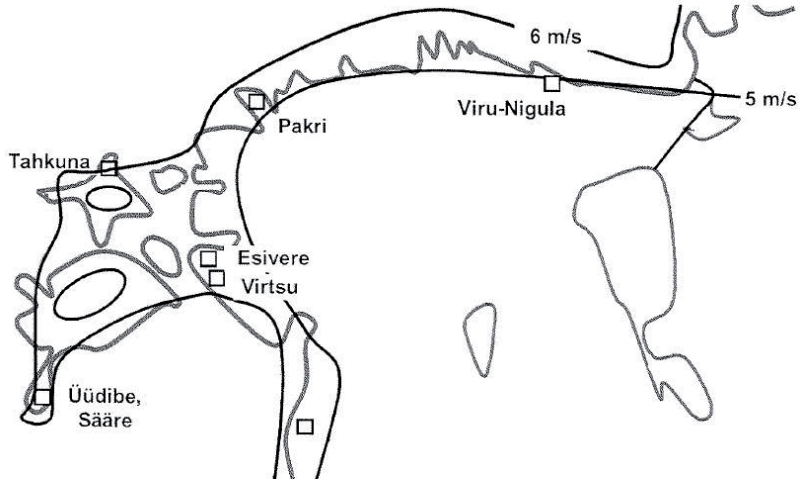

Fig. 1. Average annual wind speed in Estonia.

Unpredictable winds make it difficult to plan production (Fig. 2), complicating parallel operation with other power plants, intended for compensating the instability of wind power production. Due to unpredictable wind the difficulty in forecasting periods of excess energy as well as lack of energy occur (Andrijanovitš et al., 2010).

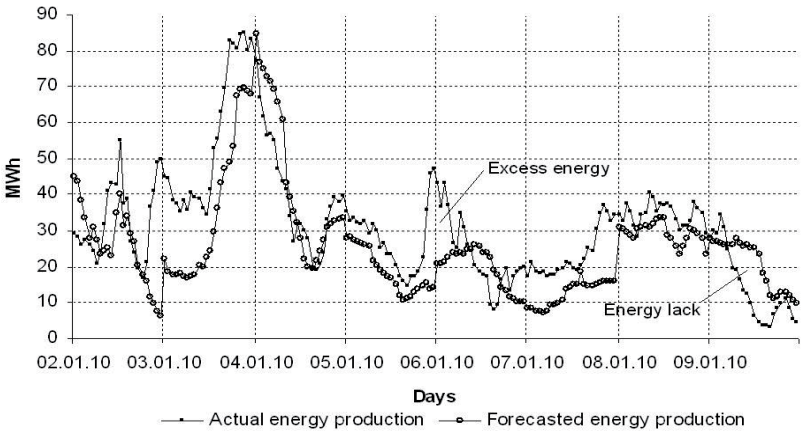

Fig. 2. An example of unpredictable energy production by Estonian wind farms.

HYDROGEN TECHNOLOGY AS A BUFFER FOR STABILIZATION OF WIND POWER GENERATION

The Department of Electrical Drives and Power Electronics has introduced the concept of using hydrogen for compensating the instability of wind production. A typical configuration of a wind farm connected to the transmission grid is formed by the set of wind generators, electrically connected through a medium voltage network, sharing one single infrastructure for access and control. A block diagram of the hydrogen buffer system for the stabilization of wind power generation is presented in Fig. 3 (Andrijanovitš et al., 2010).

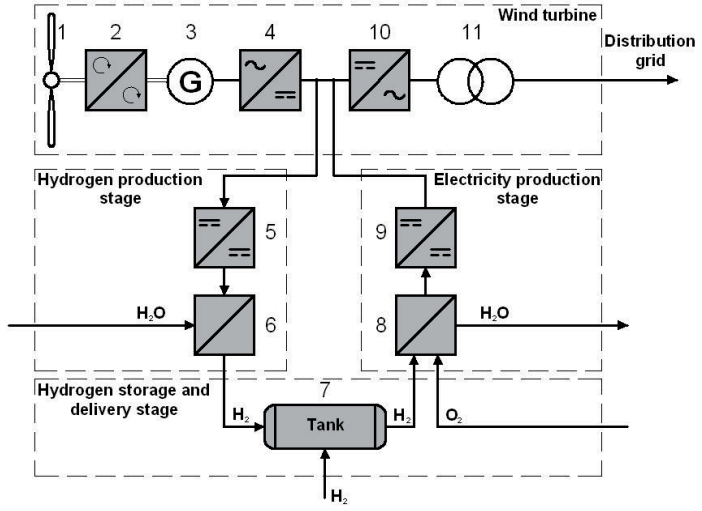

Fig. 3. Block diagram of the proposed hydrogen buffer: 1 – Blades; 2 - Gearbox; 3 - Generator; 4 – Rectifier; 5 - Interface DC/DC converter, 6 – Electrolyser; 7 - Storage tank; 8 - Fuel cell; 9 - Interface DC/DC converter; 10 – Inverter; 11 - Transformer.

Because of unregulated energy production (Fig. 2), the fluctuation of wind speed leads to a fluctuating output. It means that at some moments excess energy and energy lack appear. As mentioned above, a hydrogen buffer is used to stabilize unregulated energy production, consisting of the following main components:

1. Hydrogen production stage,
2. Hydrogen storage and delivery stage,
3. Electricity production stage.

HYDROGEN PRODUCTION STAGE

In periods of excess energy, the hydrogen generation system is connected to the internal grid. In this stage, electrical energy from the wind generator is converted into chemical energy by using water electrolysis. Because of low input voltage of an electrolyser it is necessary to decrease high output voltage of the grid with the help of interface DC/DC converter with a step-down isolation transformer.

The hydrogen generation system consists of two main parts:

1. Interface DC/DC converter with a step-down isolation transformer, which allows interfacing the high voltage DC output of converter with a low voltage input of the electrolyser,

2. Electrolyser, allowing electrical energy storage and producing hydrogen from water electrolysis using excess electricity from the wind generator.

There are three basic types of electrolysers: alkaline, proton exchange membrane (PEM) and high-temperature solid oxide (Fig. 4). Common characteristics of electrolysers are shown in Table 2 (Gamburg et al., 1989, Eg & G technical services Inc., 2004, Egorov et al., 2008). Advantages and disadvantages of different types of electrolysers are shown in Table 3.

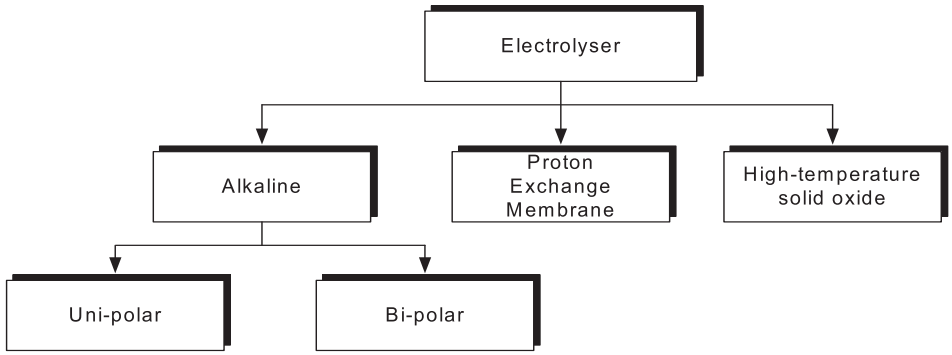

Fig. 4. General classification of electrolysers.

Alkaline electrolysers could be subdivided into unipolar or bipolar electrolysers (Fig. 4). The unipolar design is composed of a series of electrodes, anodes and cathodes alternatively suspended in a tank, filled with a 20–30% solution of electrolyte. In this design, each of the cells is connected in parallel. The bipolar electrolysers have alternating layers of electrodes and separation diaphragms, which are clamped together. The cells are connected in series and can

result in higher stack voltages. Since the cells are relatively thin, the overall stack can be considerably smaller in size than the unipolar design (Kroposki et al., 2006).

Table 2. Common characteristics of electrolysers

Characteristic	Uni–polar	Bi–polar	Proton Exchange membrane	High–temperature solid oxide
Current density, A $(cm^2)^{-1}$	0.1–0.2	0.2–0.4	0.4	1.1–2.0
Voltage cell, V	2.04–2.14	1.87–2.10	1.65–1.85	1.78–1.85
Production, $(m^3\ H_2)\ h^{-1}$	Up to 80,000	Up to 200,000	Up to 25,000	Up to 25,000
Energy demand, $(\kappa W \cdot h^{-1})\ (m^3)^{-1}$	5.0	4.3–4.6	4.5	3.9–4.0
Temperature, °C	50–100	50–100	80–100	120
Pressure, MPa	0.01–0.10	0.01–0.10	Up to 3.0	0.2–6.0
Efficiency, %	75–90	75–90	80–90	80–90

In the PEM electrolysers the electrolyte is contained in a thin, solid ion conducting membrane as opposed to the aqueous solution in the alkaline electrolysers. This allows the H+ ion to transfer from the anode side of the membrane to the cathode side and serves to separate the hydrogen and oxygen gasses. Oxygen is produced on the anode side and hydrogen is produced on the cathode side. PEM electrolysers use the bipolar design and can be made to operate at high differential pressure across the membrane (Kroposki et al., 2006).

High-temperature electrolysis (HTE) is different from the conventional electrolytic process. Some of the energy needed to split water is provided as thermal energy instead of electricity. It occurs because conventional electrolysis usually operates at temperatures below 100ºC. HTE generally refers to an electrolytic process operating at temperatures above 100ºC. As HTE curtails the relatively inefficient step of conversion of heat to electricity, it is more efficient than the conventional electrolysis (Sadhankar et al., 2006). In a HTE system using nuclear energy, a nuclear reactor supplies thermal energy that both generates electricity and heats up the steam needed for electrolysis. The HTE system is supported by nuclear process heat and electricity has the potential to produce hydrogen with overall system efficiency near that of the thermochemical processes. HTE cells consist of two porous electrodes separated by a dense ceramic electrolyte. HTE cells with oxygen ion conducting ceramic as electrolyte are often called solid oxide electrolysis cells (SOECs).

Table 3. Advantages and disadvantages of electrolysis

Type of electrolysis	Advantages	Disadvantages
Alkaline unipolar	this design is extremely simple to manufacture and repair	usually operates at lower current densities and lower temperatures
Alkaline bipolar	reduced stack footprints and higher current densities as well as the ability to produce higher pressure gas	can not be repaired without servicing the entire stack although this is rare
Proton exchange membrane	requires no liquid electrolyte, which simplifies the design significantly, the electrolyte is an acidic polymer membrane. PEM electrolysers can potentially be designed for operating pressures up to several hundred bar, and are suited for both stationary and mobile applications, increased safety due to the absence of KOH electrolytes, a more compact design due to higher densities, and higher operating pressures	limited lifetime of the membranes, membranes must use very pure deionized water, otherwise, they will accumulate cations that displace protons and increase cell resistance over time
High-temperature solid oxide	can operate at significantly higher overall process efficiencies than regular low-temperature electrolysers	requires large amounts of energy and heat, it is working with a nuclear power plant

Today's most widespread industrial electrolysers are alkaline and proton exchange membrane. These two types of electrolysers allow higher operating pressures, higher current density and low applied voltage to the cell.

ELECTRICITY PRODUCTION STAGE

In order to stabilize energy production, during the absence of wind or in conditions of a light wind, stored hydrogen could be reused. In this stage, hydrogen is converted into electrical energy by using a fuel cell (FC). The fuel cell takes the hydrogen from the tanks to generate electricity, plus water and heat as byproducts. The produced electrical energy is in DC form, thus a power converter is required to change DC voltage level required by the grid. Because of low output voltage of a fuel cell it is necessary to boost it with the help of the interface DC/DC converter with a step-up isolation transformer. A hydrogen-powered fuel cell system consists of two main parts:

1. Interface DC/DC converter with a step-up isolation transformer, which allows interfacing a low voltage DC output of fuel cell with a high voltage DC-link of the converter,
2. Fuel cell allows producing chemical energy into electrical energy in order to stabilize energy production of wind generator.

General classification of modern fuel cells (Fig. 5).

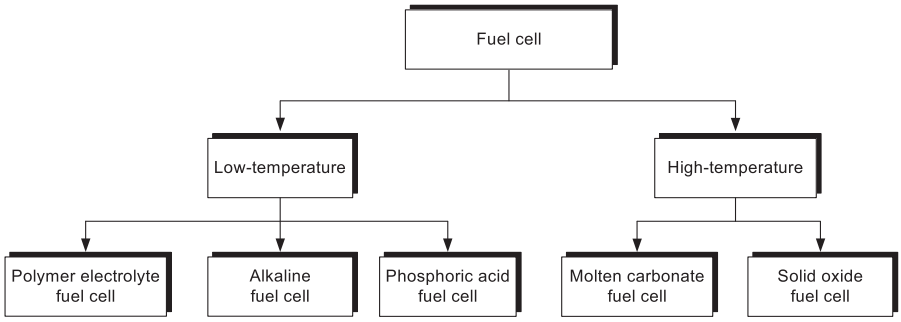

Fig. 5. General classification of fuel cells.

The electrolyte in polymer electrolyte fuel cell is an ion exchange membrane (fluorinated sulfonic acid polymer or other similar polymer), which is an excellent proton conductor. The only liquid in this fuel cell is water, thus the corrosion problems are minimal. Typically, carbon electrodes with platinum electrocatalyst are used for both anode and cathode and with either carbon or metal interconnects. Water management in the membrane is critical for efficient performance, the fuel cell must operate under conditions where the byproduct water does not evaporate faster than it is produced because the membrane must be hydrated. Higher catalyst loading than used in phosphoric acid fuel cell is required for both the anode and the cathode (Eg & G technical services Inc., 2004).

Alkaline fuel cells are one of the most developed technologies and have been used to provide power and drinking water in space missions, including the US Space Shuttle. The design of an alkaline fuel cell is similar to a proton exchange membrane (PEM) cell but with an aqueous solution or stabilized matrix of potassium hydroxide as the electrolyte. Alkaline cells operate at a similar temperature to PEM cells (around 80°C) and therefore start quickly, but their power density is around ten times lower than the power density of a PEM cell. As a result they are too bulky for using in car engines. Nevertheless, they are the cheapest type of a fuel cell to manufacture, so it is possible that they could be used in small stationary power generation units. Like the PEM cell, alkaline fuel cells are extremely sensitive to carbon monoxide and other impurities that would contaminate the catalyst (Eg & G technical services Inc., 2004).

In the phosphoric acid fuel cells, typically operating at 150 to 220°C, the concentrated phosphoric acid (close to 100%) is used as the electrolyte. The relative stability of the concentrated phosphoric acid is high compared to other common acids. Consequently the phosphoric acid fuel cell (PAFC) is capable of operating at the high end of the acid temperature range (100 to 220°C). The anode and cathode reactions are the same as in the PEM fuel cell with the cathode reaction occurring at a faster rate due to the higher operating temperature (Eg & G technical services Inc., 2004).

The electrolyte in the molten carbonate fuel cells is usually a combination of alkali carbonates, which is retained in a ceramic matrix. The fuel cell operates at 600 to 700°C where the alkaline carbonates form a highly conductive molten salt, with carbonate ions providing ionic conduction. At the high operating temperatures in MCFCs, Ni (anode) and nickel oxide (cathode) are adequate to promote a

reaction. Noble metals are not required for operation, and many common hydrocarbon fuels can be reformed internally. The focus of MCFC development has been on larger stationary and marine applications, where the relatively large size and weight of MCFC and slow start-up time are not an issue (Eg & G technical services Inc., 2004).

In the solid oxide fuel cells, the electrolyte is a solid, nonporous metal oxide. The cell operates at 600-1,000°C where ionic conduction by oxygen ions takes place. The limited conductivity of solid electrolytes required cell operation at around 1,000°C, but more recently thin electrolyte cells with improved cathodes have allowed the reduction of operating temperatures to 650-850°C. SOFCs are considered for a wide range of applications, including stationary power generation, mobile power, auxiliary power for vehicles, and specialty applications (Eg & G technical services Inc., 2004).

In accordance with the classification of fuel cells (Fig. 5), common characteristics of fuel cells are shown in Table 4, their advantages and disadvantages (Eg & G technical services Inc., 2004, Matthew M., 2008) are given in Table 5.

Table 4. Common characteristics of fuel cells

Type of fuel cell	Electrolyte	Qualified power	Operating temperature	Electrical efficiency
Proton exchange membrane	polymer membrane	100 W to 500 kW	30–100°C	cell: 50–70% system: 30–50%
Alkaline	aqueous alkaline solution	10 kW to 100 kW	under 80°C	cell: 60–70% system: 62%
Phosphoric acid	molten phosphoric acid	up to 10 MW	150–200°C	cell: 55% system: 40%
Molten carbonate	molten alkaline carbonate	100 MW	600–700°C	cell: 55% system: 47%
Solid oxide	O_2–conducting ceramic oxide	up to 100 MW	850–1,100°C	cell: 60–65% system: 55–60%

Table 5. Advantages and disadvantages of a fuel cell

Type of FC	Application	Advantages	Limitations
Proton exchange membrane	cars, buses, portable power supplies, medium to large-scale stationary power generation	compact design; relatively long operating life; adapted by major automakers; offers quick start-up, low temperature operation	high manufacturing costs, needs pure hydrogen; heavy auxiliary equipment and complex heat and water management
Alkaline	space (NASA), terrestrial transport	low manufacturing and operation costs; does not need heavy compressor, fast cathode kinetics	large size; needs pure hydrogen and oxygen; use of corrosive liquid electrolyte
Phosphoric acid	medium to large-scale power generation	commercially available; heat for co-generation	low efficiency, limited service life, expensive catalyst

Molten carbonate	large-scale power generation	highly efficient; utilizes heat for co-generation	electrolyte instability; limited service life
Solid oxide	medium to large-scale power generation	high efficiency, takes natural gas directly, no reformer needed. Operates at 60% efficiency; co-generation	high operating temp; rare metals, high manufacturing costs, oxidation issues; low specific power

Technical properties of fuel cell (Table 6).

Table 6. Fuel cell technical properties

Characteristics of fuel cell	Polymer electrolyte	Alkaline	Phosphoric acid	Molten carbonate	Solid oxide
Current density, A $(cm^2)^{-1}$	0.1–0.9	0.1–0.9	0.1–0.9	0.1–0.9	0.1–0.9
Voltage cell, V	0.8–0.6	0.8–0.6	0.8–0.6	0.8–0.6	0.8–0.6
Power density, W $(cm^2)^{-1}$	0.35–0.7	0.1–0.3	~0.14	0.1–0.12	0.15–0.7
H_2 consumption, $(cm^3\ H_2)\ (min\ A)^{-1}$	7.0	7.0	7.0	7.0	7.0
O_2 consumption, $(cm^3\ O_2)\ (min\ A)^{-1}$	3.5	3.5	3.5	3.5	3.5
Pressure, bar	1–2	1	1	1–10	1

Having considered all the fuel cells explained the authors conclude that there are several perspective types of fuel cells that can be used. First a low-temperature fuel cell that is an alkaline fuel cell with a high efficiency and low oxygen reduction reaction losses. Second, a high-temperature fuel cell, a solid oxide and molten carbonate fuel cell.

HYDROGEN STORAGE

In an ideal system, supply will match demand. Energy storage enables the supply to be shifted to meet the demand. Electricity can be drawn from the primary supply during periods of excess availability, stored and then returned during periods of excess demand. Correct sizing of the storage should allow the generation plant to operate closer to its optimal efficiency, making thus better economic use of the existing assets. According to the International Energy Agency classification (Yartys & Lototsky, 2004), hydrogen storage methods can be divided into two groups:

The first group includes physical methods which use physical processes (compression or liquefaction) to compact hydrogen gas. Hydrogen being stored by physical methods contains H_2 molecules, which do not interact with the storage medium. The following physical methods of hydrogen storage are available:

1. Compressed hydrogen gas,
2. Liquid hydrogen: stationary and mobile cryogenic reservoirs.

The second group includes chemical (or physical-chemical) methods that provide hydrogen storage using physical chemical processes of its interaction with some materials. The methods are characterized by an essential interaction of molecular or atomic hydrogen with the storage environment. The chemical methods of hydrogen storage include:

1. Adsorption,
2. Bulk absorption in solids (metal hydrides),
3. Chemical interaction.

Comparison of hydrogen storage methods in accordance with the above mentioned methods (Tables 7, 8), (Yartys & Lototsky, 2004).

Table 7. Comparison of physical hydrogen storage methods

Group	Subgroup	Method	Storage conditions		Storage performances	
			P, bar	T,ºC	Volume density, g $(dm^3)^{-1}$	Energy consumption, %
Physical	compressed gas storage	steel cylinders	200	20	17.8	9
		commercial composite cylinders	250	20	22.3	10
		advanced composite cylinders	690	20	29.7	12.5
		glass micro–spheres	350–630	200–400	20	25
	cryogenic (LH_2)		1	–252	71	27.9

Table 8. Comparison of chemical hydrogen storage methods

Group	Subgroup	Method	Storage conditions		Storage performances	
			P, bar	T,ºC	Volume density, g $(dm^3)^{-1}$	Energy consumption, %
Chemical	cryo–adsorption		2–40	–208…–195	15–30	8.1
	metal hydrides	'low–temperature' (20–100ºC)	0.01–20	20–100	90–100 / 60–70	10.4
		'high–temperature' (250–400ºC)	1–20	250–350	90–100 / 60–70	20.6

	complex hydrides (alanates)	1–20	125–165	30	13.4
organic hydrides		10–100	300–400	70–100	28

From the data (Tables 7, 8), it can be concluded that each method has its advantages and disadvantages and none of the specific hydrogen storage methods is superior to the remaining alternative ones. Cost, volume, weight and performance should be considered together in selecting an optimal storage method that suits the specific requirements.

HYDROGEN DELIVERY

Between the two ends of the economic chain, hydrogen has to be packaged by compression or liquefaction to become a commodity. In the transportation, hydrogen has to be produced, packaged, transported, stored, transferred to cars, then stored and transported again before it is finally admitted to fuel cells.

There are two possibilities of hydrogen delivery (Leighty, 2006):

1. Road delivery,
2. Pipeline delivery.

Because of the low density of the gaseous energy carrier, transport of pressurized or liquid hydrogen is extremely inefficient. Forty-ton trucks can carry only 350 kg of hydrogen at 200 bars in the gaseous or 3,500 kg in the liquid state (Leighty et al., 2006).

The energy required to deliver the gas is part of the production costs. Parasitic energy losses reduce the amount of available energy. Hydrogen transport by pipelines has to compete with electricity transport by wires.

Design and construction of large, long-distance, high pressure gaseous hydrogen pipelines and conventional natural gas (NG) transmission lines are similar. Four technological aspects differentiate the gaseous hydrogen (GH_2) line from the NG line and need to be addressed for the concept to be attractive to industry (Leighty et al., 2006):

1. The volumetric energy density of hydrogen is one third of that of methane,
2. High pipeline utilization is critical for economic feasibility,
3. Hydrogen embrittlement of pipeline steel must be prevented and controlled,
4. Compression is very costly.

Most of the analyses show that pipelining GH_2 costs approximately 1.3 to 1.8 times more per unit energy-distance than NG, because of these four factors. Pipelines are very expensive to design and construct, which is why they must have high utilization to justify the initial capital cost.

CONCLUSIONS AND FUTURE WORK

This paper is devoted to study of a new concept of using hydrogen for compensating the instability of wind power production. This concept has been considered in three main stages:

1. Hydrogen production stage allows excess energy of a wind power plant to be stored,

2. Hydrogen storage technologies, safety, automation and transportation system have to be developed in the future,

3. At moments when wind is low or absent the stage of electricity production allows wind power operation to be stabilized. Because all of the components of hydrogen buffer require DC power supply, interface converters were implemented.

In terms of ecology, the proposed method provides perspectives of significant decrease in fossil fuel extraction and accompanying environmental pollution. As Estonia depends on foreign energy supplies, the use of our own considerable wind potential will promote the promising field of energy development.

ACKNOWLEDGEMENTS. This research work has been supported by the Estonian Science Foundation (Grant ETF7425) and Archimedes Foundation (Project DAR8130 'Doctoral School of Energy and Geotechnology II') and base financing (Grant BF123) from Tallinn University of Technology.

REFERENCES

Solovjev, A. A. 2006. *Renewable power sources: Materials of scientific school.* Geographical faculty MSU, Moskva, 158 pp. (in Russian).

Andrijanovitš, A., Vinnikov, D., Hõimoja, H. & Klytta, M. 2009. Comparison of Interface Converter Topologies for Small– or Medium–Power Wind–Hydrogen Systems. In: Lahtmets R. *6th International Symposium 'Topical Problems in the Field of Electrical and Power Engineering'*, Doctoral School of Energy and Geotechnology. Estonian Society of Moritz Hermann Jacobi, Tallinn, Estonia, pp. 122–127.

Risthein, E. 2007. *Introduction to the power engineering*. Tallinn book printers. Tallinn, Estonia, 260 pp. (in Estonian).

Andrijanovitš, A., Egorov, M., Lehtla, M. & Vinnikov, D. 2010. A hydrogen technology as buffer for stabilization of wind power generation. In: Lahtmets R. *8th International Symposium 'Topical Problems in the Field of Electrical and Power Engineering'*, Doctoral School of Energy and Geotechnology, Elektriajam, Tallinn, Estonia, pp. 62–70.

Egorov, M., Vinnikov, D., Vodovozov, V. 2008. Электролиз как способ аккумулирования избыточной энергии ветроэнергетических установок. Редактор Т.І. Майбора. *Силовая электроника и энергоэффективность СЭЭ–2008*. Поліграфична дільниця Інституту електродинамики НАН України, м. Київ-57. Україна, с. 42–47.

Gamburg, D. Y., Semenov, V. P., Dubovkin, N. F., Smirnova, L. N. 1989. *Hydrogen. Properties, obtaining, storage, delivery, application*. Himija, Moskva, 672 pp. (in Russian).

Kroposki, B., Levene, J., Harrison, K., Sen, P. K. & Novachek, F. 2006. Electrolysis: Opportunities for Electric Power Utilities in a Hydrogen Economy. *38th North American*. Power Symposium. NAPS, pp. 567–576.

Sadhankar, R. R., Li, J., Li, H., Ryland, D. K. & Suppiah, S., 2006. Future Hydrogen Production Using Nuclear Reactors. IEEE. *EIC Climate Change Technology*. pp. 1–9.

Eg & G technical services, Inc. 2004. *Fuel cell handbook*. Morgantown, West Virginia, 427 pp.

Matthew M. 2008. *Fuel cell engines.* John Wiley & Sons, Inc. Hoboken, New Jersey. 515 pp.

Miaosen, S., Joseph, A., Jin W, Peng, F. Z. & Adams, D.J. 2005 Comparison of Traditional Inverters and Z–Source Inverter. *Power Electronics Specialists Conference, PESC '05. IEEE 36th*, pp. 1692–1698.

Yartys, V. A., Lototsky, M. V. 2004. An overview of hydrogen storage methods. In: Veziroglu T. N. et al (eds). *Hydrogen Materials Science and Chemistry of Carbon Nanomaterials*, Kluwer Academic Publishers. Netherlands. pp. 75–104.

Leighty, W., Holloway, J., Merer, R., Somerday, B., San Marchi, C., Keith, G. & White, D., 2006. Compressorless hydrogen transmission pipelines deliver large scale stranded renewable energy at competitive cost. *16th World Hydrogen Energy Conference*, Lyon, pp. 1–14.

[PAPER-III] **Andrijanovitsh, A.**; Steiks, I.; Zakis, J.; Vinnikov, D. Analysis of State of the Art Converter Topologies for Interfacing of Hydrogen Buffer with Renewable Energy Systems. Scientific Journal of Riga Technical University. Power and Electrical Engineering, 29, pp. 87 – 94, 2011.

Scientific Journal of Riga Technical University
Power and Electrical Engineering

2011
Volume 29

Analysis of State-of-the-Art Converter Topologies for Interfacing of Hydrogen Buffer with Renewable Energy Systems

Anna Andrijanovitsh[1], *Tallinn University of Technology*, Ingars Steiks, *Riga Technical University*,
Janis Zakis, *Tallinn University of Technology*,
Dmitri Vinnikov, *Tallinn University of Technology*

Abstract **– This paper compares state-of-the-art DC/DC converter topologies for electrolyzer and fuel cell applications in renewable energy systems (RES). The main components of the hydrogen-based energy storage system should be connected to the DC-bus of a RES via separate interface converters: the electrolyzer is interfaced by the step-down DC/DC converter, while the fuel cell is connected through the step-up DC/DC converter. Because of the high input and output voltage differences the topologies with a high-frequency voltage matching transformer are analyzed. The inverter and rectifier sides of the discussed DC/DC converters presented in schemes are analyzed in detail.**

Keywords **– Renewable energy, hydrogen, electrolyzer, fuel cell, DC/DC converter.**

I. Introduction

Use of alternative energy sources is an urgent issue today. Main advantages of renewable energy are zero fuel costs and lower impact on the environment. However, renewable energy sources, such as solar and wind power, are difficult to forecast. To compensate unstable operation of a renewable energy system (RES) the concept of hydrogen use was introduced in [1-4].

Fig. 1 shows a hydrogen-based energy storage system or a hydrogen buffer that stabilizes unregulated renewable energy generation. It consists of the following stages: hydrogen production, hydrogen storage and electricity production. In the excess energy periods the hydrogen generation system is connected to the DC-bus of the RES. In this stage electrical energy from the renewable energy source is converted into chemical energy by using water electrolysis and this energy is stored in a tank. In order to stabilize energy production during the absence of the renewable energy, stored hydrogen could be re-used. In this stage, hydrogen is converted into electrical energy by using a fuel cell (FC). The FC takes the hydrogen from the tanks to generate electricity, plus water and heat as by-products. Combination of an energy storage system and an RES allows controllable power production [5-6].

Typically, the electrolyzer (EL) and the FC are connected to the RES via separate interface converters. The EL is connected to the DC-bus of the RES through the step-down DC/DC converter, while the FC should be interfaced by the step-up DC/DC converter.

DC/DC converters can provide interfaces of different voltage levels in the hydrogen buffer system. In principle, many basic power converter topologies can be used for the EL and the FC interconnections with the DC-bus of the RES. Because of comparatively high input and output voltage differences the DC/DC converters with a high-frequency voltage matching transformer are used more frequently. For reasons of safety this transformer should also perform the function of galvanic isolation of the primary and the secondary side. In this paper, state-of-the-art DC/DC converter topologies for the EL and FC applications are analyzed in detail and compared.

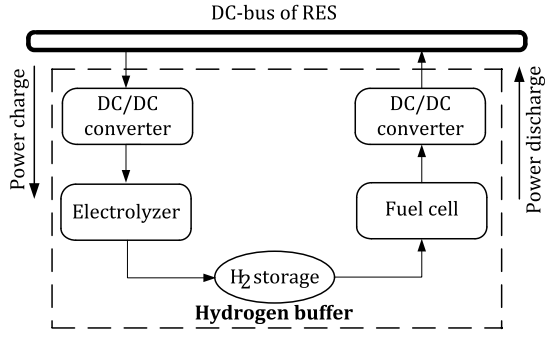

Fig. 1. Energy exchange processes in the hydrogen buffer.

II. DC/DC Converter Topologies for the Electrolyzer Application

The EL and the FC perform opposite functions. Instead of generating electrical energy as the FC does, the EL consumes it. The EL is a low DC voltage sensitive load [7] and it cannot be directly connected to uncontrolled high DC voltages. To connect the EL to the DC-bus, it is required to buck the voltage of the DC-bus to the level of the EL [8]. The DC/DC converters with a high-frequency transformer fulfill these requirements. The DC/DC converter structure for the EL integration to the system of the RES is shown in Fig. 2. In FC applications, this DC/DC converter consists of the following main components: 1 – inverter, 2 – isolation transformer, 3 – rectifier, 4 – output filter.

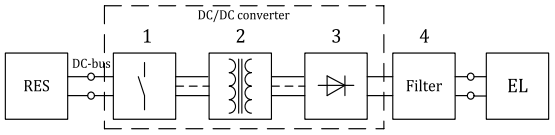

Fig. 2. Required structure of the DC/DC converter for an electrolyzer application.

The DC-bus voltage is converted to AC voltage by means of an inverter. To step down the voltage an isolation transformer is employed. The secondary side of the voltage is rectified by help of a rectifier. The output filter is used to improve the quality of the output voltage. It should be taken into account that the frequency of the current ripple at the output of the DC converter should be kept low, as higher frequencies increase the power losses in the electrolyzer [9]. The inverter side and the rectifier side topologies of DC/DC converters are described below.

As a result of the analysis of the references according to the DC/DC converter applications of electrolyzers [10-19], topologies of inverters can be classified into full-bridge (FB) [10-17] and half-bridge (HB) [17-19].

A. Inverter Side Topologies

In [10-12] a classical single-phase FB topology with an inductance and a capacitor in series is analyzed (Fig. 3). The case where only an inductance is presented (Fig. 3(a)) is called a phase-shifted zero-voltage-switching (ZVS) PWM bridge inverter. It is called an LCL series resonant inverter (SRC) if a capacitor is added in series (Fig. 3(b)). It has been approved in [10] that an LCL SRC with capacitance output has desirable features over a phase-shifted ZVS PWM bridge inverter in applications where the low DC-bus voltage is applied. In [12] a boost zero-voltage-transition (ZVT) is added to improve the LCL SRC and make it more suitable for electrolyzer applications.

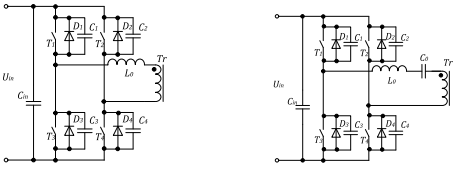

(a) (b)

Fig. 3. Single-phase FB topology with: (a) inductance; (b) inductance and capacitor.

Different phase-shifted FB ZVS topologies (Fig. 4(a)) of an inverter are proposed in [13-14]. Presented circuits are based on the usage of two transformers, connecting them in various ways and combining with capacitors. It has been reported that this topology can achieve complete ZVS in a wide range of load current and input voltage [13-14]. One of the transformers is used to achieve ZVS, but other or power transfer. As in [13-14], in [15] an FB inverter with ZVS over the entire power conversion range is proposed. Inverter topology in [15] also consists of two transformers (Fig. 4(b)), only in this case both transformers are used for power transfer.

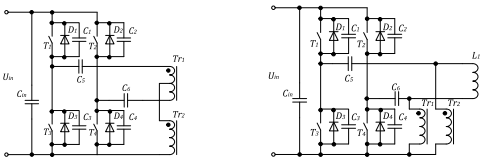

(a) (b)

Fig. 4. Implementation of phase-shifted FB ZVS PWM inverter with two transformers: (a) one auxiliary transformer for ZVS; (b) both transformers for power transfer.

L, LC, and LCL filter and LCL series-parallel resonance inverters (SPRC) have been analyzed in [16] (Fig. 5(a)), but the scope of the converter was to convert DC voltage from 48V at the input to 5V at the output of the converter. Instead of low voltage conversions in [16], high voltage and high power converter application is analyzed in [17]. In [17], in the analysis of ZVS and zero current switching (ZCS), a zero voltage zero current switching (ZVZCS) PWM inverter is described. ZVZCS PWM inverter is derived from the phase-shifted FB ZVS PWM inverters.

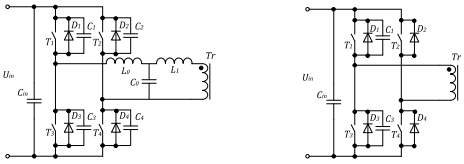

(a) (b)

Fig. 5. FB topology: (a) ZVS PWM inverter with LCL filter; (b) ZVZCS PWM inverter.

No new trends relevant to HB topology inverters have been found if they are regarded as high-frequency inverters for EL applications. In fact, HB topology inverters were analyzed more than 20 years ago [18-19]. General comparisons are reported in [17] with an analysis of HB vs. FB whereas FB is chosen. In [18], an LCL resonance inverter for telecommunication power systems is analyzed, while in [19] pure series and parallel, series-parallel inverters are compared for low voltage applications. Topologies considered in [17-19] are depicted in Fig. 6.

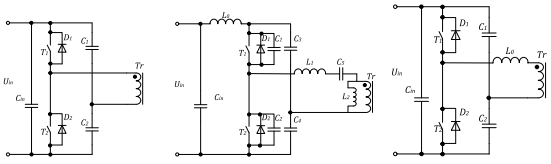

(a) (b) (c)

Fig. 6. Single-phase HB topology inverters: (a) fundamental; (b) LCL; (c) series-parallel.

B. Rectifier Side Topologies

As a DC/DC converter requires DC voltage at the output, AC voltage must be rectified. Usually rectification of the voltage is realized by the single-phase FB topology [10, 12,

16, 18] or by the current doubler topology [11, 13-15, 17, 19]. Rectifier topologies: single-phase FB (a) and current doubler (b) are shown in Fig. 7. As rectified voltage contains voltage/current ripples, they must be filtered to operate the EL efficiently. A typical DC/DC converter output filter contains an inductor and a capacitor (Fig. 7(c)).

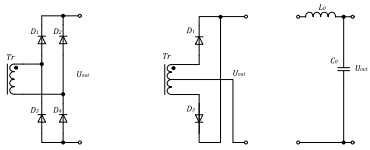

(a) (b) (c)

Fig. 7. Rectifier side topologies: (a) single-phase FB; (b) current doubler; (c) LC output filter.

Single-phase FB rectifiers are used with FB LCL inverters [10, 12, 16, 18], as they require one transformer secondary winding to add an inductor or a capacitor as required. A two transformer current doubler rectifier with two inductors is presented in [15], but in [11] a current doubler rectifier with one transformer secondary winding is shown (Fig. 8).

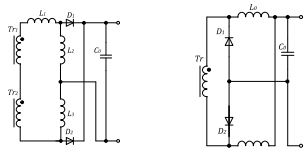

(a) (b)

Fig. 8. Current doubler topologies: (a) with two transformers; (b) with one transformer secondary winding.

More common DC/DC converter topologies for electrolyzer applications are classified in Fig. 9.

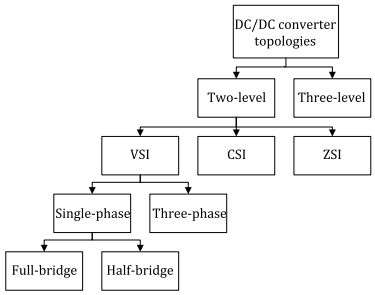

Fig. 9. The general classification of DC/DC converters for electrolyzer applications.

III. DC/DC Converter Topologies for the Fuel Cell Application

FC is a power source with low unregulated DC output voltage. To connect a FC to the load, it is necessary to boost and stabilize the relatively low output voltage of the FC to a certain operating voltage level. The DC/DC converter accomplishes both functions. Fig. 10 shows the DC/DC converter structure for the FC integration to the RES. This converter includes the following main components: 1 – inverter, 2 – isolation transformer, 3 – rectifier, 4 – output filter.

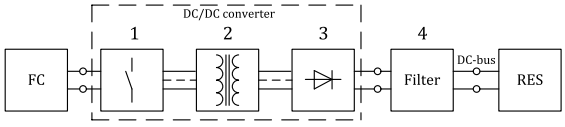

Fig. 10. Required structure of the DC/DC converter for fuel cell applications.

Low output DC voltage of a FC is converted to AC voltage by means of an inverter. For voltage step-up an isolation transformer is employed. The secondary side voltage is rectified by help of a rectifier. The output filter is an optional component. It is used to improve voltage quality. The inverter side and the rectifier side topologies of a DC/DC converter are described below.

A. Inverter Side Topologies

The inverters used in the DC/DC converters could be subdivided as two-level [20-43] and three-level [44-46]. In turn, both types of inverters can be classified into voltage source inverters (VSI) [20-25], current source inverters (CSI) [26-36] and Z-source (impedance source) inverters (ZSI) [37-43]. All these inverter types can be used for FC applications. More popular inverter topologies are as follows: single-phase (FB, HB, push-pull (PP)), and three-phase (FB, PP). Different types of switches can be used (MOSFET or IGBT technologies) for the inverter.

1. Two-Level Inverters

The single-phase FB VSI topology in Fig. 11(a) was presented in [20-23]. This inverter consists of two legs. Each leg consists of two switches and their anti-parallel diodes. The FB VSI eliminates the need for a separate filter inductor. Lack of separate inductance helps reduce the cost of the DC/DC converter. In the FB VSI the voltage and current stress of the switch is lower than in the HB topology.

In [24] the FB VSI is used with a start-up additional circuit to avoid an FC peak current demand at the system start-up. The additional diode in series with the FC stack prevents from any reverse current inside the stack.

The circuit of the three-phase PP VSI, as shown in Fig. 11(b), is proposed in [25]. The advantage of this inverter is the lower rms current through the switches. In the three-phase PP VSI topology the number of components is reduced in comparison with the three-phase FB topology.

In [26] it is shown that the single-phase FB VSI topology is less efficient for the FC application than the FB CSI topology. The FB CSI has stronger reliability for the inherent short current protection. The input current is continuous, and it prolongs the lifetime of the FC. As a result, in paper [27] the FB CSI has been chosen as an appropriate solution. Because of the high transient overvoltage across the semiconductors the CSI needs an additional clamping circuit to absorb this

overvoltage. The FB CSI topologies with two different regenerative clamping circuits are presented in [27]. The circuit with external clamping energy feedback (Fig. 12(a)) consists of the diode and the capacitance. The circuit with internal clamping energy feedback (Fig. 12(a)) has an additional transistor in parallel to the diode. This transistor is responsible for feeding the stored energy in the capacitor back into the circuit [27].

In the circuit of a single-phase FB CSI instead of MOSFET a reverse block IGBT can be used [28]. Elimination of the diodes in the reverse block IGBT should lead to such benefits as lower cost, smaller packages and lower conduction loss [28].

The single-phase HB CSI topology in Fig. 12(b) was presented in [29] as a suitable topology. This inverter topology shows higher efficiency and has higher input current ripple frequency than the FB CSI topology. The HB CSI reduces the need of two switches and the transformer turns ratio to half. The additional snubber capacitors are in parallel to the diode. The HB topology is popular for the power range around 1 kW. [29-30].

In [31] the single-phase PP CSI topology presented in Fig. 12(c) is analyzed. In this paper the CSI of the DC/DC converter was selected because of less input filtering in order to minimize the high frequency current ripple. The PP CSI provides high efficiency and has a good utilization of the transformer.

The single-phase PP CSI proposed in [32] is shown in Fig. 12(d). This topology includes an auxiliary circuit for protection of the switches against overvoltage. The auxiliary circuit is basically a flyback converter, which converts the stored energy of the clamp capacitor to the DC-bus [32].

The single-phase PP CSI topology described in [33] was modified by adding two coupled inductors to expand the duty cycle operation of the DC/DC converter. The proposed double-coupled PP CSI is shown in Fig. 12(e). The DC/DC converter with an inverter of such type can operate from 0 to 100% of the duty cycle.

The three-phase FB CSI topology with an active clamp in Fig. 12(f) was presented in [34]. The proposed converter includes the following features: increased power converter rating by employing three phases instead of a single phase; lower transformer turn-ratio by using a boost stage inherited by the current-fed type; achieve zero voltage switching in three-phase FB switches by a single common active clamp branch [34].

The circuit of the three-phase PP CSI illustrated in Fig. 12(g) is proposed in [35]. In this converter, the input boost inductor is placed in series with the power source. Three-phase transformers are generally smaller and lighter than single-phase ones for the same processed power due to reduced voltage and magnetic stresses. Thus, the losses in the three-phase PP CSI are better distributed than in the single-phase PP CSI.

In [36] the three-phase PP CSI topology with an active clamping (Fig. 12(h)) was analyzed. This clamp circuit consists of three clamp switches and a clamp capacitor at the low voltage primary side of the DC/DC converter. The active clamp limits the transient overvoltage caused by transformer leakage inductances and helps improve the efficiency by enabling soft switching of the main switches [36]. Thus, the active clamping method achieves higher efficiency and higher power density.

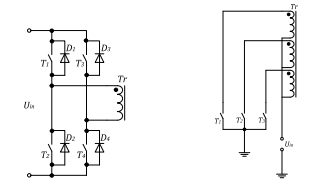

(a) (b)

Fig. 11. VSI topologies: (a) single-phase FB; (b) three-phase PP.

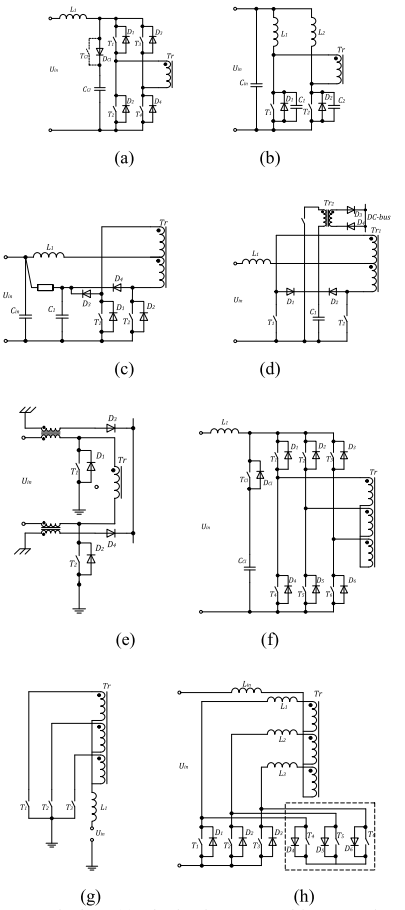

(a) (b) (c) (d) (e) (f) (g) (h)

Fig. 12. CSI topologies: (a) single-phase FB with external and internal clamping energy feedback, (b) single-phase HB; (c) single-phase PP; (d) single-phase PP with an auxiliary circuit; (e) single-phase double-coupled PP; (f) three-phase FB with active clamp; (g) three-phase PP; (h) three-phase PP with active clamp.

In [37] the single-phase FB ZSI topology is presented, shown in Fig. 13(a). The single-phase FB topology is most useful in terms of cost and efficiency, especially when implemented for power levels higher than 3 kW [37]. The ZSI can boost or buck voltage, minimize component count, increase efficiency, and reduce the cost. This impedance source consists of a split-inductor and capacitors connected in X shape.

The application of the three-phase FB ZSI [38] (Fig. 13(b)) has one extra zero state when the load terminals are shorted through both the upper and lower devices of any one phase leg, any two phase legs, or all three phase legs. This shoot-through zero state provides the unique buck-boost feature to the inverter [38-39].

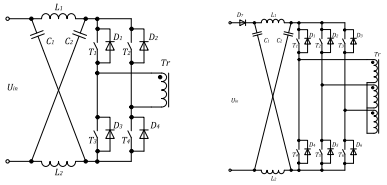

(a) (b)

Fig. 13. ZSI topologies: (a) single-phase FB; (b) three-phase FB.

The single-phase and three-phase FB quasi-Z-source inverter (qZSI) proposed in [40-41] is derived from a traditional ZSI (Fig. 14(a, b), respectively). As compared to the ZSI, the qZSI has two distinctive advantages, such as continuous constant DC current from the source and lower operating voltage of the capacitor C2. To further improve the boost properties of the qZSI topology the cascaded quasi-Z-source circuit was introduced [42-43].

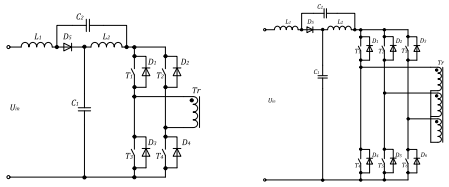

(a) (b)

Fig. 14. qZSI topologies: (a) single-phase FB; (b) three-phase FB.

2. Three-Level Inverters

In contrast to the traditional two-level converters, the primary advantage of the multilevel converters is their smaller output voltage step, which results in high power quality, lower harmonic components, better electromagnetic compatibility, and lower switching losses. The disadvantage of the multilevel converters is the need for a large number of power semiconductor switches. Although low-voltage-rated switches can be utilized in a multilevel converter, each switch requires a related gate driver and protection circuits. This may result in higher costs and higher complexity of the overall system [44].

In [45] the three-level single-phase PP forward inverter topology (Fig. 15(a)) was analyzed. Half of the switches sustain half of the input voltage, and others sustain one and a half of the input voltage.

The three-level single-phase FB circuit illustrated in Fig. 15(b) was proposed in [46]. This converter can operate in three-level and two-level modes, so the output filter and input current ripple can be reduced. Lower output current ripple leads to higher efficiency and longer lifetime [46].

Since the three-level topologies are not so popular, in the next comparative analysis they are not used.

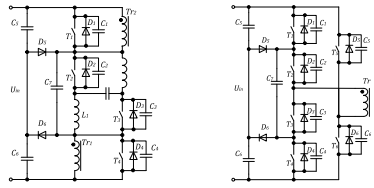

(a) (b)

Fig. 15. Three-level topologies: (a) single-phase PP forward; (b) single-phase FB.

B. Rectifier Side Topologies

Papers [22-24, 27, 31-32, 37, 42, 45, 46] report rectification on the secondary side of the DC/DC converter realized by an FB rectifier consisting of the diodes D1-D4, as shown in Fig. 16(a). In [29] to improve the efficiency as well as reduce the size and cost the output rectifier diodes are replaced with active switches.

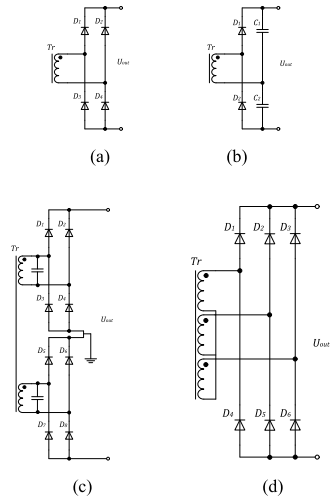

(a) (b) (c) (d)

Fig. 16. Rectifier topologies: (a) single-phase FB; (c) single-phase FB with two separated outputs; (d) three-phase FB.

The secondary side of the DC/DC converter is connected to the voltage doubler rectifier in [40]. This type of the rectifier (Fig. 16(b)) is derived from the FB rectifier by the replacement of diodes in one leg by the capacitors with an

equal capacity. The main advantages of the voltage doubler rectifier are the doubling effect of the secondary winding voltage of the isolation transformer and reduced power dissipation due to a smaller number of rectifying diodes [40].

In the rectifier topology proposed in [20, 28], two DC output sources could be obtained with two separated output windings, as shown in Fig. 16(c). The output voltage can be fully controlled by changing the phase shift angle between the two legs. In [28] in this rectifier the additional resonant component Cr, which can help achieve zero current switching operation, is also used.

According to [34-36], the circuit of the secondary side of the DC/DC converter consists of a three-phase FB diode rectifier connected through a three-phase transformer, as shown in Fig. 16(d).

More common DC/DC converter topologies for fuel cell applications are classified in Fig. 17.

IV. Comparative Analysis of DC/DC Converters

The main converter ratings used to compare the efficiency of the above converter structures are presented in Table I.

TABLE I

Main Ratings of the Considered DC/DC Converters for Electrolyzer and Fuel Cell Applications

Parameters \ Topologies	Single-phase			Three-phase	
	Full-bridge	Half-bridge	Push-pull	Full-bridge	Push-pull
Input voltage, U_{in} (p.u.)	1	1	1	1	1
Rated power of the converter, P (p.u.)	1	1	1	1	1
Number of switches	4	2	2	6	3
Current rating of the switch, I_{sw} (p.u.)	1	2	1	0,7	0,7
Voltage across the switch, U_{sw} (p.u.)	1	1	2	1	2
Transformer primary windings	1	1	2	3	3
Transformer turns ratio, $n=Tr_2/Tr_1$ (p.u.)	2	1	2	2	2

A comparative analysis of the advantages and disadvantages of the DC/DC converters was made. In Table II the discussed DC/DC converters are compared side by side [47].

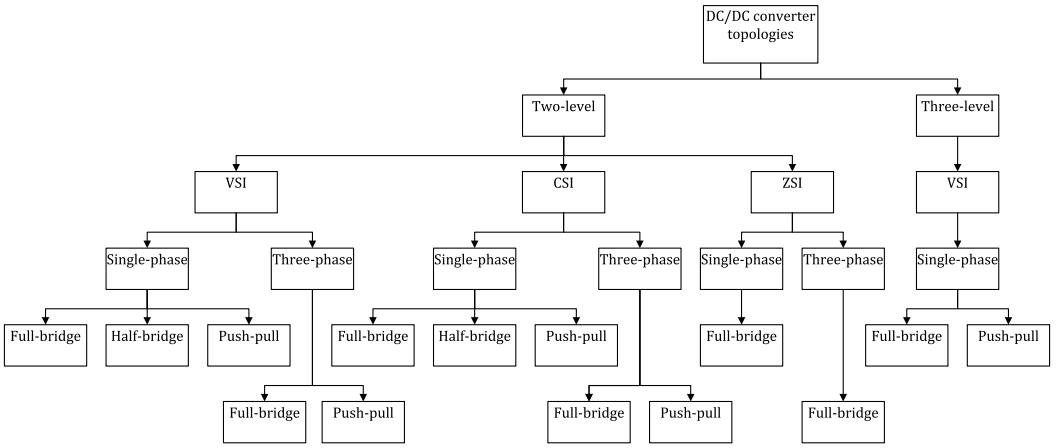

Fig. 17. The general classification of DC/DC converters for fuel cell applications.

TABLE II

Comparative Analysis of the Basic Structures of the DC/DC Converter Topologies for Electrolyzer and Fuel Cell Applications

Features \ Topologies	Single-phase			Three-phase	
	FB	HB	PP	FB	PP
Advantages	The voltage and current stress of the switch is lower than in HB. Higher possible switching frequency. Lower isolation transformer primary current.	Reduces the need of two switches and the transformer turns ratio to half. Lower isolation transformer primary voltage.	Provides a high efficiency and has a good utilization of the transformer. No more than one switch in series conducts at any instant time. It can generate multiple output voltages.	Increases power converter rating by employing three phases. The losses in the three-phase FB are better distributed than in the single-phase. Inverter switch rating is better than in a single-phase topology.	Lower rms current through the switches. Number of components is lower than with the FB. The losses in the three-phase PP are better distributed than in the single-phase.

Topologies / Features	Single phase			Three-phase	
	FB	HB	PP	FB	PP
Disadvantages	Higher number of switches. Higher conduction number. Higher isolation transformer primary voltage.	Limited switching frequency. Higher isolation transformer current.	It requires very good matching of the switch transistors to prevent unequal on times, since this will result in saturation of the transformer core.	Active inverter switch utilization is lower than in the single-phase topology. More components than with the PP.	Control circuit is complexity.
Implementation possibilities	Most useful in terms of cost and efficiency, especially when implemented for power levels higher than 3 kW.	Feasible for the power range around 1 kW.	Feasible for the power range around 1 kW.	A three-phase transformer gives a potential feedom and flexibility to choose voltages and currents in the inverter, transformer and rectifier.	A three-phase transformer gives a potential feedom and flexibility to choose voltages and currents in the inverter, transformer and rectifier.

V. CONCLUSIONS

The DC/DC converter topologies that can be considered for EL and FC applications have been presented in this paper. All these converters have a high-frequency voltage matching transformer, which should also perform the function of galvanic isolation of the inverter and rectifier side. This paper gives an opportunity to compare the basic parameters of the DC/DC converters and select more feasible topology for particular applications.

In electrolyzer applications of the inverter side of the DC/DC converter, switching losses must be kept as low as possible. Thus, ZVS or ZCS is preferred. In the case of a rectifier side, a low component count is preferred, as the current is relatively high.

The FC is one of the promising technologies for RES. It can provide higher efficiency and enhanced reliability of the long-term energy storage systems. Because of the FC disadvantage due to high variations in its output voltage when the load changes, the DC/DC converter is used to supply a smooth output voltage to other electrical loads. According to power the discussed DC/DC converters can be classified like converters for small or medium power systems. In a power range about 1-3 kW, converters like half-bridge or push-pull are suitable topologies utilizing high-frequency transformer. For a power range higher then 3 kW, the full-bridge converter is an appropriate solution for fuel cell applications. The three-phase configurations of the DC/DC converter topology can be used to improve the losses distribution in the converter and to increase power converter ratings. However, the three-phase topology applications increase the number of components that may not be feasible. As an example, the discussed DC/DC converter circuits have been illustrated in this paper.

REFERENCES

[1] C. Cavallaro, F. Chimento, S. Musumeci, C. Sapuppo, C. Santonocito, "Electrolyser in H2 self-producing systems connected to DC link with dedicated phase shift converter", International Conference on Clean Electrical Power, ICCEP '2007, pp. 632-638, 21-23 May 2007.

[2] F. Ibanez, A. Perez-Navarro, C. Sanchez, I. Segura, E. Bernal, J. Paya, "Wind generation stabilization using a hydrogen buffer", European Conference on Power Electronics and Applications, pp. 1-10, 2-5 Sept. 2007.

[3] C. Cavallaro, V. Cecconi, F. Chimento, S. Musumeci, C. Santonocito, C. Sapuppo, "A phase-shift full bridge converter for the energy management of electrolyzer systems", IEEE International Symposium on Industrial Electronics, ISIE'2007, pp. 2649-2654, 4-7 June 2007.

[4] J. J. Ugartemendia, X. Ostolaza, V. Moreno, J. J. Molina, I. Zubia; "Wind generation stabilization of fixed speed wind turbine farms with hydrogen buffer", 11th. Spanish-Portuguese Conference on Electrical Engineering (11CHLIE), pp. 1-5, 1-4 July 2009.

[5] A. Andrijanovitš, M. Egorov, M. Lehtla, D. Vinnikov, "New method for stabilization of wind power generation using an energy storage technology", Journal on Agronomy Research, vol. 8, (S1), pp. 12-24, May 2010.

[6] J. A. Carr, J. C. Balda, "A grid interface for distributed energy resources with integrated energy storage using a high frequency AC link", IEEE Power Electronics Specialists Conference, pp. 3774-3779, June 2008.

[7] Supramaniam Srinivasan "Fuel Cells: from fundamentals to applications" Springer, USA, 2006.

[8] C. Wang, M. H. Nehrir, "Power management of a stand-alone wind/photovoltaic/fuel cell energy system", IEEE Transactions on Energy Conversion, September 2008.

[9] F. da Costa Lopes, E. H. Watanabe, "Experimental and theoretical development of a PEM electrolyzer model applied to energy storage systems", IEEE, September 2009.

[10] D. S. Gautam, A. K. S. Bhat, "A comparison of soft-switched DC to DC converters for electrolyser application", Proceedings of India International Conference on Power Electronics 2006,pp.274-279, 2006.

[11] C. Cavallaro, V. Cecconi, F. Chimento, S. Musumeci, C. Santonocito, C. Sapuppo, "A phase-shift full-bridge converter for the energy management of electrolyzer systems", IEEE, July 2007.

[12] D. S. Gautam, A. K. S. Bhat, "A two-stage soft-switched converter for electrolyser application", Fifteenth National Power Systems Conference (NPSC), IIT Bombay, December 2008.

[13] Y. Jang and M. M. Jovanović, "A new family of full-bridge ZVS converters", IEEE, pp. 622-628, March 2003.

[14] D. K. Nayak and S. R. Reddy, "Simulation of soft switched PWM ZVS full-bridge converter", International Journal of Computer and Electrical Engineering, Vol. 2, No. 3, June 2010.

[15] M. Borage, S. Tiwari, S. Bhardwaj, and S. Kotaiah, "A full-bridge DC/DC converter with zero-voltage-switching over the entire conversion range", IEEE Transactions on Power Electronics, Vol. 23, No. 4, July 2008.

[16] P. Chandrasekhar, S. Rama Reddy, "Design of LCL resonant converter for electrolyser", International Journal of Electronic Engineering Research, Vol. 2, No. 3, 2010.

[17] J.Dudrik, J.Oetter, "High-frequency soft-switching DC/DC converters for voltage and current DC power sources", Acta Polytechnica Hungarica, Vol. 4, No. 2, 2007.

[18] A. K. S. Bhat, "Analysis and design of LCL-type series resonant converter", IEEE, pp.172-178, 1990.

[19] R. L. Steigerwald, "A comparison of half-bridge resonant converter topologies", IEEE Transactions on Power Electronics, Vol. 3, No. 2, April 1988.

[20] Z. B. Shen, E. F. El-Saadany, "Novel interfacing for fuel cell based distributed generation", IEEE Power Engineering Society General Meeting, June 2007.
[21] R. Sharma, H. Gao, "A new DC/DC converter for fuel cell powered distributed residential power generation systems", IEEE, pp. 1014-1018, 2006.
[22] M. A. A. Younis, N. A. Rahim, S. Mekhilef, "Dynamic and control of fuel cell system", IEEE Industrial Electronics and Applications, pp. 2063-2067, June 2008.
[23] H. Xu, L. Kong, X. Wen, "Fuel cell power system and high power DC/DC converter", IEEE Transaction on Power Electronics, vol. 19, no. 5, pp. 1250-1255, September 2004.
[24] A. Narjiss, D. Depernet, F. Gustin, D. Hissel, A. Berthon, "Design and control of a fuel cell DC/DC converter for embedded applications", IEEE, 2008.
[25] H. R. E. Larico, I. Barbi, "Voltage-fed three-phase push-pull DC/DC converter", IECON´09, 35th Annual Conference of IEEE, pp. 956-961, November 2009.
[26] M. Mohr, F. Fuchs, "Voltage-fed and current-fed full-bridge converter for the use in three-phase grid connected fuel cell systems", IEEE Power Electronics and Motion Control Conference, August 2006.
[27] M. Mohr, F. Fuchs, "Current-fed full-bridge converters for fuel cell systems connected to the three phase grid", IEEE, pp. 4313-4318, 2006.
[28] X. Zhu, D. Xu, G. Shen, D. Xi, K. Mino, H. Umida, "Current-fed DC/DC converter with reverse block IGBT for fuel cell distributing power system", Industry Applications Conference, pp. 2043-2048, October 2005.
[29] A. K. Rathore, S. K. Mazumder, "Novel zero-current switching current-fed half-bridge isolated DC/DC converter for fuel cell based applications", Energy Conversion Congress and Exposition, pp. 3523-3529, September 2010.
[30] S. Meo, A. Perfetto, L. Piegari, F. Esposito, "A ZVS current-fed DC/DC converter oriented for applications fuel-cell-based", The 30th Annual Conference of the IEEE Industrial Electronics Society, pp. 932-937, November 2004.
[31] G. K. Andersen, C. Klumpner, S. B. Kjaer, F. Blaabjerg, "A new green power inverter for fuel cells", IEEE Power Electronics Specialists Conference, pp. 727-733, 2002.
[32] R. Bojoi, C. Pica, A. Tenconi, "New DC/DC converter with reduced low-frequency current ripple for fuel cell in single-phase distributed generation", IEEE Industrial Technology (ICIT), pp. 1213-1218, March 2010.
[33] H. R. E. Larico, I. Barbi, "Double-coupled current-fed push-pull DC/DC converter: analysis and experimentation", IEEE Power Electronics Conference, COBEP´09, pp. 305-312, October 2009.
[34] H. Cha, P. Enjeti, "A novel three-phase high power current-fed DC/DC converter with active clemp for fuel cells", IEEE Power Electronics Specialists Conference, pp. 2485-2489, June 2007.
[35] R. L. Andersen, I. Barbi, "A three-phase current-fed push-pull DC/DC converter", IEEE Transaction on Power Electronics, vol. 24, no. 2, pp. 358-368, February 2009.
[36] S. Lee, J. Park, S. Choi, "A three-phase current-fed push-pull DC/DC converter with active clemp for fuel cell applications", IEEE.
[37] D. Vinnikov, I. Roasto, T. Jalakas, "New step-up DC/DC converter with high-frequency isolation", IEEE, pp. 670-675, 2009.
[38] F. Z. Peng, "Z-source inverter", IEEE Transactions on Industry Applications, vol. 39, no. 2, pp. 504-510, April 2003.
[39] M. Shen, A. Joseph, J. Wang, F. Z. Peng, D. J. Adams, "Comparison of traditional inverters and Z-source inverter for fuel cell vehicles, IEEE Transactions on Power Electronics, vol. 22, no. 4, pp. 1453-1463, July 2007.
[40] D. Vinnikov, I. Roasto, J. Zakis, R. Strzelecki, "New step-up DC/DC converter for fuel cell powered distributed generation systems: some design guidelines", Journal of Electrical Review, vol. 86, no. 8, pp. 245-252, 2010.
[41] Y. Li, J. Anderson, F. Z. Peng, D. Liu, "Quasi-Z-source inverter for photovoltaic power generation systems", IEEE Applied Power Electronics Conference and Exposition, pp. 918-924, February 2009.
[42] D. Vinnikov, I. Roasto, J. Zakis, "New bi-directional DC/DC converter for supercapacitor interfacing in high-power applications", IEEE Power Electronics and Motion Control Conference, September 2010.
[43] D. Vinnikov, I. Roasto, J. Zakis, "Mathematical models of cascaded quasi-impedance source converter", Технічна електродинаміка, 59-64, 2010.
[44] M. Harfman Todorovic, L. Palma, P. N. Enjeti, "Design of a wide input range DC/DC converter with a robust power control scheme suitable for fuel cell power conversion", IEEE Transactions of Industrial Electronics, Vol. 55, No. 3, pp. 1247-1255, March 2008.
[45] Z. Yao, L. Xiao, Y. Huang, C. Gong, "Push-pull forward three-level converter with reduced rectifier voltage stress", IEEE, pp. 1654-1660, 2009.
[46] K. Jin, X. Ruan, M. Yang, M. Xu, "A hybrid fuel cell power system", IEEE Transactions of Industrial Electronics, Vol. 56, No. 4, pp. 1212-1222, April 2009.
[47] D. Vinnikov, "Research, design and implementation of auxiliary power supplies for the light rail vehicles", Ph.D. dissertation, Dept. El. Drives Pow. Elec., Tallinn Univ. Tech., Estonia, 2005.

Anna Andrijanovitsh received B.Sc. and M.Sc. degrees in electrical engineering from Tallinn University of Technology, Tallinn, Estonia, in 2006 and 2008, respectively.

She is presently PhD student in the Department of Electrical Drives and Power Electronics, Tallinn University of Technology.

Her research interests include switchmode power converters, modeling and simulation of power systems, applied design of power converters and development of energy storage systems.

Ingars Steiks received the B.sc.ing. and M.sc.ing. degrees from the Faculty of Power and Electrical Engineering, Riga Technical University, Riga, Latvia, in 2003 and 2005, respectively.

Since 2006, he has been a Researcher in the Institute of Industrial Electronics and Electrical Engineering, Riga Technical University.

His main research interests include modular multilevel power converter applications for fuel cells. Mr. Steiks is a Student Member of the IEEE Industrial Electronics Society since 2006.

Janis Zakis received B.Sc., M.Sc. and Dr.Sc.ing. degrees in electrical engineering from Riga Technical University, Riga, Latvia, in 2002, 2004 and 2008, respectively.

He is presently a Senior Researcher in the Department of Electrical Drives and Power Electronics, Tallinn University of Technology.

He has over 20 publications and is the holder of one Utility Model in power converter design. His research interests include flexible ac transmission systems (FACTS), simulation of power systems, switching mode power converters, applied design of power converters and energy storage systems.

Dmitri Vinnikov received the Dipl.Eng, M.Sc. and Dr.Sc.techn. degrees in electrical engineering from Tallinn University of Technology, Tallinn, Estonia, in 1999, 2001 and 2005, respectively.

He is presently a Senior Researcher in the Department of Electrical Drives and Power Electronics, Tallinn University of Technology.

He has authored more than 100 published papers on power converters design and development and is the holder of several Utility Models in this application field. His research interests include switchmode power converters, modeling and simulation of power systems, applied design of power converters and control systems and application and development of energy storage systems.

[PAPER-IV] **Andrijanovits, A.;** Beldjajev, V. Techno-Economic Analysis of Hydrogen Buffers for Distributed Energy Systems. Power Electronics, Electrical Drives, Automation and Motion (SPEEDAM), pp. 1401 – 1406, 2012.

2012
International Symposium on Power Electronics,
Electrical Drives, Automation and Motion

Techno-Economic Analysis of Hydrogen Buffers for Distributed Energy Systems

A. Andrijanovits, V. Beldjajev
Tallinn University of Technology, Ehitajate tee 5, 19086 Tallinn (Estonia)

***Abstract*—Massive utilization of fossil fuels presents serious environmental threats. In this context, today the development of renewable energies is an urgent issue. Due to the stochastic nature of renewable energy sources an energy storage is needed in renewable energy generation systems. Hydrogen-based energy storage system or hydrogen buffer can help to stabilize unregulated renewable energy generation. In the hydrogen buffer system, the excess wind energy is stored in the form of hydrogen via conversion through the electrolyzer. The fuel cell is used to produce electrical power when the load demand exceeds that produced by the renewable energy sources. Hydrogen buffer includes two main operational stages: electrochemical and power electrical. This paper explores the techno-economic analysis of the electrochemical stage of the hydrogen buffer in order to increase the efficiency of hydrogen production in the renewable energy system.**

***Index Terms*—Electrolyzer, fuel cell, hydrogen buffer, renewable energy.**

I. Introduction

Use of alternative energy sources is an urgent issue today. Main advantages of renewable energy are zero fuel costs and lower impact on the environment. However, renewable energy sources, such as solar and wind power, are difficult to use due to their stochastic variability. In order for renewable energy to be generally used for regular consumers, the concept of hydrogen use needs to be introduced to stabilize unregulated renewable energy generation [1-11]. A typical renewable energy system (RES) must include both short-term and long-term energy storage. A short-term energy storage system is commonly used due to its high round-trip efficiency, convenience for charging/discharging. In addition, it can take care of the effects caused by instantaneous load ripples/spikes, electrolyzer transients and wind energy peaks. However, batteries alone are not appropriate for long-term energy storage because of their low energy density, self-discharge, and leakage. The combination of short-term energy storage with long-term energy storage in the form of hydrogen can improve the performance of stand-alone RES significantly [12-17].

Fig. 1 shows a hydrogen-based energy storage system or a hydrogen buffer consisting of two layers: electrochemical and power electrical stage. The electrochemical stage includes hydrogen production, hydrogen storage and electricity production. In the excess energy periods the hydrogen generation system is connected to the DC-bus of the (RES). In this stage electrical energy from the renewable energy source is converted into chemical energy by using water electrolysis and this energy is stored in a tank. In order to stabilize energy production during the absence of the renewable energy, stored hydrogen could be re-used. In this stage, hydrogen is converted into electrical energy by using a fuel cell (FC). The FC takes the hydrogen from the tanks to generate electricity, plus water and heat as by-products. Combination of an energy storage system and an RES allows controllable power production [18-19].

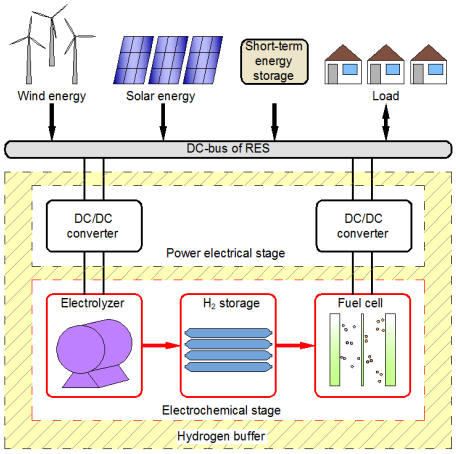

Fig. 1. Energy exchange processes in the hydrogen buffer.

At the power electrical stage, the interconnection of the EL and the FC with the DC-bus of RES is implemented. The EL is connected through the step-down DC/DC converter, while the FC should be interfaced by the step-up DC/DC converter. The description of the power electrical stage was presented in [20-22]. This paper focuses on the techno-economic analysis of the electrochemical stage of the hydrogen buffer. In this analysis the efficiency, response time and economic reasoning of the hydrogen buffer are discussed in detail.

II. Efficiency

A. Electrolyzer

The EL is used for splitting water into hydrogen and oxygen by the supply of direct current to its electrodes. Fig. 2 shows three basic types of electrolyzers: alkaline, proton exchange membrane (PEM) and high–temperature

This research work has been supported by Estonian Ministry of Education and Research (project SF0140016s11) and Estonian Archimedes Foundation (projects „Doctoral School of Energy and Geotechnology II“ and DoRa8).

978-1-4673-1301-8/12/$31.00 ©2012 IEEE

solid oxide [23]. Today's most widespread industrial electrolyzers are alkaline and PEM [24]. These two types of electrolyzers allow higher operating pressures, higher current density and low applied voltage to the cell. Table I shows that the total electrolyzer efficiency varies between 75% and 90%. The EL coupled to a hydrogen compressor is used to produce hydrogen. It should be noted that the efficiency of the electrolyzer output power decreases by 5% if the compressor energy is taken into account [25-28].

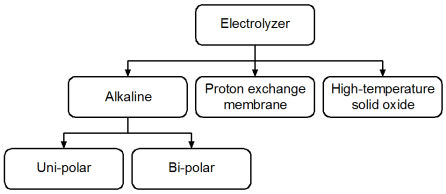

Fig. 2. General classification of electrolyzers.

Common characteristics of electrolyzers are shown in Table I.

TABLE I. COMMON CHARACTERISTICS OF ELECTROLYZERS

Characteristic	Alkaline		Proton Exchange membrane	High–temperature solid oxide
	Uni–polar	Bi–polar		
Current density, A $(cm^2)^{-1}$	0.1–0.2	0.2–0.4	0.4	1.1–2.0
Voltage cell, V	2.04–2.14	1.87–2.10	1.65–1.85	1.78–1.85
Production, $(m^3\ H_2)\ h^{-1}$	up to 80000	up to 200000	up to 25000	up to 25000
Energy demand, $(\kappa W{\cdot}h)\ (m^3)^{-1}$	5.0	4.3–4.6	4.5	3.9–4.0
Temperature, °C	50–100	50–100	80–100	120
Pressure, MPa	0.01–0.10	0.01–0.10	up to 3.0	0.2–6.0
Efficiency, %	75–90	75–90	80–90	80–90

Fig. 3 shows the experimental efficiency of the PEM electrolyzer.

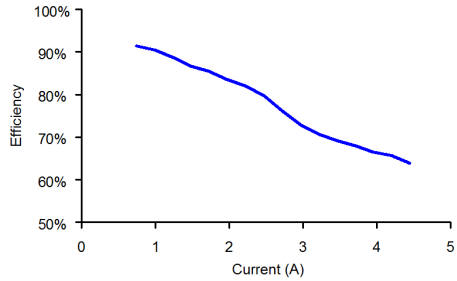

Fig. 3. Experimental efficiency of a PEM electrolyzer.

The graph shows that at higher currents the efficiency is reduced. This is explained by the fact that the losses increase with higher currents, as presented in [29]. However, it is clear that the electrolyzer is very efficient in converting electrical energy to electrochemical energy. The high efficiency of the electrolyzer makes it suitable to be employed in energy storage systems [29-30].

B. Fuel Cell

The FC converts chemical energy to electrical energy by oxidizing hydrogen, also producing water and heat as by-products. The fuel cells can be classified to low-temperature and high-temperature types, as shown in Fig. 4. The low-temperature fuel cells could be subdivided as proton exchange membrane, alkaline and phosphoric acid fuel cells. The high-temperature fuel cells include molten carbonate and solid oxide fuel cells.

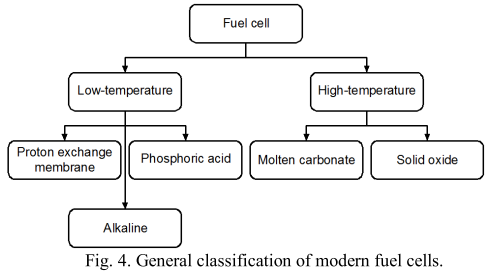

Fig. 4. General classification of modern fuel cells.

Common characteristics of fuel cells are shown in Table II.

TABLE II. COMMON CHARACTERISTICS OF FUEL CELLS

Characteristic	Proton exchange membrane	Alkaline	Phosphoric acid	Molten carbonate	Solid oxyde
Current density, A $(cm^2)^{-1}$	0.1–0.9	0.1–0.9	0.1–0.9	0.1–0.9	0.1–0.9
Voltage cell, V	0.8–0.6	0.8–0.6	0.8–0.6	0.8–0,6	0.8–0.6
Power density, W $(cm^2)^{-1}$	0.35–0.7	0.1–0.3	~0.14	0.1–0.12	0.15–0.7
H_2 consumption, $(cm^3\ H_2)(min\ A)^{-1}$	7.0	7.0	7.0	7.0	7.0
O_2 consumption, $(cm^3\ O_2)(min\ A)^{-1}$	3.5	3.5	3.5	3.5	3.5
Pressure, bar	1–2	1	1	1–10	1
Temperature, °C	30–100	below 80	150–200	600–700	850–1100
Efficiency, %	cell: 50–70 system: 30–50	cell: 60–70 system: 62	cell: 55 system: 40	cell: 55 system: 47	cell: 60–65 system: 55–60

Across the entire range of applicable sizes, fuel cell systems offer attractive electrical conversion efficiencies. As shown in Table II, the efficiency of various fuel cell systems ranges from 30% to 62% [25-26, 31]. Few small to medium-sized conventional systems can achieve efficiencies comparable to those provided by fuel cell systems at design conditions [31]. An alkaline fuel cell is a more prospective type that can be used for hydrogen buffer systems because of high efficiency and low reaction losses of oxygen reduction [23, 32].

Fig. 5 shows the efficiency of the PEM fuel cell as a function of power density [33]. The efficiency increases with a decreasing load.

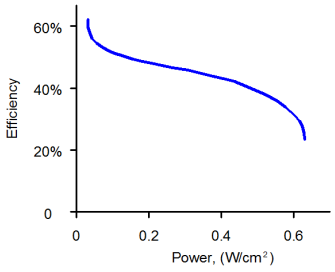

Fig. 5. Efficiency of the PEM fuel cell.

C. Hydrogen Storage

Hydrogen is one of the promising alternatives that can be used as an energy carrier. The universality of hydrogen implies that it can replace other fuels for stationary generating units for power generation in various industries. On the other hand, hydrogen storage adds complexity to system design and operation, and it is inevitable that the overall hydrogen buffer efficiency decreases. Hydrogen can be stored as compressed gas, as cryogenic liquid, in solids (metal hydrides, carbon materials) and in liquid hydrogen carriers (methanol, ammonia). Compressed gas storage is most relevant for large-scale stationary storage systems [5, 8, 34-35]. Specialized high pressure containers for hydrogen storage production are shown in Fig. 6.

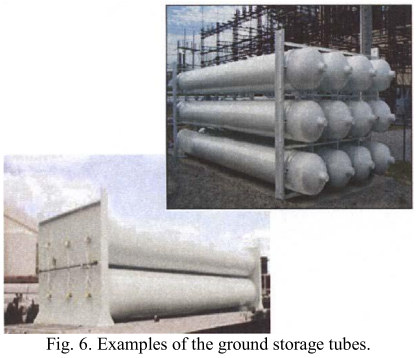

Fig. 6. Examples of the ground storage tubes.

The efficiency of the hydrogen storage methods and their leakage characteristics are summarized in Table III [36].

TABLE III. COMPARISON OF THE HYDROGEN STORAGE METHODS

Hydrogen storage methods		Efficiency, %	Leakage rate (/day)
Compressed gas	300 bar	91.5	0.000024 %
	700 bar	90.5	0.000033 %
Liquid		62.5 – 77	1%
Activated carbon (77 K)		91.7 – 93.3	0.2%
Hydrides	Low temperature (<100˚C)	90 – 93.3	-
	High temperature (>300˚C)	79 - 83	-

From Table III it can be seen that the energy lost to compress the gas is relatively low and therefore yields higher conversion efficiency [36]. Activated carbon has also high efficiency; however, a very low temperature is required during the process. Because the required energy storage time could be long due to the strong wind periods, lasting extended periods of time, a low leak rate is critical to preventing additional dynamic energy loss. The compressed gas method has a very low leakage rate compared to the other methods, high capacity and dynamic energy efficiency [37].

Hydrogen is the lightest chemical element in the periodic table. Because of this, it is rather difficult to confine. Lighter than air, it rises faster than helium when released, dispersing quickly. In order for hydrogen to combust, an oxidizer must be present, which leaves confined tanks safe from combustion. Hydrogen burns very quickly, and it takes very little energy, comparatively, for it to combust. At low concentrations, however, the energy required to combust is similar to that of other fuels. Hydrogen flames have a low radiant heat. This low level of heat near the flame lowers the risk of secondary fires compared to that of a hydrocarbon fire. Hydrogen is non-toxic, and it will not contaminate groundwater. A release of hydrogen is not known to increase any kind of pollution or contribute to it in any way. The compressed hydrogen system poses a risk in that energy is stored in the form of pressure. A rupture in a high-pressure tank is a potentially dangerous event. Clever design of tank technology is minimizing these risks, and extensive testing is being conducted to demonstrate the safety of these systems in even the most trying circumstances [6, 38].

The total energy loss of this whole system over time is plotted in Fig. 7 [36]. The total energy loss is calculated including the efficiency of the electrolyzer, that of the dynamic energy of the hydrogen storage and of the fuel cell. Others hydrogen storage methods are also plotted for comparison. This result confirms that the compressed gas method was the best solution for the hydrogen buffer system, with the maximum total efficiency being about 50%. Although half of the energy was lost during the process, it is clearly still better to recover this energy rather than just to abandon the excess renewable energy.

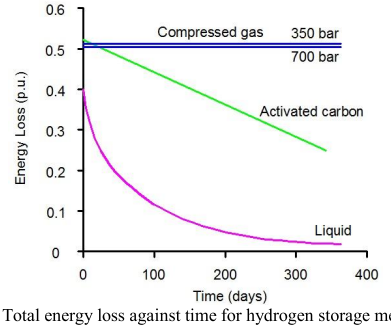

Fig. 7. Total energy loss against time for hydrogen storage methods.

III. Response Time

A. Electrolyzer

Traditionally, electrolyzers have been designed for constant hydrogen production rates. The electrolyzer must be able to follow sudden changes of operating conditions because of unforecastable periods of renewable energy production. Intermittent operation may cause impurity of hydrogen in oxygen and vice versa. The alkaline electrolyzers have increased the power consumption during start-up. PEM electrolyzers are easier to operate and provide fast start-up [5]. Fig. 8 shows the experimental response of the PEM electrolyzer voltage to a current step from 0 to 1 A [29].

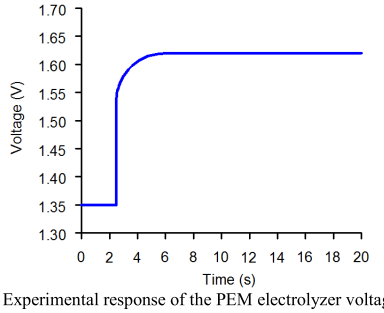

Fig. 8. Experimental response of the PEM electrolyzer voltage to a current step.

B. Fuel Cell

Renewable energy sources are connected to a local grid that feeds electricity to one or several consumers. The stochastic nature of the renewable energy requires that the source of energy should be able to respond to fast changing loads. Fuel cells do not have the capacity to respond to fast changing loads. Thus there is a need for additional energy storage (battery, supercapacitor), which can respond to the increased load instantly in order to improve the power quality of the fuel cell output [15, 39-40]. It can demand a short high power for starting or changing operating modes [27]. In renewable hydrogen systems, the low-temperature cells are considered as most interesting because of their operating flexibility regarding start-up and shut-down procedures as well as intermittent operation [5]. They can respond to load changes on the order of 0.3% to 10% per second.

C. Hydrogen Storage

Hydrogen storage systems also have a time lag in start-up, and if the storage system start-up time is longer than the fuel cell start time, the size of the battery pack must be increased to make up the difference. Minimizing the start-up time will benefit the system by reducing maintenance and operating expense [6]. Compressed hydrogen has the best start time, as hydrogen gas is available as soon as the regulator to the tank is open.

IV. Economic Reasoning

The current cost of an electrolyzer is 170$/kW, values up to 1000$/kW depending on the size of the electrolysis system [24]. The cost of the fuel cell system also starts from 175$/kW. The cost of hydrogen fuel will be an important factor for hydrogen acceptance in the commercial marketplace. Hydrogen fuel prices are typically reported on a "$/kg H2" basis. The processing cost ranges between 4 and 20 dollars per kilogram of hydrogen.

For compressed hydrogen, storage tanks are aluminum reinforced with carbon fiber. This is the cheapest type of storage vessels capable of handling 350 bar of hydrogen and is about 50000$. Vessels made entirely of carbon are available at 350 and 700 bar, but these tanks are more expensive. The cost of the compressor is approximately 50000$ [6].

For large-scale storages of hydrogen, underground storages are expected to be two orders of magnitude cheaper. However, this option requires a hydrogen storage in, for example, salt caverns or depleted natural gas reservoirs, which limits the potential usage [5-34].

Between the two ends of the economic chain, hydrogen has to be packaged by compression or liquefaction to become a commodity. In the transportation, hydrogen has to be produced, packaged, transported, stored, transferred to cars, then stored and transported again before it is finally admitted to fuel cells. There are two possibilities of hydrogen delivery:

1. road delivery,
2. pipeline delivery.

Surface transportation of hydrogen gas is expensive, especially over long distances, because of the amount of pressure required to store the hydrogen. Liquified hydrogen is denser, but liquefaction is extremely costly and energy inefficient. Nevertheless, transport using cryogenic tankers is currently the most common method because of the lack of underground pipelines. Hydrogen has a very small amount of energy by volume as compared to other fuels. Because of that, distribution and delivery are costly and result in inefficiencies associated with it. Most of the analyses show that gaseous hydrogen pipelining costs approximately 1.3 to 1.8 times more per unit energy distance than natural gas. Pipelines are very expensive to design and construct and must have high utilization to justify the initial capital cost [23, 38, 41-42].

V. Conclusions

This paper characterizes the main components of the hydrogen buffer: the electrolyzer, the hydrogen storage system and the fuel cell. In the technical economic analysis of the electrochemical stage of the hydrogen buffer the efficiency, response time and economic reasoning of the main components of the hydrogen buffer were discussed. Results showed that the efficiency of the electrolyzer (including the compressor) varies between 70% and 85%, the the efficiency of the fuel cell is in the range of 30%-62% and the efficiency of the hydrogen storage system is 90.5%. The power efficiency of the step-down and step-up DC/DC converters varies between 92% and 96%. The maximum total efficiency of the hydrogen buffer is about 50%. The diagram in Fig. 9 shows the distribution of losses between the main components of the hydrogen buffer.

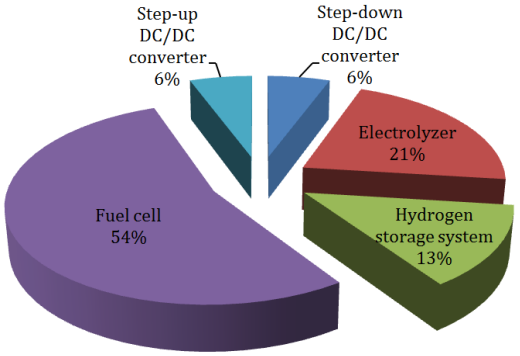

Fig. 9. Losses distribution in the hydrogen buffer system.

As it can be seen from Fig. 9, the majority of the losses occur at the stage of hydrogen conversion into electrical energy by using a fuel cell. It is impossible to improve the performance of the existing models of an electrolyzer and a fuel cell. However, it may be feasible to increase the efficiency of the interface converters that give a reduction of the overall losses. In the power electrical stage, losses of about 12% of the total efficiency are significant. Thus, it should be given special attention when modeling DC/DC converters for the power electrical stage in the hydrogen buffer.

The technical analysis of the hydrogen buffer components has revealed that the response time of the process is an insignificant parameter in the scale of the overall system and should not have an important role.

In terms of economic reasoning, the hydrogen buffer is quite an expensive system, but as time progresses, renewable energy technologies generally get cheaper, while fossil fuels get more expensive. The renewable energy penetration inevitably increases. Thus, an energy storage system is needed to stabilize renewable energy generation. Hydrogen is considered to be a versatile energy carrier for the future, complementary to electricity and with the potential to replace fossil fuels due to its characteristic of zero carbon emissions.

Acknowledgment

This research work has been supported by Estonian Ministry of Education and Research (project SF0140016s11) and Estonian Archimedes Foundation (projects „Doctoral School of Energy and Geotechnology II“ and DoRa8).

References

[1] Cavallaro, C., Chimento, F., Musumeci, S., Sapuppo, C., Santonocito, C.: *Electrolyser in H2 self-producing systems connected to DC link with dedicated phase shift converter*, International Conference on Clean Electrical Power, ICCEP ‘2007, 21-23 May 2007, pp. 632-638.

[2] Ibanez, F., Perez-Navarro, A., Sanchez, C., Segura, I., Bernal, E., Paya, J.: *Wind generation stabilization using a hydrogen buffer*, European Conference on Power Electronics and Applications, 2-5 Sept. 2007, pp. 1-10.

[3] Cavallaro, C., Cecconi, V., Chimento, F., Musumeci, S., Santonocito, C., Sapuppo, C.: *A phase-shift full bridge converter for the energy management of electrolyzer systems*, IEEE International Symposium on Industrial Electronics, ISIE’2007, 4-7 June 2007, pp. 2649-2654.

[4] Ugartemendia, J. J., Ostolaza, X., Moreno, V., Molina, J. J., Zubia, I.: *Wind generation stabilization of fixed speed wind turbine farms with hydrogen buffer*, 11th. Spanish-Portuguese Conference on Electrical Engineering (11CHLIE), 1-4 July 2009, pp. 1-5.

[5] Korpas, M., Gjengedal, T.: *Opportunities for hydrogen storage in connection with stochastic distributed generation*, 9th International Conference on Probabilistic Methods Applied to Power Systems, June 2006, pp. 1-8.

[6] Kelly, M., Briggs, A.: *Methods of hydrogen storage for standby power units*, IEEE, 2002, pp. 331-337.

[7] Takahashi, R., Otsuki, Y., Tamura, J., Sugimasa, M., Komura, A., Futami, M., Ichinose, M., Ide, K.: *A new wind generation system cooperatively controlled with hydrogen electrolyzer*, IEEE XIX International Conference on Electrical Machines, ICEM 2010, 2010, pp. 1-10.

[8] Nigim, K., Reiser, H.: *Energy storage for renewable energy combined heat, power and hydrogen fuel ($CHPH_2$) infrastructure*, IEEE Electrical Power and Energy Conference, 2009, pp. 1-6.

[9] http://www.chfca.ca

[10] Sick, N., Blug, M., Leker, J.: *The influence of raw material prices on the development of hydrogen storage materials: the case of metal hydrides*, IEEE, 2011, pp. 1-12.

[11] Nelson, D. B., Nehrir, M. H., Wang, C.: *Unit sizing of stand-alone hybrid wind/PV/fuel cell power generation systems*, IEEE, 2005, pp. 1-7.

[12] Korpaas, M., Hildrum, R., Holen, A. T.: *Optimal operation of hydrogen storage for energy sources with stochastic input*, IEEE Bologna PowerTech Conference, June 2003, pp. 1-8.

[13] Bapu, B. R. R., Karthikeyan, J., Reddy, K. V. K.: *Hydrogen storage in wind turbine tower – a review*, IEEE, 2010, pp. 308-312.

[14] Iannuzzi, D., Pagano, M.: *Efficiency of hydrogen based storage systems for stand-alone PV applications: numerical and experimental results*, IEEE, 2009, pp. 555-561.

[15] Gao, W., Zheglov, V., Wang, G., Mahajan, S. M.: *PV-wind-fuel cell-electrolyzer micro-grid modeling and control in real time digital simulator*, IEEE, 2008, pp. 29-34.

[16] Chedid, R., Chaaban, F. B., Shihab, R.: *A simplified electric circuit model for the analysis of hybrid wind-fuel cell systems*, IEEE, 2007, pp. 1-6.
[17] Doumbia, M. L., Agbossou, K., Granger, E.: *Modelling and simulations of a hydrogen based photovoltaic/wind energy system*, IEEE, 2007, pp. 2601-2606.
[18] Carr, J. A., Balda, J. C.: *A grid interface for distributed energy resources with integrated energy storage using a high frequency AC link*, IEEE Power Electronics Specialists Conference, June 2008, pp. 3774-3779.
[19] Maloney, T. M.: *An electrolysis-based pathway towards hydrogen fueling*, IEEE, 2005, pp. 487-491.
[20] Vinnikov, D., Hoimoja, H., Andrijanovits, A., Roasto, I., Lehtla, T., Klytta, M.: *An improved interface converter for a medium-power wind-hydrogen system*, IEEE Clean Electrical Power, 2009, pp. 426-432.
[21] Vinnikov, D., Andrijanovits, A., Roasto, I., Jalakas, T.: *Experimental study of new integrated DC/DC converter for hydrogen-based energy storage*, Environment and Electrical Engineering, 2011, pp. 1-4.
[22] Andrijanovits, A., Vinnikov, D., Roasto, I., Blinov, A.: *Three-level half-bridge ZVS DC/DC converter for electrolyzer integration with renewable energy systems*, Environment and Electrical Engineering, 2011, pp. 1-4.
[23] Andrijanovits, A., Egorov, M., Lehtla, M., Vinnikov, D.: *New method for stabilization of wind power generation using an energy storage technology*, Journal on Agronomy Research, vol. 8, (S1), May 2010, pp. 12-24.
[24] Ursua, A., Gandia, L. M., Sanchis, P.: *Hydrogen production from water electrolysis: current status and future trends*, IEEE, 2011, pp. 1-17.
[25] Korpas, M., Holen, A. T.: *Operation planning of hydrogen storage connected to wind power operating in a power market*, IEEE Transaction on Energy Conversion, vol. 21, no. 3, September 2006, pp. 742-749.
[26] Agbossou, K., Kolhe, M., Hamelin, J., Bose, T. K.: *Performance of a stand-alone renewable energy system based on energy storage as hydrogen*, IEEE Transaction on Energy Conversion, vol. 19, no. 3, September 2004, pp. 633-640.
[27] Agbossou, K., Doumbia, M. L., Anouar, A.: *Optimal Hydrogen production in a stand-alone renewable energy system*, IEEE, 2005, pp. 2932-2936.
[28] Wang, C., Nehrir, M. H.: *Power management of stand-alone wind/photovoltaic/fuel cell energy system*, IEEE Transaction on Energy Conversion, vol. 23, no. 3, 2008, pp. 1-11.
[29] Lopes, F. C., Watanabe, E. H.: *Experimental and theoretical development of a PEM electrolyzer model applied to energy storage system*, IEEE, 2009, pp. 775-782.
[30] Ursua, A., Gubia, E., Lopez, J., Marroyo, L., Sanchis, P.: *Electronic device for the emulation of wind system and analysis of alkaline water electrolysers*, IEEE, 2010, pp. 1-5.
[31] Ellis, M. W., Von Spakovsky, M. R., Nelson, D. J.: *Fuel cell systems: efficient, flexible energy conversion for the 21st century*, IEEE, vol. 89, no. 12, December 2001, pp. 1808-1818.
[32] T-Raissi, A., Banerjee, A., Sheinkopf, K. G.: *Current technology of fuel cell systems*, pp. 1953-1957.
[33] Laughton, M. A.: *Fuel cells*, Engineering Science and Education Journal, February 2002, pp. 7-16.
[34] Cohen, M., Snow, G. C.: *Hydrogen delivery and storage options for backup power and off-grid primary power fuel cell systems*, IEEE, 2008, pp. 1-8.
[35] Cohen, M., Kenny, K.: *Hydrogen delivery and storage options for backup power and off-grid primary power fuel cell systems: two years later*, IEEE, 2010, pp. 1-8.
[36] Yu, S., Mays, T. J., Dunn, R. W.: *A new methodology for designing hydrogen energy storage in wind power systems to balance generation and demand*, IEEE, 2009, pp. 1-2.
[37] Yu, S., Mays, T. Y., Dunn, R. W.: *Hydrogen energy storage in isolated micro-grids with wind generation*, UPEC 2010, 2010, pp. 1-5.
[38] http://h2101.harc.edu
[39] Thounthong, P., Sethakul, P., Rael, S., Davat, B.: *Performance investigation of fuel cell/battery and fuel cell/supercapacitor hybrid sources for electric vehicle applications*, IEEE, 2009, pp. 455-459.
[40] Boscaino, V., Capponi, G., Livreri, P., Marino, F.: *Fuel cell modeling for power supply systems design*, IEEE, 2008, pp. 1-4.
[41] Cohen, M., Snow, G. C.: *Hydrogen delivery and storage options for backup power and off-grid primary power fuel cell systems*, IEEE, 2008, pp. 1-8.
[42] Al-Ahmed, A., Hossain, S., Mukhtar, B., Rahman, S. U., Abualhamayel, H., Zaidi, J.: *Hydrogen highway: An overview*, Energy Conference and Exhibition (EnergyCon), 2010 IEEE International, 18-22 December 2010, pp. 642-647.

[PAPER-V] Blinov, A.; **Andrijanovits, A.** New DC/DC Converter for Electrolyzer Interfacing with Stand-Alone Renewable Energy System. Electrical, Control and Communication Engineering, Vol. 1, Issue 1, pp. 24–29, 2013.

VERSITA
Electrical, Control and Communication Engineering
doi: 10.2478/v10314-012-0004-1
2012 / 1

New DC/DC Converter for Electrolyser Interfacing with Stand-Alone Renewable Energy System

Andrei Blinov (*Research Fellow, Tallinn University of Technology*),
Anna Andrijanovits (*Doctoral student, Tallinn University of Technology*).

***Abstract* - This paper presents findings of a R&D project targeted to the development of a galvanically isolated step-down DC/DC converter for electrolyzer integration with renewable energy systems. The presented converter with an improved control algorithm for the full-bridge active rectifier features reduced energy circulation and switching losses. The performance can be improved under wide input voltage and load variations. The advantages of the converter were verified with a 1 kW converter prototype and the test results were in full agreement with the expected waveforms. The presented steady-state operation principle and mathematical analysis of the converter based on the simulation and experimental results can be used as design guidelines for component and parameter estimation in practical applications.**

***Keywords* - Distributed power generation, energy storage, hydrogen storage, zero current switching, zero voltage switching.**

I. Introduction

Use of alternative energy sources is an urgent issue today. Main advantages of renewable energy are zero fuel costs and lower impact on the environment. However, renewable energy sources, such as solar and wind power, are difficult to use due to their stochastic variability. In order for renewable energy to be generally used for regular consumers, the concept of hydrogen use needs to be introduced to stabilize unregulated renewable energy generation [1]-[4]. A typical renewable energy system (RES) must include both short-term and long-term energy storage. A short-term energy storage system is commonly used due to its high round-trip efficiency, convenience for charging/discharging. In addition, it can take care of the effects caused by instantaneous load ripples/spikes, electrolyzer transients and wind energy peaks. However, batteries alone are not appropriate for long-term energy storage because of their low energy density, self-discharge, and leakage. The combination of short-term energy storage with long-term energy storage in the form of hydrogen can improve the performance of stand-alone RES significantly.

Fig. 1 shows a hydrogen-based energy storage system or a hydrogen buffer (HB) consisting of two layers: electrochemical and power electrical stage. The electrochemical stage includes hydrogen production, hydrogen storage and electricity production. In the excess energy periods the hydrogen generation system is connected to the DC-bus of the RES. In this stage electrical energy from the renewable energy source is converted into chemical energy by using water electrolysis and this energy is stored in a tank. In order to stabilize energy production during the absence of the renewable energy, stored hydrogen could be re-used. In this stage, hydrogen is converted into electrical energy by using a fuel cell (FC). The FC takes the hydrogen from the tanks to generate electricity, plus water and heat as by-products. Combination of an energy storage system and an RES allows controllable power production.

To achieve proper voltage matching the main components of the HB should be connected to the DC-bus of RES via different power electronic converters: the electrolyzer is interfaced by help of a step-down DC/DC converter, while the fuel cell is connected by help of a step-up DC/DC converter. In principle, any basic power converter topology can be used to design a power interface for a fuel cell and an electrolyzer. Typically, these converters have a high-frequency voltage matching transformer, which could also perform the function of galvanic isolation demanded in several applications. The main technology development trend here is to reduce the power losses in the interface converters in order to obtain the highest possible energy efficiency of the HB.

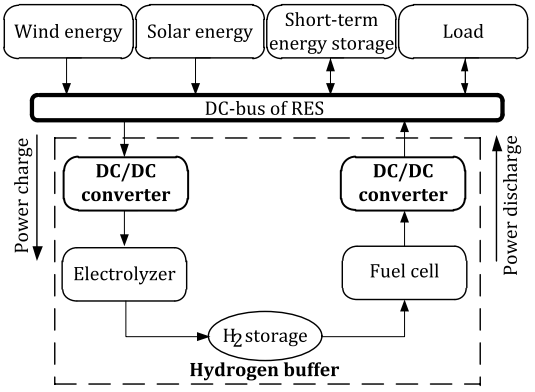

Fig. 1. Energy exchange processes in the hydrogen buffer connected to a stand-alone renewable energy system.

In the analysis of the state-of-the-art converters for the HB application it was stated that the majority of presented topologies are meant for the fuel cell integration to the RES and only minor publications [2], [3], [5]-[7] are related to the interface converters for electrolyzers.

This paper presents a new galvanically isolated step-down DC/DC converter (Fig. 2). The converter has a half-bridge inverter on its primary side, high-frequency step-down transformer and a full-bridge phase-shifted active rectifier based on reverse blocking (RB) switches on the secondary side.

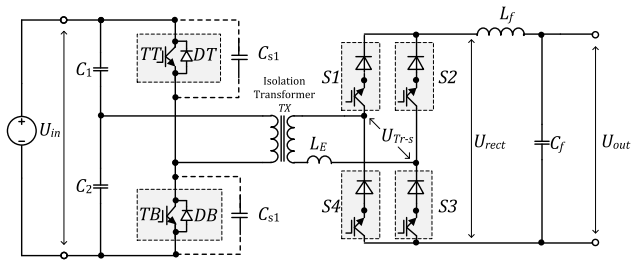

Fig. 2. Investigated half-bridge converter circuit with controlled RB switches at the secondary side.

II. Step-Down DC/DC Converter with a Full-Bridge Phase-Shifted Active Rectifier

The phase-shifted synchronous rectifier concept is a well-known method to reduce the ringing, increase the efficiency and achieve ZVS (zero voltage switching) of converter switches. The other advantages are the possibility of using non-dissipative capacitive snubbers in the inverter and constant frequency operation, allowing for simple control of the converter. Generally, these converters comprise a half- or a full-bridge inverter, a high-frequency transformer and a rectifier [8], [9]. The rectifier part could be classified as: full-bridge, central-tapped and current-doubler [10].

In converters with a synchronous rectifier the output voltage is generally controlled by the varying delay time between the turn-on of the switches in the rectifier and the turn-on of the IGBTs in the inverter. At the beginning of each half-period, the transformer current will have the same direction as in the previous one and will only change it when the other switch pair in the rectifier turns on. Therefore, at the beginning of each half-period the current will flow through the freewheeling diode of the IGBT module to be turned on next, allowing the ZVS of both inverter transistors. This switching algorithm allows non-dissipative capacitive snubbers to be used in the inverter and the inductive ones in the rectifier. The role of the latter ones could be performed by the transformer leakage inductance. The disadvantage of such control algorithms is the presence of the intervals of energy return from the load to the power supply (time intervals of the opposite sign of the current and voltage of the primary transformer winding during the delay time). If the energy return is not possible, there will be an increase of the input voltage of the inverter and a deviation of the midpoint potential of the capacitor input voltage divider. Moreover, energy circulation corresponds to the generation of the reactive power, resulting in the reduction of the converter power factor and the efficiency due to increased conduction losses. In the case of high input voltage (large periods of energy return), the effects of these drawbacks could be inacceptable. One of the ways to reduce such effects is to increase the capacitance value of the input voltage divider, however, that leads to an increase in the dimensions and cost of the converter.

III. Operating Principle

To overcome the disadvantages of a conventional phase-shifted synchronous rectifier, the control algorithm of the rectifier switches could be modified, at the same time keeping the advantages of the reference phase-shifted control algorithm [11]. A similar concept for the full-bridge converter was first introduced in [12]. The proposed algorithm provides phase-shifted control whereas practically no energy is returned into the power supply. This is achieved by introducing two additional switching states of the rectifier switches. The voltage and current waveforms of the converter are presented in Fig. 3 with the associated switching states shown in Fig. 4.

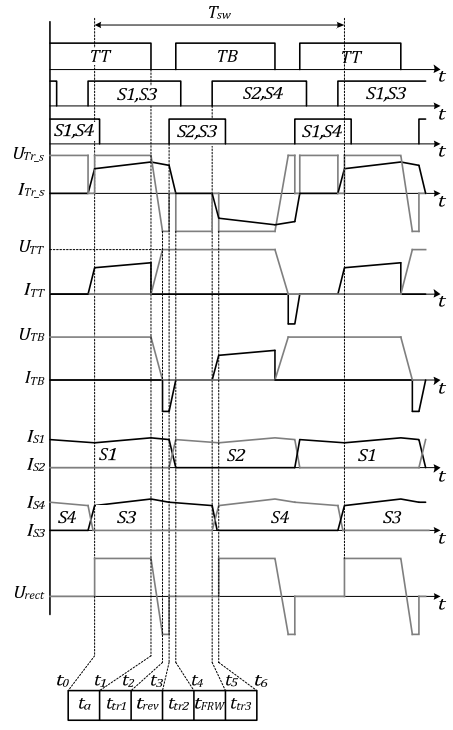

Fig. 3. Generalised operation principle of a proposed converter with a phase-shifted active full-bridge rectifier.

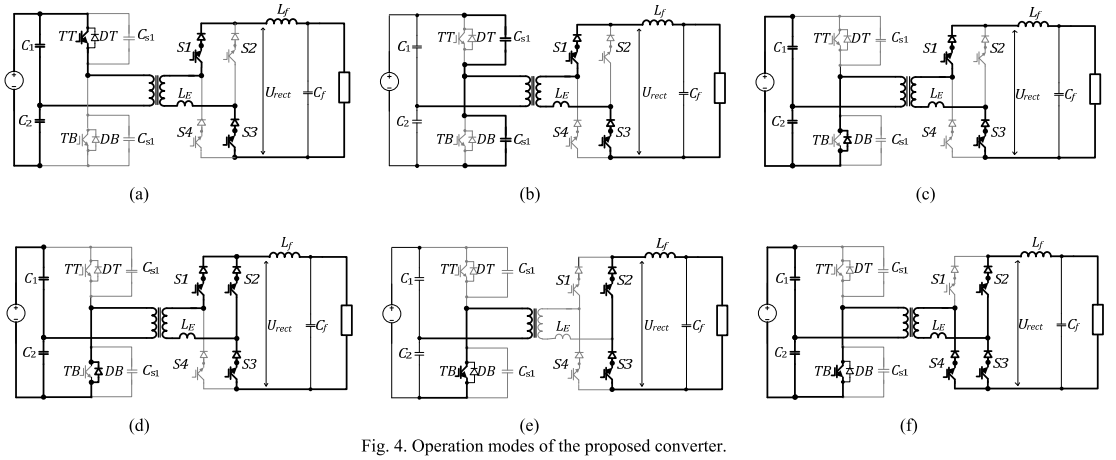

Fig. 4. Operation modes of the proposed converter.

The following events during the switching half-period could be distinguished:

t_0-t_1 – transistor *TT* and switches *S1*, *S3* are conducting (Fig. 4a). The voltage of the transformer primary winding is $+U_{in}/2$, and at the output, the voltage of the rectifier is $+U_{Tr\text{-}s}$. Switch *S4* could be turned off with ZCS.

t_1-t_2 – transistor *TT* is turned off. The transformer voltage and U_{rect} change their sign as the snubber capacitors are recharged (Fig. 4b).

t_2-t_3 – the snubber capacitors are recharged and the transformer primary voltage reaches $-U_{in}/2$. The freewheeling diode *DB* opens, starting the energy return interval and the transistor *TB* could be opened with ZVS from now on. The output voltage of the rectifier is now $-U_{Tr\text{-}s}$ (Fig. 4c). Until the moment t_3 the processes do not differ from the corresponding ones in the conventional phase-shifted synchronous rectifier.

t_3-t_4 – switch *S2* is now opened (Fig. 4d). The voltage across the transformer secondary drops to zero and the transformer current decreases gradually, as the load current transfers from *S1* to *S2* with *di/dt* limited by the circuit equivalent inductance.

t_4-t_5 – the energy return interval is over, the negative voltage $-U_{Tr\text{-}s}$ is applied to the transformer secondary and switch *S1*, which can be turned off now with ZCS. Only small magnetising current is flowing through the transformer primary. The load current freewheels through *S3*, *S2*, L_f and the load (Fig. 4e).

t_5-t_6 – switch *S4* is opened (Fig. 4f). The voltage across the transformer secondary drops to zero and the transformer and the *TB* current increase gradually, as the load current transfers from *S3* to *S4* with *di/dt* limited by the circuit equivalent inductance.

The processes are then repeated with the difference that the transistors and the primary side diodes replace each other, so do switches *S1*, *S2* and *S3*, *S4*.

The control of the output voltage can be achieved by varying the current freewheeling duration *ts* (time interval *t3*-*t6*). The energy return interval (time interval *t2*-*t3*) could be constant and should be kept as short as possible in order to maintain high power factor and reduce conduction losses.

IV. Some Design Guidelines

This section provides guidelines for the selection of the parameters for the experimental converter with the phase-shifted active full-bridge rectifier (AFBR). In order to simplify the calculations it is assumed that the opponents are lossless, the input capacitors and the transformer magnetising inductance are large enough and therefore the input voltage ripple and the magnetising current are negligible. For the introduced modified control algorithm, six PWM channels are used. The inverted control signals of *S1* and *S2* are shifted by the ratio D_γ relative to the turn-off of inverter switches (Fig. 5). The inverted control signals for *S3* and *S4* are shifted by the ratio D_s relative to *S1* and *S2*. Rectifier channels have a constant duty cycle and the output voltage is regulated by varying the ratio D_s. The values of D_γ and D_s are defined as follows:

$$D_\gamma = \frac{t_3 - t_1}{T}, \tag{1}$$

$$D_s = \frac{t_6 - t_3}{T} = \frac{t_s}{T}. \tag{2}$$

The active state duty cycle D_a of the converter can be calculated by

$$D_a = \frac{t_a}{T} = \frac{T_{sw} - 2 \cdot t_s - 2 \cdot t_{tr1} - 2 \cdot t_{rev}}{2 \cdot T_{sw}}. \quad (3)$$

The output voltage can be expressed by the following equation:

$$U_{out} = \frac{N_s}{N_p} \cdot \frac{U_{in} \cdot (t_a - t_{rev})}{T_{sw}}, \quad (4)$$

and the amplitude voltage across the transformer secondary is

$$U_{Tr-s} = \frac{U_{out} \cdot T_{sw}}{2 \cdot (t_a - t_{rev})}. \quad (5)$$

The average and maximum collector currents of inverter transistors are calculated by

$$I_C = \frac{P_{out} \cdot T}{U_{in} \cdot (t_a - t_{rev})}, \quad (6)$$

$$I_{C(max)} = I_C + \frac{N_s}{N_p} \cdot \frac{\Delta I_{ripple}}{2}, \quad (7)$$

where ΔI_{ripple} is the filter inductor L_f peak-to-peak current ripple.

The inverter switches require a certain dead time t_d to recharge snubber capacitors to maintain the ZVS condition, hence the following expression must be satisfied:

$$t_d \geq t_{tr1} = \frac{2 \cdot U_{in} \cdot C_s}{I_{C(max)}}. \quad (8)$$

According to this equation, the most demanding point is at the minimum load and the maximum input voltage.

Certain time is required for the current of the rectifier switches to fall to zero during the natural commutation, therefore the rectifier switches should operate with a duty cycle higher than 0.5 to maintain the ZCS condition and exclude the situation when only one transistor in the rectifier is turned on. The additional time required can be equal for all the rectifier switches and is estimated from t_{tr2}:

$$D_{rect} \geq \frac{1}{2} + \frac{t_{tr2}}{T_{sw}} = \frac{1}{2} + L_E \cdot \frac{2 \cdot P_{out} \cdot (t_a - t_{rev})}{U_{out}^2 \cdot T_{sw}}, \quad (9)$$

where L_E is the equivalent inductance, which is mainly represented by the leakage inductance of the transformer secondary winding.

To estimate the parameters of the output filter inductor it is assumed that the current of the inductor is continuous:

$$L_f = \frac{(U_{Tr-s} - U_{out}) \cdot t_a}{\Delta I_{ripple}} = \frac{t_a \cdot U_{out}^2}{P_{out} \cdot k_L} \cdot \left[\frac{1}{2 \cdot f_{sw} \cdot (t_a - t_{rev})} - 1 \right], \quad (10)$$

where k_L is the relative current ripple of the output filter inductor :

$$k_L = \frac{\Delta I_{ripple} \cdot U_{out}}{P_{out}}. \quad (11)$$

The capacitance of the output filter capacitor can be approximated as:

$$C_f = \frac{\Delta I_{ripple} \cdot t_a}{\Delta U_{ripple}} = \frac{t_a \cdot k_L \cdot P_{out}}{k_U \cdot U_{out}^2}, \quad (12)$$

where ΔU_{out} is the peak-to-peak output voltage ripple and k_U is the relative voltage ripple.

$$k_U = \frac{\Delta U_{out}}{U_{out}}, \quad (13)$$

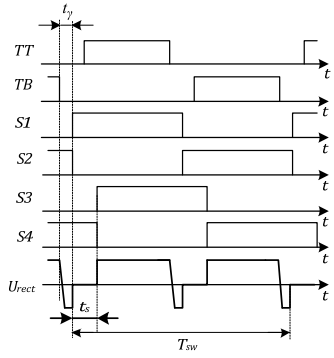

(a)

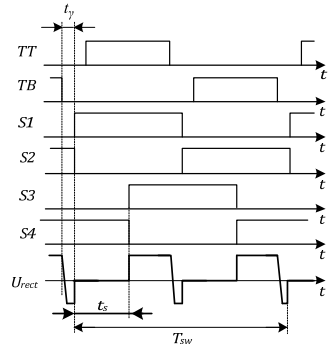

(b)

Fig. 5. New control algorithm for the converter with a phase-shifted active rectifier at maximal (a) and minimal (b) input voltages.

Fig. 6 presents the relationship between the normalised output voltage ($U_{out}/U_{Tr\text{-}s}$) and the freewheeling state duty ratio D_s.

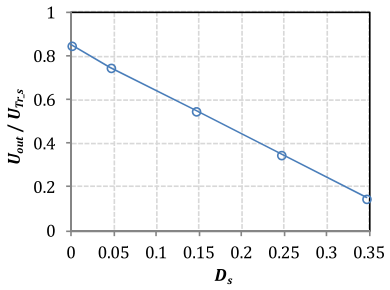

Fig. 6. Output voltage regulation characteristics ($D\gamma$=0.025).

V. Simulation and Experimental Results

In order to verify the theoretical approach the proposed converter was simulated using PSIM software. The simulation parameters were selected to the data presented in Table I.

TABLE I

Parameters and Components of the Experimental Prototype

Parameter	Symbol	Value / Type
Input voltage, V	U_{in}	500…620
Output voltage, V	U_{out}	70
Switching frequency, kHz	f_{sw}	10
Transformer turns ratio	N_s/N_p	0.5
Output filter capacitance, uF	C_f	220
Output filter inductance, mH	L_f	1.5
Inverter switch	*TT*, *TB*	BSM75GB120DLC
Rectifier switch	*S1-S4*	IXFX 48N60P
Rectifier diode		ON MBR40250
Output power, W	P_{out}	2000

As shown in Fig. 7, the simulation results were in full agreement with the estimated waveforms.

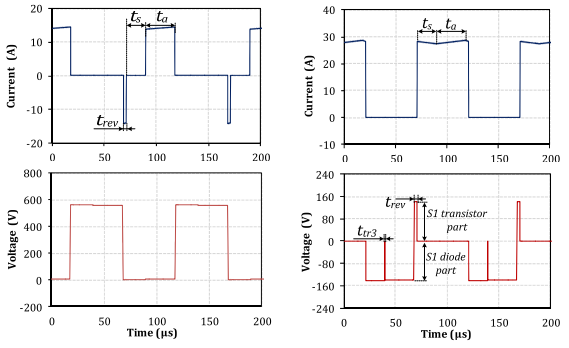

(a) (b)

Fig. 7. Simulated voltage and current waveforms of the *TT* IGBT module (a) and *S1* switch (b).

To experimentally validate a theoretical background a small-scale prototype with the output power of 1 kW was assembled. Six independent PWM channels were used. Two channels with small dead time were used to drive IGBTs in the inverter and four channels were used to control the rectifier. As mentioned, rectifier switches should have reverse blocking capability. In the prototype, MOSFETs with series connected diodes were used. In practical applications these switches could be replaced by reverse-blocking IGBTs or fast thyristors for reduced power dissipation during the on- state. The main parameters and components are presented in Table I.

The experimental waveforms are presented in Fig. 8. As shown, the test results completely correspond to the theoretically predicted waveforms.

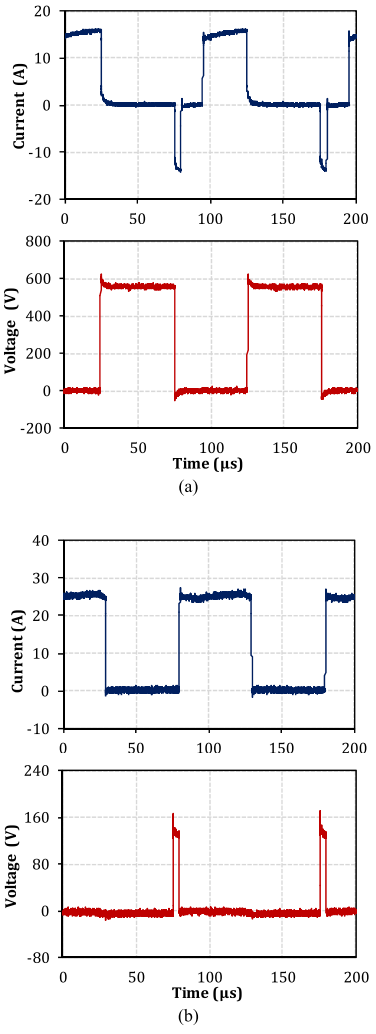

(a)

(b)

Fig. 8. Experimental voltage and current waveforms of the *TT* IGBT module (a); *S1* transistor (b) (*Uin*=350 V; *fsw*=10 kHz, 800 W load).

VI. Conclusions

This paper presents a novel galvanically isolated step-down DC/DC converter for electrolyzer integration with stand-alone renewable energy systems. The design of the converter with several recommendations and guidelines are outlined. To validate the topology, the simulation and experimental results are presented and discussed. According to the results, the presented step-down DC/DC converter topology with a phase-shifted active rectifier could be one of the most promising candidates for high-power conversion systems due to its reduced switching losses and a wide regulation range.

References

[1] Andrijanovitš, A.; Egorov, M.; Lehtla, M.; Vinnikov, D. "New Method for Stabilization of Wind Power Generation Using an Energy Storage Technology". Journal on Agronomy Research, vol. 8, (S1), pp. 12-24, May 2010.

[2] Cavallaro, C.; Chimento, F.; Musumeci, S.; Sapuppo, C.; Santonocito, C. "Electrolyser in H2 Self-Producing Systems Connected to DC Link with Dedicated Phase Shift Converter", International Conference on Clean Electrical Power, ICCEP '2007, pp. 632-638, 21-23 May 2007.

[3] Cavallaro, C.; Cecconi, V.; Chimento, F.; Musumeci, S.; Santonocito, C.; Sapuppo, C. "A Phase-Shift Full Bridge Converter for the Energy Management of Electrolyzer Systems", IEEE International Symposium on Industrial Electronics, ISIE'2007, pp. 2649-2654, 4-7 June 2007

[4] Ugartemendia, J.J.; Ostolaza, X.; Moreno, V.; Molina, J.J.; Zubia; I. "Wind generation stabilization of fixed speed wind turbine farms with hydrogen buffer", 11th. Spanish-Portuguese Conference on Electrical Engineering (11CHLIE), pp. 1-5, 1-4 July 2009.

[5] Vinnikov, D.; Hõimoja, H.; Andrijanovits, A.; Roasto, I.; Lehtla, T.; Klytta, M. "An improved interface converter for a medium-power wind-hydrogen system", 2009 International Conference on Clean Electrical Power, pp.426-432, 9-11 June 2009.

[6] Gautam, D.S.; Bhat, A.K.S. "A comparison of soft-switched DC-to-DC converters for electrolyser application", 2006. India International Conference on Power Electronics (IICPE'2006), pp. 274-279, 19-21 Dec. 2006.

[7] Andrijanovits, A.; Vinnikov, D.; Roasto, I.; Blinov, A.; , "Three-level half-bridge ZVS DC/DC converter for electrolyzer integration with renewable energy systems," Environment and Electrical Engineering (EEEIC), 2011 10th International Conference on , vol., no., pp.1-4, 8-11 May 2011.

[8] Yingqi Zhang; Sen, P.C.; "A new ZVS phase-shifted PWM DC/DC converter with push-pull type synchronous rectifier", Canadian Conference on Electrical and Computer Engineering, IEEE CCECE'03, vol.1, pp. 395- 398 vol.1, 4-7 May 2003.

[9] Hong Mao; Abu-Qahouq, J.A.; Shiguo Luo; Batarseh, I.; "Zero-voltage-switching (ZVS) two-stage approaches with output current sharing for 48 V input DC-DC converter", Nineteenth Annual IEEE Applied Power Electronics Conference and Exposition, APEC'04, vol.2, pp. 1078- 1082 vol.2, 2004.

[10] Chiu, H.J.; Lin, L.W.; Mou, S.C.; Chen, C.C.; "A soft switched DC/DC converter with current-doubler synchronous rectification", The 4th International Power Electronics and Motion Control Conference, IPEMC'04, vol.2, pp.526-531 Vol.2, 14-16 Aug. 2004

[11] Blinov, A.; Ivakhno, V.; Zamaruev, V.; Vinnikov, D.; Husev, O. "A Novel High-Voltage Half-Bridge Converter with Phase-Shifted Active Rectifier", IEEE International Conference on Industrial technology, ICIT'2012, pp.967-970, 19-21 March 2012.

[12] Moisseev, S.; Soshin, K.; Sato, S.; Gamage, L.; Nakaoka, M.; "Novel soft-commutation DC-DC power converter with high-frequency transformer secondary side phase-shifted PWM active rectifier", IEE Proceedings - Electric Power Applications, vol.151, no.3, pp. 260- 267, 8 May 2004.

Andrei Blinov received his B.Sc. and M.Sc. techn. in electrical drives and power electronics from Tallinn University of Technology, Tallinn, Estonia, in 2005 and 2008, respectively. From 2008 he pursues doctoral studies in Tallinn University of Technology.

Andrei Blinov is a Research Fellow in the Department of Electrical Drives and Power Electronics, Tallinn University of Technology. His research interests are in simulation and research of switchmode power converters, semiconductor heat dissipation and different cooling systems.

Anna Andrijanovitsh received B.Sc. and M.Sc. degrees in electrical engineering from Tallinn University of Technology, Tallinn, Estonia, in 2006 and 2008, respectively.

She is presently PhD student in the Department of Electrical Drives and Power Electronics, Tallinn University of Technology.

Her research interests include switchmode power converters, modeling and simulation of power systems, applied design of power converters and development of energy storage systems.

[PAPER-VI] **Andrijanovitš, A.**; Vinnikov, D.; Roasto, I.; Blinov, A. Three-Level Half-Bridge ZVS DC/DC Converter for Electrolyzer Integration with Renewable Energy Systems. 10th International Conference on Environment and Electrical Engineering (EEEIC´11), Rome (Italy), IEEE, pp. 683 – 686, 2011.

Three-Level Half-Bridge ZVS DC/DC Converter for Electrolyzer Integration with Renewable Energy Systems

Anna Andrijanovitš, Dmitri Vinnikov, Indrek Roasto and Andrei Blinov
Department of Electrical Drives and Power Electronics
Tallinn University of Technology
Ehitajate tee 5, 19086 Tallinn, Estonia
dmitri.vinnikov@ieee.org

Abstract— **This paper presents findings of a R&D project targeted to the development of a galvanically isolated step-down DC/DC converter for electrolyzer integration with renewable energy systems. The topology proposed is a three-level neutral point clamped half-bridge with a high-frequency isolation transformer and a current doubler rectifier that fulfils all the targets set by the designers. Despite an increased component count the proposed converter is very simple in design and operation. The paper outlines the design with several recommendations and guidelines, and also discusses the experimental results obtained.**

Keywords- renewable energy systems, electrolyzer, interface converter, control methodology, efficiency

I. INTRODUCTION

Hydrogen is one of the promising alternatives that can be used as an energy carrier. The universality of hydrogen implies that it can replace other fuels for stationary generating units for power generation in various industries. Having all the advantages of fossil fuels, hydrogen is free of harmful emissions when used with dosed amount of oxygen, thus reducing the greenhouse effect [1].

In recent years, implementation of hydrogen-based long-term energy storages in renewable energy systems (RES) has attracted much attention [1-4]. Essential elements of such a hydrogen buffer (HB) comprise an electrolyzer, a hydrogen storage system and a fuel cell. Outside peak periods, excess electricity of a RES would be converted to hydrogen by help of an electrolyzer and during the peak demands when more power is needed, hydrogen could be converted to electricity by help of a fuel cell. Water to hydrogen conversion efficiency is averaged at 65 % and fuel cell conversion efficiency is 65 - 70 %, which ends up to 20 - 40 % overall efficiency of the hydrogen buffer [5-7].

To achieve proper voltage matching the main components of the HB should be connected to the DC-bus of RES via different power electronic converters: the electrolyzer is interfaced by help of a step-down DC/DC converter, while the fuel cell is connected by help of a step-up DC/DC converter. In principle, any basic power converter topology can be used to design a power interface for a fuel cell and an electrolyzer. Typically, these converters have a high-frequency voltage matching transformer, which could also perform the function of galvanic isolation demanded in several applications. The main technology development trend here is to reduce the power losses in the interface converters in order to obtain the highest possible energy efficiency of the HB.

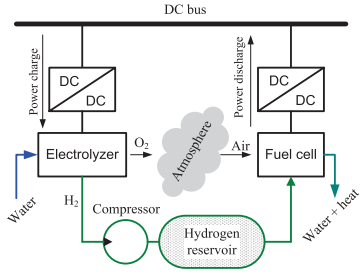

Figure 1. Energy exchange processes of the hydrogen based energy storage [8]

In the analysis of the state-of-the-art converters for the HB application it was stated that the majority of presented topologies are meant for the fuel cell integration to the RES and only minor publications [2, 3, 9, 10] are related to the interface converters for electrolyzers.

This paper proposes a new galvanically isolated step-down DC/DC converter for electrolyzer integration with renewable energy systems (Fig. 2). The three-level neutral point clamped (3L-NPC) half-bridge inverter implemented in the primary side of the converter features inherent zero-voltage switching (ZVS), thus increasing the efficiency of the interface converter. The PMW control algorithm presented permits all transistors to be operated under ZVS without additional components merely utilizing parasitic elements of the circuit, such as junction and freewheeling diode capacitances across each IGBT, and leakage inductance of the isolation transformer. Moreover, the current doubler rectifier (CDR) introduced with coupled inductors offers loss reduction in the secondary side of the converter in contrast to the traditional full-bridge rectifier due to the twice reduced operation current of the rectifier diodes and the secondary winding of the transformer.

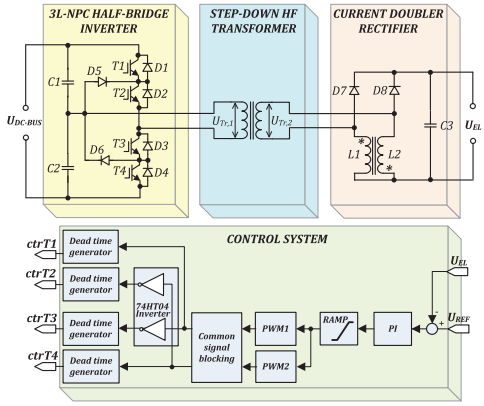

Figure 2. Step-down DC/DC converter for electrolyzer integration with renewable energy systems.

II. New Step-Down DC/DC Converter for Electrolyzer Integration

The proposed converter is very simple in design and operation. The terminal voltage of the electrolyzer could be simply regulated by the duty cycle variation of the transistors *T1…T4*. Neglecting losses in components, the voltage U_{EL} could be estimated as

$$U_{EL} = \frac{U_{DC-BUS}}{2 \cdot n} \cdot D, \quad (1)$$

where U_{DC-BUS} is the DC-bus voltage of the main system (input voltage of the converter), D is the duty cycle of the inverter switches (*T1…T4*) and n is the turns ratio of the isolation transformer:

$$n = \frac{U_{Tr,1}}{U_{Tr,2}}, \quad (2)$$

where $U_{Tr,1}$ and $U_{Tr,2}$ are the amplitude voltages of the primary and secondary windings of the isolation transformer, respectively.

To validate the proposed topology the experimental setup with the power rating of 2kW was assembled. Operating parameters and component values of the experimental setup are listed in Table I.

TABLE I. Operating Parameters of the Experimental Setup

PARAMETER	VALUE
Nominal input voltage, U_{DC-BUS}	560 V
Rated voltage of electrolyzer, U_{EL}	70 V
Switching frequency, f	20 kHz
Capacitance of *C1* and *C2*	60 uF
Capacitance of *C3*	220 uF
Inductance of *L1* and *L2*	1.2 mH
Nominal duty cycle of inverter, D	0.40

The experimental converter was comprehensively tested in different operation conditions and has shown excellent performance despite its simple structure and control principle. In the following sections practical novelties introduced in the converter as well as some experimental results will be presented, analyzed and discussed.

III. 3L-NPC Half-Bridge Inverter with ZVS Capability

A. Operation and control principle

The operation of a 3L-NPC half-bridge inverter can be generally divided into four operating modes: two conduction and two freewheeling modes. The first - the positive conduction mode - operates when *T1* and *T2* are on and *T3* and *T4* are off. In that mode the current flows from the input and through transistors *T1* and *T2*, the isolation transformer, and the capacitor *C2*. The second mode - the positive freewheeling mode - when *T1* and *T4* are off, *T2* and *T3* are on and *D5* is conducting. This mode is followed by the negative conduction mode (*T1* and *T2* are off and *T3* and *T4* are on) and the negative freewheeling mode (*T1* and *T4* are off, *T2* and *T3* are on and *D6* is conducting). An explanatory timing diagram of the inverter switches and the resulting primary winding voltage of the isolation transformer are presented in Fig. 3.

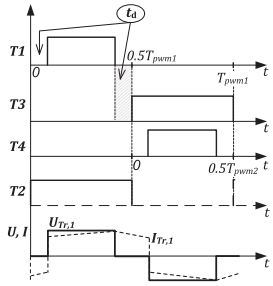

Figure 3. Generalized timing diagram of transistors *T1...T4* of 3L-NPC half-bridge inverter and the resulting primary winding voltage and current of the isolation transformer.

Since the 3L-NPC half-bridge inverter has four transistors, four independent PWM channels are also required, which increase the complexity of the control program and load the controller. A new concept that uses hardware based signal multiplication circuit was proposed in the current research project. By use of this method, only two independent PWM channels (*PWM1* and *PWM2*, Fig. 2) are needed. The control is made very easy: outer transistors *T1* and *T4* are controlled directly from the PWM generators of a microcontroller, while

inner switches *T3* and *T2* are driven by the inversions of the corresponding control PWM signals. These inversions are derived by the external inverter logic (NOT gate) realized by the logic IC - 74HT04 HEX inverter. The resulting four control signals (*ctrT1*, *ctrT2*, *ctrT3*, *ctrT4*) are provided with a dead time t_d (Fig. 3) that is generated by the simple RC delay circuit presented in Fig. 4*a*.

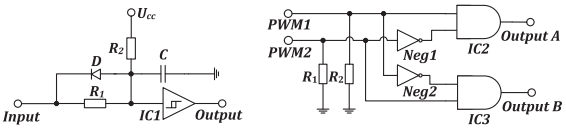

(a) (b)

Figure 4. Implemented dead time generator with the Schmidt trigger (a) and the common signal blocking circuit (b).

The dead time circuit (Fig. 4*a*) provides no protection against common signals, which can be caused by some software error or EMI impact. In order to ensure the required protection the common signal blocking circuit was introduced, as shown in Fig. 4*b*. The negation gates (*Neg1, Neg2*) block the common signal while the "pull down" resistors (*R1* and *R2*) force the PWM outputs to zero during microcontroller reset or a failure situation.

As shown in Fig. 2, the output voltage of the converter is controlled with the classical voltage mode control algorithm. Thus, the output voltage is measured for the control loop feedback. Also, the control system receives feedback signals from three additional sensors: the output current is used to identify overload conditions. In order to detect volt-second unbalance of the transformer primary, the capacitor voltage U_{C2} is measured. The input voltage $U_{DC\text{-}BUS}$ is sensed to detect over- and undervoltage situations.

B. Inherent zero-voltage switching of 3L-NPC half-bridge inverter

The presented PWM control method (Fig. 3) provides the 3L-NPC half-bridge inverter with the zero-voltage switching of all transistors without any additional components (Figs. 5 and 6). The sufficient condition for ZVS is that the isolation transformer should have relatively high leakage inductance of windings and the dead time implemented should be smaller than the time needed to utilize the leakage energy. Also, Figs. 5 and 6 show that all the transistors have a hard turn-off, which results in remarkable turn-off losses. However, reducing the leakage inductance of the isolation transformer together with the 20-40% decrease of the duty cycle will result in zero-voltage/zero-current switching of the inner transistors *T2* and *T3*.

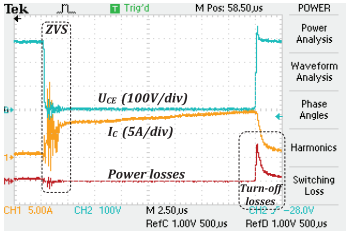

Figure 5. ZVS operation of outer transistors *T1* and *T4* in 3L-NPC half-bridge inverter (duty cycle *D*=0.4).

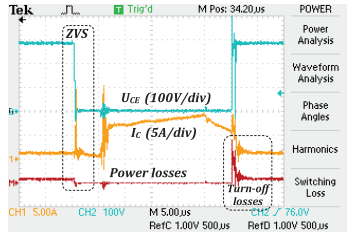

Figure 6. ZVS operation of inner transistors *T2* and *T3* in 3L-NPC half-bridge inverter (duty cycle *D*=0.4).

IV. Isolation Transformer and Current Doubler Rectifier

A. Isolation transformer

The isolation transformer is required for voltage matching between the primary and secondary parts of the converter as well as for providing galvanic isolation between the DC-link of a RES and the electrolyzer. The desired turns ratio of the isolation transformer could be derived from (1) as follows:

$$n = \frac{U_{Tr,1}}{U_{Tr,2}} = \frac{D}{2} \cdot \frac{U_{DC-BUS}}{U_{EL}} = \frac{0.4}{2} \cdot \frac{560}{70} = 1.6\,.$$

The 2 kW prototype transformer assembled for the project has been constructed on the EPCOS UI93/104/30 ferrite core (A_e=840 mm^2, V_e=217·10^3 mm^3) and has 24 turns of 135x0.2mm litz wire on the primary and 15 turns of the copper foil tape 40x0.4mm on its secondary side. The experimental voltage and current waveforms of the developed transformer are presented in Fig. 7.

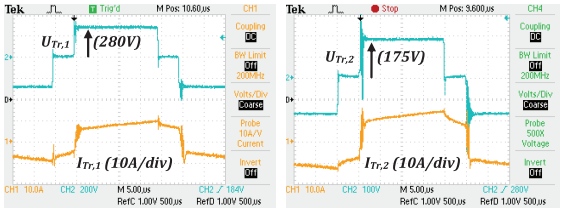

(a) (b)

Figure 7. Experimental voltage and current waveforms of the isolation transformer: primary (a) and secondary (b) winding.

B. Ripple current calcellation effect of CDR

To improve the power density of the interface converter it was decided to implement the current doubler rectifier (Fig. 2). The main problem of the full-bridge rectifier (FBR) based topologies is the increased losses in the converter secondary side, which are caused by the higher current in the transformer secondary winding and increased conduction losses of the rectifier bridge caused by the current having to go through two diodes in each half-cycle. The filter inductances can be estimated by

$$L_1 = L_2 = \frac{U_{EL} \cdot (1 - D)}{\Delta I_L \cdot f_{sw}}\,, \qquad (3)$$

where U_{EL} is the output voltage, D is the duty cycle, ΔI_L is the inductor ripple current, and f_{sw} is the switching frequency.

In contrast to the FBR, the CDR adds one more inductor to the circuit. However, this penalty could be partially alleviated by the implementation of the coupled inductors concept, where both inductors *L1* and *L2* share a common magnetic core. In the current project in order to match the 25% peak-to-peak output current ripple the 2 kW coupled inductor was designed (Fig. 8*a*). Final specifications are: Metglas AMCC -200 core (A_C=7.8 cm^2, W_A=20.8 cm^2, air gap 2x1.4 mm), *N1*=*N2*=34 turns of copper foil tape 58x0.2mm. The inductor was implemented in combination with ultrafast recovery diodes (*D7* and *D8*) and experimental current waveforms of coupled inductor windings and the resulting output current of the converter are shown in Fig. 8*b*. Thanks to the high coupling coefficient used in the current design (k>0.94) the operating currents of windings have significantly reduced ripple, which finally features at around 1.14 and 1.3 times decreased rms current values in both windings of the inductor as well as in the secondary winding of the isolation transformer, respectively. As a consequence, the winding losses of the isolation transformer and the coupled inductor were proportionally reduced. Moreover, thanks to the ripple cancellation effect of the CDR the output current of the converter (sum of the two winding currents) has the twice reduced ripple as compared to that of each winding of the coupled inductor (Fig. 8*b*).

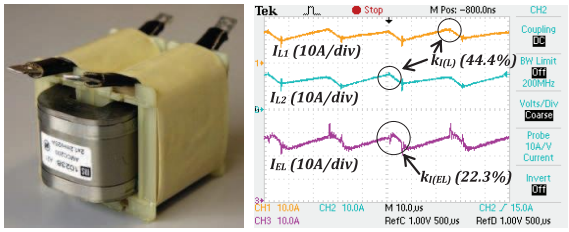

(a) (b)

Figure 8. Developed 2 kW coupled inductor (a) and measured current waveforms of coupled inductor windings and the resulting output current (b).

The CDR based secondary side of the converter could be further optimized by the implementation of fully integrated magnetic structures that implement the transformer and two inductors on a single magnetic core [11]. It will lead to the reduction of interconnection losses as well as to an increase in power density.

V. CONCLUSIONS

This paper presents a new galvanically isolated step-down DC/DC converter for electrolyzer integration with renewable energy systems. The design of the converter with several recommendations and guidelines are outlined. To validate the topology, the experimental results are presented and discussed.

The three-level neutral point clamped (3L-NPC) half-bridge inverter implemented in the primary side of the converter provides a possibility of transistor implementation with the blocking voltage twice reduced in comparison with the traditional two-level configuration. This finally means that faster IGBTs with reduced saturation voltage could be implemented to achieve more compact design and higher efficiency of the converter. Moreover, the 3L-NPC half-bridge inverter together with the presented PWM control permits all the transistors to be operated under ZVS without additional components merely utilizing parasitic elements of the circuit.

To decrease the losses caused by the high operation currents in the secondary side of the converter the current doubler rectifier was introduced. Thanks to the implemented coupled inductor with a high coupling coefficient the rms currents (and losses also) were reduced in both windings of the inductor as well as in the secondary winding of the isolation transformer. The discussed topology has shown an efficiency of 95% at maximum power and could be recommended for implementation in residential renewable energy systems.

ACKNOWLEDGMENT

This research work has been supported by Estonian Ministry of Education and Research (Project SF0140016s11), Estonian Science Foundation (Grant ETF8538), Estonian Archimedes Foundation (project ”Doctoral School of Energy and Geotechnology-II“).

REFERENCES

[1] Andrijanovitš, A.; Egorov, M.; Lehtla, M.; Vinnikov, D. "New Method for Stabilization of Wind Power Generation Using an Energy Storage Technology". Journal on Agronomy Research, vol. 8, (S1), pp. 12-24, May 2010.

[2] Cavallaro, C.; Chimento, F.; Musumeci, S.; Sapuppo, C.; Santonocito, C. "Electrolyser in H2 Self-Producing Systems Connected to DC Link with Dedicated Phase Shift Converter", International Conference on Clean Electrical Power, ICCEP ‘2007, pp. 632-638, 21-23 May 2007.

[3] Cavallaro, C.; Cecconi, V.; Chimento, F.; Musumeci, S.; Santonocito, C.; Sapuppo, C. "A Phase-Shift Full Bridge Converter for the Energy Management of Electrolyzer Systems", IEEE International Symposium on Industrial Electronics, ISIE’2007, pp. 2649-2654, 4-7 June 2007.

[4] Ugartemendia, J.J.; Ostolaza, X.; Moreno, V.; Molina, J.J.; Zubia; I. "Wind generation stabilization of fixed speed wind turbine farms with hydrogen buffer", 11th. Spanish-Portuguese Conference on Electrical Engineering (11CHLIE), pp. 1-5, 1-4 July 2009.

[5] Smith, S.C.; Sen, P.K.; Kroposki, B. "Advancement of energy storage devices and applications in electrical power system", 2008 IEEE Power and Energy Society General Meeting - Conversion and Delivery of Electrical Energy in the 21st Century, pp. 1-8, 20-24 July 2008.

[6] Nigim, K.; Reiser, H. "Energy storage for renewable energy combined heat, power and hydrogen fuel (CHPH2) infrastructure", 2009 IEEE Electrical Power & Energy Conference (EPEC), pp.1-6, 22-23 Oct. 2009.

[7] Choi, S.S.; Tseng, K.J.; Vilathgamuwa, D.M.; Nguyen, T.D. "Energy storage systems in distributed generation schemes", 2008 IEEE Power and Energy Society General Meeting - Conversion and Delivery of Electrical Energy in the 21st Century, pp. 1-8, 20-24 July 2008.

[8] S. Faias, P. Santos, J. Sousa, R. Castro. "An Overview on Short and Long-Term Response Energy Storage Devices for Power Systems Applications", International Conference On Renewable Energies and Power Quality (ICREPQ'08), 6 p., 2008.

[9] Vinnikov, D.; Hõimoja, H.; Andrijanovits, A.; Roasto, I.; Lehtla, T.; Klytta, M. "An improved interface converter for a medium-power wind-hydrogen system", 2009 International Conference on Clean Electrical Power, pp.426-432, 9-11 June 2009.

[10] Gautam, D.S.; Bhat, A.K.S. "A comparison of soft-switched DC-to-DC converters for electrolyser application", 2006. India International Conference on Power Electronics (IICPE’2006), pp. 274-279, 19-21 Dec. 2006.

[11] Jian Sun; Webb, K.F.; Mehrotra, V. "An improved current-doubler rectifier with integrated magnetics", Seventeenth Annual IEEE Applied Power Electronics Conference and Exposition (APEC 2002), vol. 2, pp. 831-837, 2002.

[PAPER-VII] Vinnikov, D.; Husev, O.; **Andrijanovitš, A.**; Roasto, I. New High-Gain Step-up DC/DC Converter for a Fuel Cell Interfacing in Hydrogen Buffer. Технічна електродинаміка, pp. 93 – 100, 2011.

NEW HIGH-GAIN STEP-UP DC/DC CONVERTER FOR A FUEL CELL INTERFACING IN HYDROGEN BUFFER

Dmitri Vinnikov[1], Oleksandr Husev[1,2], Anna Andrijanovitš[1], Indrek Roasto[1]
[1]Department of Electrical Drives and Power Electronics
Tallinn University of Technology
Ehitajate str. 5, 19086, Tallinn, Estonia
Tel. (+372) 6 20 3705, fax. (+372) 6 20 3701, e-mail: dmitri.vinnikov@ieee.org
[2]Department of Industrial Electronics
Chernihiv State Technological University
Shevchenko str. 95, 14027, Chernihiv, Ukraine
Tel. (+380 04622) 31695, fax: (+380 04622) 34244, e-mail: gsfki@ukr.net

Аннотация **– В данной статье представлен новый повышающий DC/DC преобразователь с гальванической изоляцией, предназначенный для работы в системе возобновляемых источников питания на основе топливных элементов. Предложенная топология состоит из квази-импедансного инвертора, повышающего трансформатора и выпрямителя. Описана система управления, показана область устойчивости преобразователя. Результаты моделирования и экспериментов подтверждают эффективность новой топологии.**

Ключевые слова **– квази-импедансный инвертор, топливные элементы, трансформатор, выпрямитель, устойчивость.**

INTRODUCTION

In recent years, implementation of hydrogen-based long-term energy storages in a renewable energy system (RES) has attracted much attention [1-4]. Essential elements of such a hydrogen buffer (HB) comprise an electrolyzer, a hydrogen storage system and a fuel cell (Fig. 1). Outside peak periods, excess electricity of a RES would be converted to hydrogen by help of an electrolyzer and during the peak demands when more power is needed, hydrogen could be converted to electricity by help of a fuel cell. Water to hydrogen conversion efficiency is averaged at 65 % and fuel cell conversion efficiency is 65-70 %, which yields an overall efficiency of the hydrogen buffer at 20-40% [5-7].

To achieve proper voltage matching the main components of the HB should be connected to the DC-bus of the RES via different power electronic converters: the electrolyzer is interfaced by help of a step-down DC/DC converter, while the fuel cell is connected by help of a step-up DC/DC converter.

Typically, these converters have a high-frequency voltage matching transformer, which could also perform the function of galvanic isolation demanded in some applications. The main trend in technology development here is to reduce the power losses in the interface converters to obtain the highest possible energy efficiency of the HB.

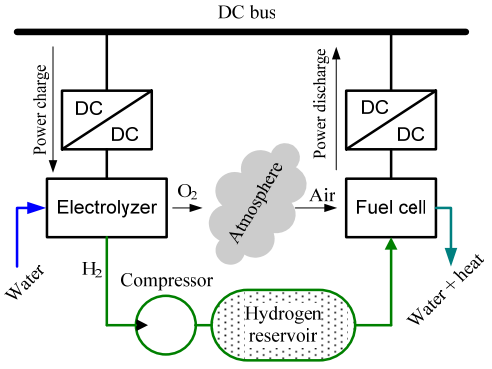

Fig. 1

This paper presents a new high-gain step-up DC/DC converter for fuel cell interfacing in a hydrogen buffer. The topology proposed (Fig. 2) contains the modified sine wave quasi-Z-source inverter

(qZSI) at the converter input side, a high-frequency step-up isolation transformer and a voltage doubler rectifier (VDR). In contrast to earlier presented topologies, the novel converter provides such advantages as increased reliability, an isolation transformer with a reduced turns ratio and reduced impact on the fuel cell due to continuous input current.

GENERAL OPERATING PRINCIPLE

The central idea implemented in the proposed converter is to keep the intermediate DC link voltage (U_{DC}) constant despite variations in the fuel cell voltage U_{FC}. By keeping the U_{DC} constant the PWM inverter could be operated with a fixed duty cycle, thus ensuring constant volt-second and flux swing of the isolation transformer [8].

The main advantage of the qZSI implemented in the input stage of the DC/DC converter is that it can boost the input voltage during special shoot-through operating states of the PWM inverter. During the shoot-through states the primary winding of the isolation transformer is shorted through all switches of both phase legs of the inverter (Fig. 3*b*, switching sequence ②). The passive qZS-network makes the shoot-through states possible, effectively protecting the circuit from damage. Moreover, the shoot-through states are used to store the magnetic energy in the inductors *L1* and *L2* without short-circuiting capacitors *C1* and *C2*. The stored magnetic energy in turn provides the boost of voltage seen on the inverter output during the active states of the inverter (Fig. 3*b*, switching sequences ③ and ⑤). Thus, by adjusting the shoot-through duty cycle D_S of the inverter switches *T1*…*T4* the U_{DC} could be preregulated to some desired voltage level (typically, this level equals the open cell voltage of the FC) despite variations in the FC voltage with a load. After the preregulation of U_{DC} the isolation transformer *TR* is being supplied from the inverter with a voltage of constant amplitude and duty cycle.

The proposed phase shift modulation (PSM) control principle of the modified sine wave qZSI is presented in Fig. 3*a*. It is seen that the switching period consists of three states: active, zero and shoot-through

$$T = t_A + t_S + t_Z , \qquad (1)$$

where t_A, t_S and t_Z are the durations of the active, shoot-through and zero states, correspondingly. In the active state only one switch in each phase leg conducts (Fig. 3*b*, switching sequences ③ and ⑤). In the zero state the primary winding of the isolation transformer is shorted through either the top- or bottom-side inverter switches (Fig. 3*b*, switching sequences ① and ④). It is seen from Fig. 3 that in the proposed control method the shoot-through states are generated during zero states. To provide a sufficient regulation margin, the zero state time t_Z should always exceed the maximum duration of the shoot-through states per one switching period. Moreover, the zero and shoot-through states are spread over the switching period so that the number of higher harmonics in the transformer primary could be reduced. To reduce switching losses of the transistors, the number of shoot-through states per period was limited by two. Moreover, in order to decrease the conduction losses of the transistors, shoot-through current is distributed between both inverter legs [9].

To reduce the turns ratio of the isolation transformer a voltage doubler rectifier (VDR) was implemented on the secondary side of the converter. During the positive half cycle, the capacitor *C3* is charged through the diode *D2* to the peak secondary voltage of the isolation transformer. During the negative half cycle the capacitor *C4* is charged through the diode *D3*. At every time instant the output voltage (U_{DC2}) from this circuit will be the sum of the two capacitor voltages or twice the peak voltage ($U_{TR,sec}$) of the secondary winding of the isolation transformer:

$$U_{DC2} = 2 \cdot U_{TR,\mathrm{sec}} . \qquad (2)$$

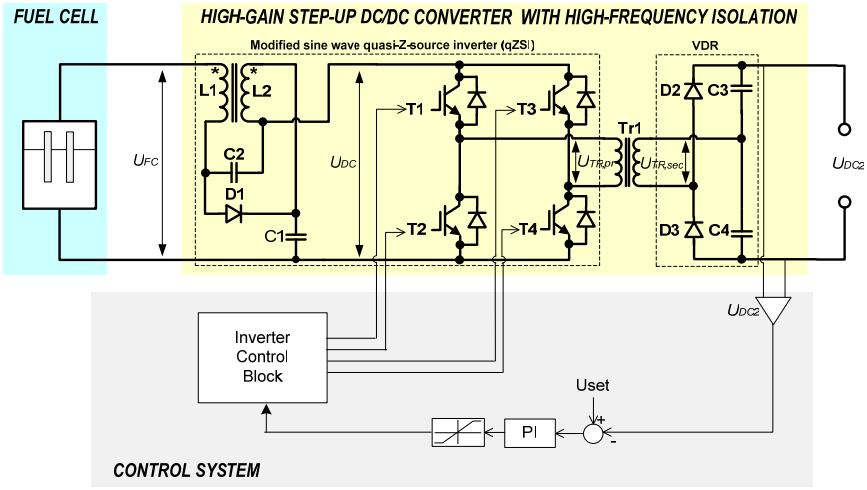

Fig. 2

The turns ratio n of an isolation transformer is defined as the relation of the primary and the secondary winding voltages:

$$n = \frac{U_{TR,pr}}{U_{TR,\text{sec}}} = \frac{U_{DC}}{U_{DC2}/2}, \qquad (3)$$

where $U_{TR,pr}$ is the primary winding voltage, $U_{TR,sec}$ is the secondary winding voltage, U_{DC} is the intermediate DC link voltage, U_{DC2} is the average output voltage of the converter.

Neglecting losses in the components, the intermediate DC link voltage of the qZS DC/DC converter could be regulated simply by the variation of a shoot-through duty cycle D_S:

$$U_{DC} = U_{FC} \cdot \frac{1}{1-2D_S}, \qquad (4)$$

where U_{FC} is the operating voltage of the fuel cell and D_S is the shoot-through duty cycle. The output voltage of the converter operating in the shoot-through mode could be estimated as

$$U_{DC2} = \frac{2 \cdot U_{FC}}{n} \cdot \left(\frac{1}{1-2 \cdot D_S} \right). \qquad (5)$$

STABILITY MARGIN AND COMPENSATION LOOP DESIGN

Since the proposed converter is a higher-order system, the stability criteria are an important issue. A good method to test system stability and dynamic behaviour is the transient response analysis.

The main task of the proposed topology is to ensure stable output voltage despite of the fuel cell voltage or converter load changes. In this case both the static error in the steady-state mode and the dynamics of the transient process are important. To evaluate the dynamic behavior of the converter it is necessary to determine its transfer functions.

Fig. 2 shows a control system that determines the state of the inverter. The output voltage of the converter is compared with the reference voltage and the resulting error is sent to the input of the PI regulator. The regulator output determines the shoot-through duty cycle D_S.

Depending on the fluctuations of the input voltage the shoot-through duty cycle is changing. That determines the gain factor of the converter. For example, with a decrease in the output voltage the error signal increases, which leads to an increase in the shoot-through duty cycle. The gain of the converter increases and, as a result, voltage on the output grows.

The ability to compensate both the input voltage and the load variations is a very important dynamic parameter of the control system.

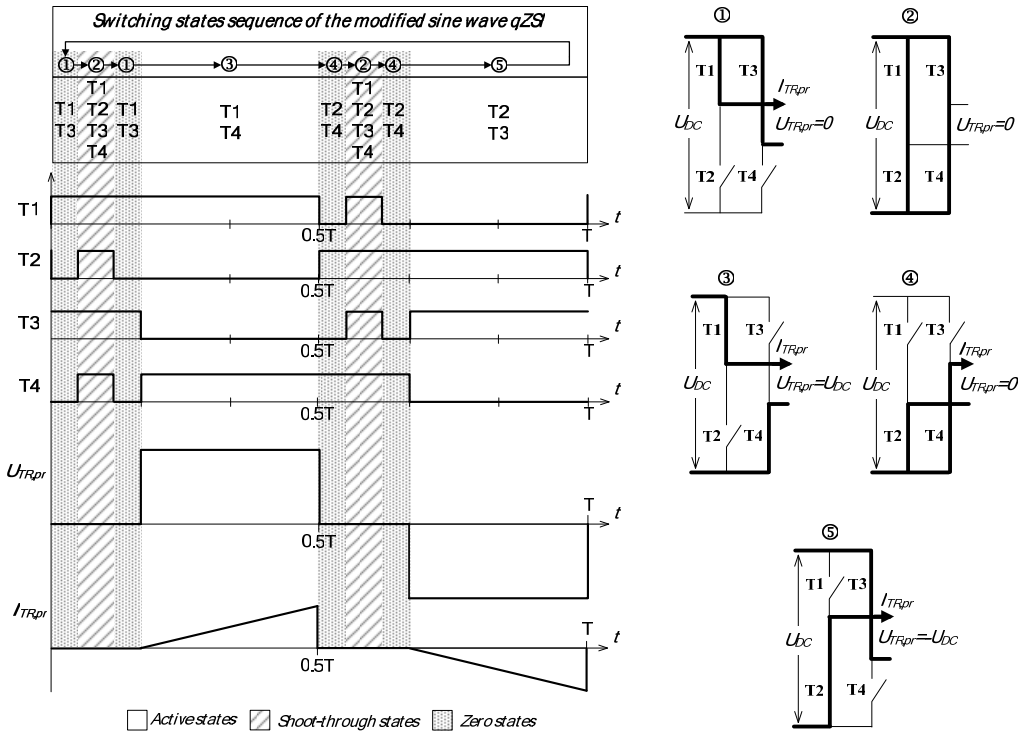

(a) (b)

Fig. 3

Based on that, it is possible to propose several approaches of the control system. Under a strict approach it is necessary to consider both the AC and the DC components of the output voltage. The switching period of the converter determines the ripple of the output voltage. To analyze the stability of the system during the disturbances with respect to the load or to the input voltage it is sufficient to consider only the DC component. Taking into account the discretion of the converter, the structure of a closed-cycle control system is shown in Fig. 4*a*. Where the inverter, transformer, rectifier and resistance load can be represented as the united continuous linear part (CLP), that gain factor is equal to

$$K_L = \frac{U_{DC2}}{U_{DC}} = \frac{2}{n}. \qquad (6)$$

The transfer function of the regulator in the *p*-space:

$$K_{PI} = K_P + \frac{1}{\tau \cdot p}, \qquad (7)$$

where K_P is the proportional gain, τ is the time constant.

It is evident from Eq. (4) that the transfer function of the qZS converter (U_{FC}=*const*) has a substantially nonlinear nature (Fig. 4*b*). Taking into account the above, it is possible to compose a block diagram of the system of automatic control both on the control and on the disturbance (Fig. 4*c*).

The basic task in the determination of transfer functions from control and disturbance respectively is reduced to the linearization of the transfer function of the qZS and the determination of its dynamic properties. It is known from the theory of the boost converters that they could work in the narrow range of the D_S value. Due to losses in the components the experimental transfer function significantly differs from that theoretically predicted (Fig. 4*b*).

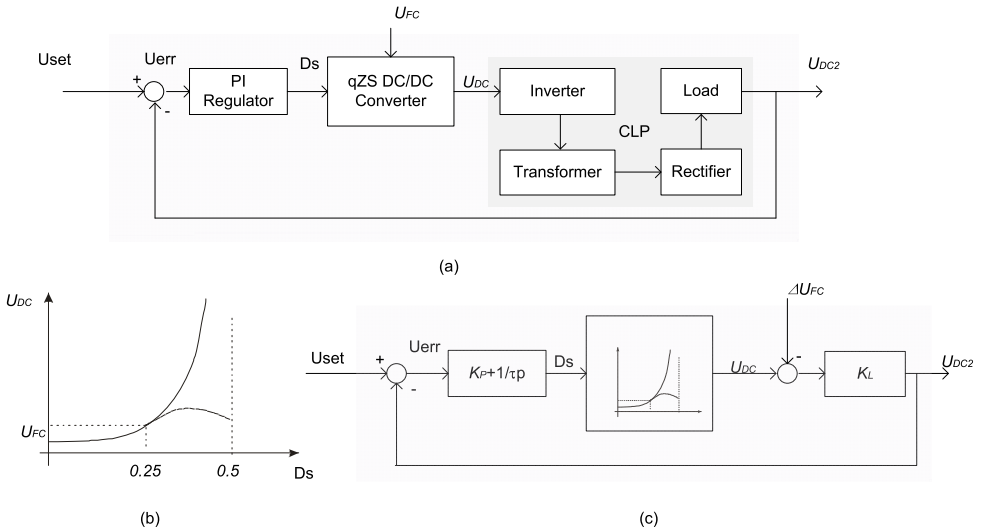

Fig. 4

In the nominal rating the shoot-through duty cycle is selected not more than 0.25. By this range expression (4) can be replaced with the linear dependence:

$$U_{DC} = \alpha \cdot U_{FC} \cdot D_S , \qquad (8)$$

where α is the liniarity coifficient. Consequently, the transfer function of the qZS without consideration of the dynamic properties of the converter can be presented in the form:

$$K_{qZS} = \alpha \cdot U_{FC} . \qquad (9)$$

It should be noted that this approach can be considered correct when the operating cycle of the impulse system for control is commensurate with the time constant of the converter. Then in a general form we can express transfer functions on control and disturbance, respectively.

$$K_C = \frac{(K_P + \frac{1}{\tau \cdot p}) \cdot K_{qZS} \cdot K_L}{1 + (K_P + \frac{1}{\tau \cdot p}) \cdot K_{qZS} \cdot K_L} = \frac{K_{qZS} \cdot K_L + K_{qZS} \cdot K_P \cdot K_L \cdot \tau \cdot p}{\tau \cdot p + K_{qZS} \cdot K_L + K_{qZS} \cdot K_P \cdot K_L \cdot \tau \cdot p} . \qquad (10)$$

$$K_D = \frac{K_L}{1 + (K_P + \frac{1}{\tau \cdot p}) \cdot K_{qZS} \cdot K_L} = \frac{K_L \cdot \tau \cdot p}{\tau \cdot p + K_{qZS} \cdot K_L + K_{qZS} \cdot K_P \cdot K_L \cdot \tau \cdot p} . \qquad (11)$$

where K_C is input to output transfer function, K_D is load disturbance output transfer function.

It is known from the general control theory that the system is steady when non of its poles are positive. In our case the first order system has one pole:

$$p_1 = -\frac{K_{qZS} \cdot K_L}{\tau + K_{qZS} \cdot K_P \cdot K_L \cdot \tau} . \qquad (12)$$

As it can be seen from the expression that the system is absolutely steady when it is possible to consider the gain K_{qZS} as a constant. The margin of relative linearity determines the space of absolute stability. Let us note that the coefficient K_p and the time constant τ in the control system determine the speed and the quality of the transient process. For more accurate results the dynamic component of the qZS transfer function that defines the speed of establishing the output voltage with the assigned shoot-through duty cycle must be taken into account.

SIMULATION RESULTS

The dynamic properties of the control system were evaluated by the help of simulations. The step response of the system is shown in Fig. 5 ($K_p = 0.003$, $\tau = 0.0005$, $U_{FC} = 30$ V).

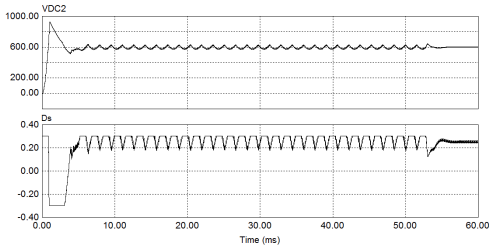

Fig. 5

Due to the high proportional gain the regulator has fast step response. In this case, as the figure shows, the output voltage has significant overregulation.

Fig. 6 shows the transient process with $K_p = 0.00003$, $\tau = 0.001$, $U_{FC} = 45$ V. The decrease of the gain factor of the proportional component leads to the decrease of the operating speed of the regulator just as an increase in the time constant of the integrator. However, in this case voltage overregulation is reduced.

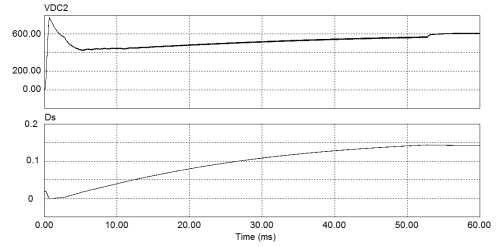

Fig. 6

Fig. 7 shows the reaction of the converter on the overvoltage from the input voltage. Voltage varies from 30 V to 60 V. At the moment of time t = 0.1 s boost voltage has occurred. This is the worst case in terms of an assumption of disturbance. As is evident, control system successfully masters the voltage disturbances (K_p=0.003, τ=0.0005).

From the simulation result it is possible to conclude that the system corresponds to the stability margin, which allows compensation of a variable input voltage.

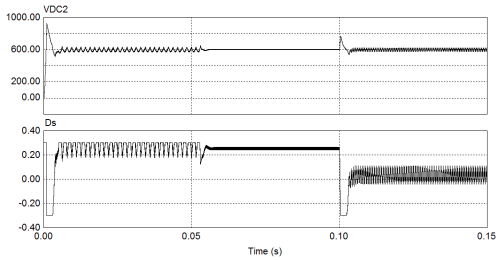

Fig. 7

PROTOTYPE

In this section the construction of a prototype assembly is shown in the first part, followed by the presentation of experimental results. General specifications of the prototype converter are indicated in Table 1. The picture of the realized converter is presented in Fig. 8. The control system is based on DSP TMS320F28335.

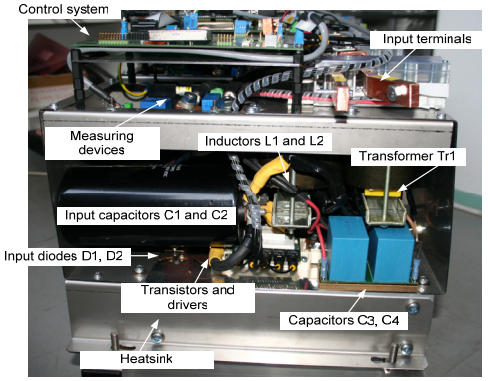

Fig. 8.

Table 1

Minimal input voltage $U_{FC,min}$	32 V
Maximal input voltage $U_{FC,max}$	60 V
Intermediate DC-link voltage U_{DC}	60 V
Output voltage U_{DC2}	600 V
Output power P	2.5 kW
Operating frequency of the qZS network f_{qZS}	30 kHz
Operating frequency of the isolation transformer f_{Tr}	15 kHz

Converter Assembly

Standard components currently available on the market were considered for the construction of the converter prototype (Table 2). The isolation transformer and the coupled inductor were built on the Epcos

UI93/104/30 core-sets [10]. Copper foils have been considered for the windings and the optimal thickness has been calculated for the inductor and transformer separately. In order to improve the service life of the converter the polypropylene capacitors were implemented in the qZS-network and in the voltage doubler rectifier.

Table 2

Isolation transformer Tr	
Core type	UI93/104/30
Primary winding turns	3
Primary winding wire	Cu-foil 40x0.4 mm (two in parallel)
Secondary winding turns	18
Secondary winding wire	Cu-foil 40x0.4 mm
Coupled inductors L1 and *L2*	
Core type	UI93/104/30
Winding turns number	13
Winding wire type	Cu-foil 40x0.3 mm
qZS capacitors C1 and C2	
Type	Cornell Dubilier 947C731K801CDMS
Rating	730 uF/800 V
VDR capacitors C3 and C4	
Type	EPCOS B32778G1256
Rating	1300 V/25 uF
qZS diode D1	
Type	STM Schottky STPS200170TV1
Rating	170 V/2x100 A
VDR diodes D2 and D3	
Type	IXYS DSEP 2x60-12A
Rating	1200 V/2x60 A
Transistors of PWM inverter T1…T4	
Type	Semikron SEMiX 202GB066HDs
Rating	600 V/200 A

EXPERIMENTAL RESULTS

General Operating Waveforms

The converter was first tested with a low FC voltage, at the terminal voltage of 40 V. To boost the FC voltage to the desired voltage level of the intermediate DC-link (60 V) the shoot-through duty cycle D_S was set to 0.19. The active state duty cycle was 0.4. Fig. 9*a* shows that the qZSI with the proposed control algorithm ensures the demanded gain of the FC voltage (U_{FC} = 40 V and U_{DC} = 60 V, as expected). Moreover, the voltage doubler rectifier provides the demanded voltage doubling effect of the peak voltage of the secondary winding of the isolation transformer, thus ensuring the ripple-free voltage of 600 V DC at the output (Fig. 9*b*). For the second operating point (Fig. 10), when the FC voltage equals the desired intermediate DC-link voltage, the shoot-through states are eliminated and the converter operates as a traditional VSI.

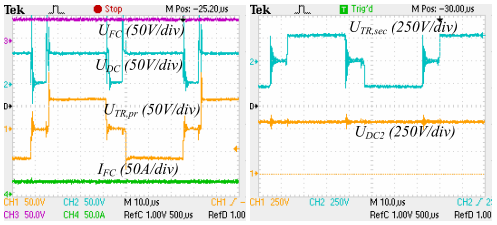

(a) (b)

Fig. 9

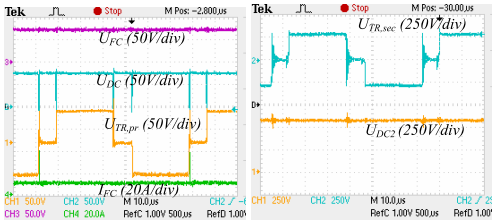

(a) (b)

Fig. 10

Dynamic Performance Tests

To evaluate the dynamic parameters of the control system and compare them with simulation results a family of experimental waveforms are represented.

Transient response of an idle and load mode are shown in Figs. 11*a* and 11*b*, respectively.

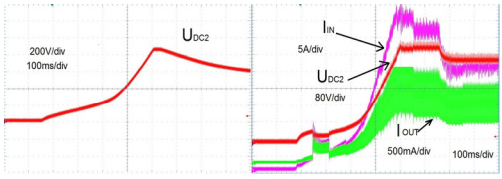

(a) (b)

Fig. 11

As it can be seen that overregulation happens during initial time, but much less

than expected. The ripple shape of the output voltage is connected with a non-ideal source of the input voltage that varies during the transient process. Thus, correct comparisons with simulation results where voltage step up is considered are not possible.

At the same time load disturbances were carried out to check the stability of the control system.

Figs. 12*a* and 12*b* show the response of the output voltage in the case of rapid current increase. Power step up is about 1.5 kW. As it can be seen the control system handles successfully such current variations.

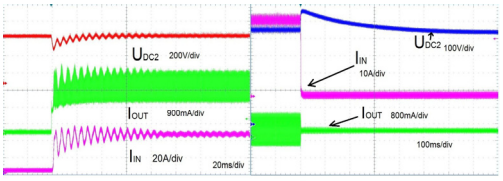

(a) (b)

Fig. 12

Fig. 12*b* shows the power drop process. No significant overvoltages occurred in the process.

As a result it can be concluded that they correspond to the results theoretically predicted. Differences are connected with limited source voltage and parameters of the regulator that were chosen to avoid significant overvoltage and make the transient process slower.

CONCLUSIONS

In this paper a new high-gain step-up DC/DC converter is proposed for the fuel cell interfacing in hydrogen-based long-term energy storages for renewable energy systems. The control system of the converter is described. The stability of the system with respect to the DC component of the output voltage is analyzed. Its absolute stability during the disturbances is shown. The margin of the relative linearity determines the space of absolute stability. The results of simulations and experiment confirm theoretical assumptions.

ACKNOWLEDGEMENT

This research work has been supported by the Estonian Ministry of Education and Research (Project SF0140016s11) and Estonian Science Foundation (Grant ETF8538).

[1] Zobaa, A.F.; Cecati, C., "A comprehensive review on distributed power generation", International Symposium on Power Electronics, Electrical Drives, Automation and Motion, SPEEDAM'2006, pp. 514-518, 23-26 May 2006.

[2] Cavallaro, C.; Chimento, F.; Musumeci, S.; Sapuppo, C.; Santonocito, C. "Electrolyser in H2 Self-Producing Systems Connected to DC Link with Dedicated Phase Shift Converter", International Conference on Clean Electrical Power, ICCEP '2007, pp. 632-638, 21-23 May 2007.

[3] del Real, A.J.; Arce, A.; Bordons, C. "Hybrid model predictive control of a two-generator power plant integrating photovoltaic panels and a fuel cell", 46th IEEE Conference on Decision and Control, pp. 5447-5452, 12-14 Dec. 2007.

[4] Ibanez, F.; Perez-Navarro, A.; Sanchez, C.; Segura, I.; Bernal, E.; Paya, J. "Wind generation stabilization using a hydrogen buffer", European Conference on Power Electronics and Applications, pp. 1-10, 2-5 Sept. 2007.

[5] Cavallaro, C.; Cecconi, V.; Chimento, F.; Musumeci, S.; Santonocito, C.; Sapuppo, C. "A Phase-Shift Full Bridge Converter for the Energy Management of Electrolyzer Systems", IEEE International Symposium on Industrial Electronics, ISIE'2007, pp. 2649-2654, 4-7 June 2007.

[6] Ugartemendia, J.J.; Ostolaza, X.; Moreno,V.; Molina, J.J.; Zubia; I. "Wind generation stabilization of fixed speed wind turbine farms with hydrogen buffer", 11th. Spanish-Portuguese Conference on Electrical Engineering (11CHLIE), pp. 1-5, 1-4 July 2009.

[7] Andrijanovitš, A.; Egorov, M.; Lehtla, M.; Vinnikov, D. "New Method for Stabilization of Wind Power Generation Using an Energy Storage Technology". Journal on Agronomy Research, vol. 8, (S1), pp. 12-24, May 2010.

[8] Vinnikov, D.; Roasto, I. "Quasi-Z-Source-Based Isolated DC/DC Converters for Distributed Power Generation", IEEE Transactions on Industrial Electronics, vol. 58, no.1, pp. 192-201, Jan. 2011.

[9] Roasto, I.; Vinnikov, D., "Analysis and evaluation of PWM and PSM shoot-through control methods for voltage-fed qZSI based DC/DC converters", in Proc. of 14th International Power Electronics and Motion Control Conference EPE-PEMC'2010, pp.T3-100-T3-105, 6-8 Sept. 2010.

[10] Available: www.epcos.com

[PAPER-VIII] Vinnikov, D.; **Andrijanovitš, A.;** Roasto, I.; Jalakas, T. Experimental Study of New Integrated DC/DC Converter for Hydrogen-Based Energy Storage. 10th International Conference on Environment and Electrical Engineering (EEEIC´11), Rome (Italy), IEEE, pp. 542 – 545, 2011.

Experimental Study of New Integrated DC/DC Converter for Hydrogen-Based Energy Storage

Dmitri Vinnikov, Anna Andrijanovitš, Indrek Roasto and Tanel Jalakas
Department of Electrical Drives and Power Electronics
Tallinn University of Technology
Ehitajate tee 5, 19086 Tallinn, Estonia
dmitri.vinnikov@ieee.org

Abstract— **This paper presents a new integrated (multiport) DC/DC converter for hydrogen-based energy storages. In comparison with traditional solutions based on individual converters for interfacing of an electrolyser and a fuel cell the proposed topology features reduced energy conversion stages. The paper analyzes and discusses the operating principle of the new converter. Several guidelines are presented for the new converter design. Finally, theoretical background was experimentally verified.**

Keywords- distributed energy systems, electrolyser, fuel cell, interface converter, multiport converter

I. INTRODUCTION

The energy conversion from renewable energy sources, such as wind turbines or photovoltaic arrays can play an important role in the development and operation of distributed energy systems (DES) [1, 2]. Due to the unpredicted nature of primary power sources (wind, solar) power fluctuations could appear in DES. Moreover, electrical production is not subject to the demand, which usually results in an unbalanced system [3]. The way to overcome these problems is to implement the long-term energy storage within the DES.

In recent years, implementation of hydrogen-based long-term energy storages in distributed energy systems has attracted much attention [2, 4-7]. Typically, the main components of such a system are an electrolyser (EL), a hydrogen storage system and a fuel cell (FC). Since the FC has a slow response time and also prefers to be operated under constant power, a battery is often used as additional energy storage in order to compensate the peak power demands.

Traditionally, individual converters are used to provide interfaces for the power inputs and outputs of the hydrogen buffer. In principle, any basic power converter topology can be used to design a power interface for a fuel cell and electrolyser. All these converters should have a high-frequency voltage matching transformer, which could also perform a function of galvanic isolation demanded in several applications. It finally leads to complex multiconverter systems with a high number of energy conversion stages, complex control and reduced efficiency.

This paper proposes the new integrated DC/DC converter for hydrogen buffer interfacing in distributed energy systems (Fig. 1). Thanks to the implemented multiport converter concept (Fig. 2) the number of energy conversion stages was significantly reduced. The resulting advantages of that include reduced component count, lower cost, and control simplicity. Moreover, the multiport converter technology may best satisfy integrated power conversion, efficient thermal management, compact packaging, and centralized control requirements [8, 9]. These advantages can potentially improve the overall cost, efficiency and flexibility of the hydrogen buffers used in distributed energy systems.

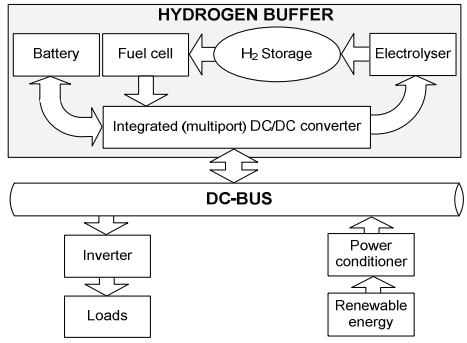

Figure 1. Proposed structure of the distributed energy system with hydrogen buffer interfaced via multiport DC/DC converter.

II. OPERATING PRINCIPLE OF NEW INTEGRATED DC/DC CONVERTER

The integrated (multiport) structure presented in Fig. 2 could be a technically feasible alternative for a small-scale DES, reducing a number of power processing stages and increasing an overall energy efficiency of the hydrogen buffer. The electrolyser and fuel cell are magnetically coupled with the DC-bus side converter by help of a multiwinding voltage matching transformer. Thus, all the ports of the interface converter are galvanically isolated, which could be a compulsory requirement for safety reasons in DES applications. The proposed converter consists of three ports: two unidirectional low-voltage ports for interconnection of electrolyser and fuel cell and one high-voltage bidirectional port for interconnection of hydrogen buffer with the main DC-bus of a DES.

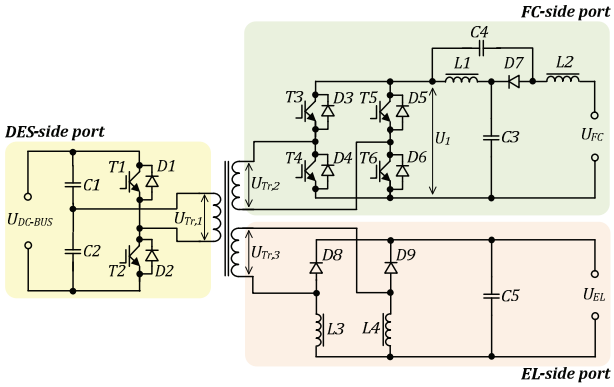

Figure 2. Power circuit layout of the proposed integrated DC/DC converter for hydrogen-based energy storage.

In accordance with its operation principle the hydrogen buffer could have two distinct operation modes: hydrogen generation from surplus energy of a DES (i.e. EL operation mode) and a power back-up mode with the electricity generation by a fuel cell (i.e. FC operation mode) [10].

A. EL operation mode

In the EL operation mode the converter acts as a traditional step-down isolated DC/DC converter with a voltage-source half-bridge inverter, step-down isolation transformer and current-doubler rectifier (Fig. 3). Implementation of half-bridge inverter together with current-doubler rectifier provides an opportunity of turns ratio reduction of the isolation transformer.

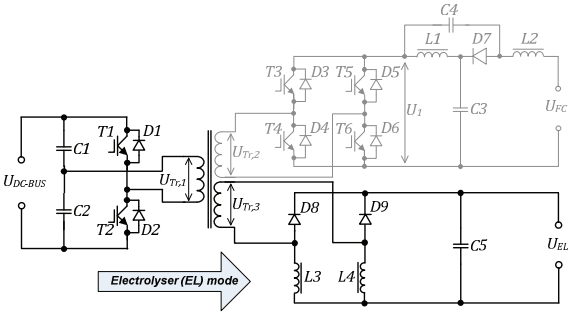

Figure 3. Power circuit configuration in the electrolyser (EL) mode.

The EL voltage could be simply controlled by the duty cycle variation of the transistors T1 and T2. Neglecting losses in components, the voltage U_{EL} during the EL mode (Fig. 3) is

$$U_{EL} = \frac{U_{DC-BUS}}{2 \cdot n_1} \cdot D, \qquad (1)$$

where U_{DC-BUS} is the DC-bus voltage of the main system, D is the duty cycle of the VSI switches (T1 and T2). Input and output sides (ports) of the converter are magnetically coupled through the isolation transformer's windings 1 and 3, respectively (Fig. 3) and the desired turns ratio of the isolation transformer n_1 is:

$$n_1 = \frac{U_{Tr,1}}{U_{Tr,3}}, \qquad (2)$$

where $U_{Tr,1}$ and $U_{Tr,3}$ is the amplitude voltages of the primary (high-voltage, DC-bus side) and tertiary (low-voltage, EL side) windings of the isolation transformer, respectively.

B. FC operation mode

In the FC operation mode the converter acts as a step-up isolated DC/DC converter and the power flows from the FC to the high-voltage DC-bus, thus performing the power back-up function. The configuration of the power circuit in FC mode is presented in Fig. 4.

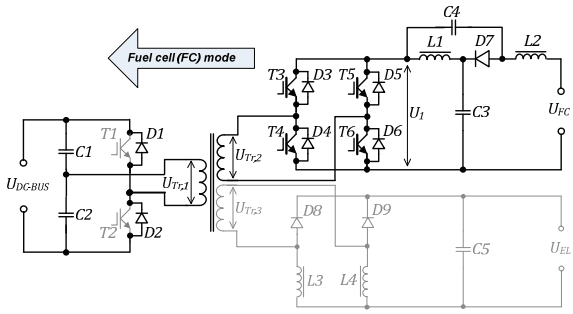

Figure 4. Power circuit configuration in the fuel cell (FC) mode.

The power flow from the FC to the DC-bus is controlled by the quasi-impedance-source inverter (qZSI). The integrated freewheeling diodes D1 and D2 of transistor modules T1 and T2 together with capacitors C1 and C2 act as the voltage-doubler rectifier. In conditions of changing FC voltage the amplitude voltage $U_{Tr,2}$ of the secondary winding of the isolation transformer is kept constant by the variation of the duration of a shoot-through switching state of qZSI. The shoot-through switching state is the simultaneous conduction of both switches of the same phase leg of the qZSI. This switching state is forbidden for the traditional voltage source converters because it could destroy the inverter. In the qZSI, the shoot-through states are used to store the magnetic energy in the DC-

side inductors L1 and L2 without short-circuiting the DC-capacitors C3 and C4. This magnetic energy in turn provides the boost of voltage $U_{Tr,2}$ seen on the transformer secondary winding during active states of the qZSI [11].

Fig. 5*a* shows the implemented PWM shoot-through control principle of a qZSI. The shoot-through states are generated during zero states. The zero and shoot-through states are spread over the switching period so that the number of higher harmonics in the transformer primary could be reduced. In order to reduce switching losses of the transistors, the number of shoot-through states per period was limited by two. Moreover, in order to decrease the conduction losses of the transistors, shoot-through current is distributed between both inverter legs. The proposed block-diagram of gating signal generator for the PWM shoot-through control is presented in Fig. 5*b*. It involves two parts: the active and the shoot-through state control. The active states are controlled by duty cycles of two PWM signal generators (*PWM1* and *PWM2*). The shoot-through states are generated using a triangle waveform generator and two comparators. When the modulation waveform is greater than the positive compare value U_P, the first shoot-through state (all the transistors turned on) appears and when the modulation signal is smaller than the value U_N, the second shoot-through state emerges. During zero states only top transistors (T3 and T5) are turned on while in the case of shoot-through both inverter legs are conducting.

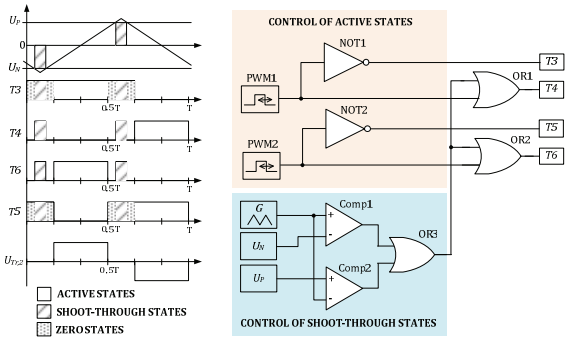

(a) (b)

Figure 5. qZSI control method implemented in proposed converter in the fuel cell (FC) mode: PWM shoot-through control principle (a) and generalized block-diagram of a gating signal generator (b).

Neglecting losses in components, the voltage $U_{DC\text{-}BUS}$ during the FC mode (Fig. 4) could be regulated by the variation of a shoot-through duty cycle D_S:

$$U_{DC-BUS} = \frac{2 \cdot U_{FC}}{n_2 \cdot (1 - 2 \cdot D_S)}, \tag{3}$$

where U_{FC} is the fuel cell voltage, D_S is the shoot-through duty cycle of the qZSI switches (T3, T4, T5 and T6). FC-side and DES-side ports of the converter are magnetically coupled through the isolation transformer's secondary and primary windings, respectively (Fig. 4) and the desired turns ratio of the isolation transformer n_2 is:

$$n_2 = \frac{U_{Tr,2}}{U_{Tr,1}}, \tag{4}$$

where $U_{Tr,1}$ and $U_{Tr,2}$ is the amplitude voltages of the primary (high-voltage, DC-bus side) and secondary (low-voltage, FC side) windings of the isolation transformer, respectively.

III. Experimental Study of Proposed Converter

In order to verify theoretical background the experimental converter with power rating of 2.4 kW was assembled in accordance with schematics shown in Fig. 2. It was assumed that the hydrogen buffer is based on the 2.4 kW electrolyser, which capable to generate 1 Nm^3 (1000 litres) of hydrogen in two hours. For electricity generation from the hydrogen two series connected 1.2 kW fuel cells were selected. The voltage selected for a DC-bus of a DES was 560 VDC (which is typical for 3×400 AC output). Operating parameters of the experimental converter are listed in Table I.

TABLE I. Desired Operating Parameters of the Experimental Converter

PARAMETER	VALUE
General	
DC-link voltage of the main system, $U_{DC\text{-}BUS}$	560 V
Rated voltage of electrolyser, U_{EL}	80 V
Light-load FC voltage, $U_{FC,max}$	70 V
Full-load FC voltage, $U_{FC,min}$	46 V
Operating frequency of isolation transformer, f	15 kHz
Number of turns of the voltage matching transformer, $N_{Tr,1} / N_{Tr,2} / N_{Tr,3}$	24 / 6 / 15
Capacitance of C1 and C2	60 uF
Capacitance of C3 and C4	180 uF
Inductance of L1 and L2	65 uH
Inductance of L3 and L4	1.2 mH
EL operation mode	
Duty cycle of VSI switches (T1 and T2), D	0.45
FC operation mode	
Desired voltage amplitude of the intermediate DC-link, U_I	70 V
Duty cycle of active states, D_A	0.4
Duty cycle variation of shoot-through states, D_S	0...0.17

A. EL operation mode

First, the system was studied in the electrolyser mode. During the experiment no control of the output voltage was performed and half-bridge VSI operated without dead time with the constant duty cycle $D = 0.45$. Figs. 6 and 7 show the experimental waveforms of the proposed converter in the EL mode. It is seen that the converter operates normally, ensuring ripple-free voltage $U_{EL} = 80$ V on the terminals of the electrolyser. The tertiary winding of the voltage matching transformer sees only half of the output current during the active time interval (Fig. 7*b*).

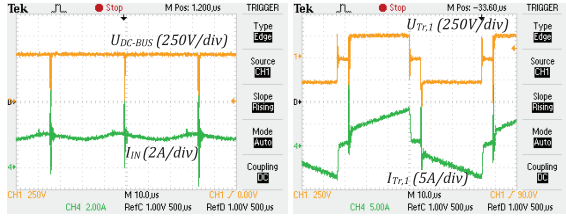

(a) (b)

Figure 6. Experimental waveforms of the proposed converter in the EL mode: DC-link voltage of the main system and input current (a); voltage and current of the primary winding of the voltage matching transformer (b).

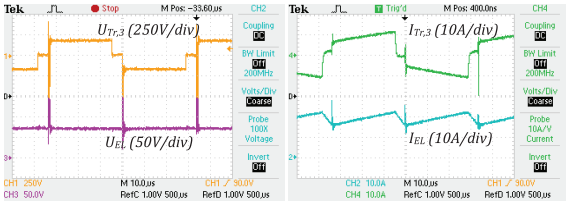

(a) (b)

Figure 7. Experimental waveforms of the proposed converter in the EL mode: voltage of the tertiary winding of the voltage matching transformer and electrolyser terminal voltage (a); current of the tertiary winding of the voltage matching transformer and electrolyser current (b).

B. FC operation mode

During the fuel cell mode the converter was first tested with the minimal FC voltage, thus having terminal voltage of 46 V. To boost the FC voltage to the desired voltage level of the intermediate DC-link (70 V) the shoot-through duty cycle D_S was set to 0.17. In active states the isolation transformer was supplied with voltage pulses with a duty cycle of 0.4. Fig. 8*a* shows that the qZSI with the proposed control algorithm ensures the demanded gain of the FC voltage ($U_{FC,min}$ = 46 V and U_I = 70 V, as expected). Moreover, the voltage doubler rectifier provides the demanded voltage doubling effect of the peak voltage of the secondary winding of the isolation transformer, thus ensuring the ripple-free voltage of 560 V DC at the DC-link of the main system (Fig. 8*b*). For the second operating point (Fig. 9), when the FC voltage equals the desired intermediate DC-link voltage, the shoot-through states are eliminated, and the converter operates as a traditional VSI.

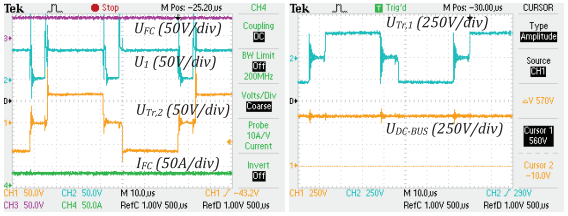

(a) (b)

Figure 8. Experimental waveforms of the proposed converter in the FC mode at the minimal FC voltage: intermediate DC-link voltage, voltage of the secondary winding of the voltage matching transformer and fuel cell current (a); voltage of the primary winding of the voltage matching transformer and DC-link voltage of the main system (b).

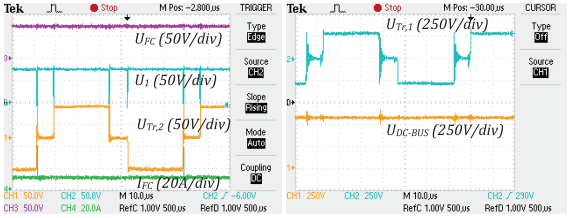

(a) (b)

Figure 9. Experimental waveforms of the proposed converter in the FC mode at the maximal FC voltage: intermediate DC-link voltage, voltage of the secondary winding of the voltage matching transformer and fuel cell current (a); voltage of the primary winding of the voltage matching transformer and DC-link voltage of the main system (b).

IV. CONCLUSIONS

This paper presents a novel integrated multiport DC/DC converter for hydrogen-based energy storages. The proposed converter has three ports: a bidirectional VSI port, a unidirectional VSI port and a unidirectional qZSI port. These three ports are magnetically coupled via a single multiwinding transformer. During the hydrogen production mode (electrolyser mode) the converter acts as a VSI-based step-down DC/DC converter, thus ensuring stabilized supply voltage for the electrolyser. In the power back-up (fuel cell) mode the converter operates as a qZSI-based step-up DC/DC converter providing the regulated voltage on the DC-bus despite the variation of the fuel cell voltage with the load. The paper has discussed the operation principle of the new converter and analyzed the experimental results.

ACKNOWLEDGMENT

This research work has been supported by Estonian Ministry of Education and Research (Project SF0140016s11) and Estonian Science Foundation (Grant ETF8538).

REFERENCES

[1] Zobaa, A.F.; Cecati, C., "A comprehensive review on distributed power generation", International Symposium on Power Electronics, Electrical Drives, Automation and Motion, SPEEDAM'2006, pp. 514-518, 23-26 May 2006.

[2] Cavallaro, C.; Chimento, F.; Musumeci, S.; Sapuppo, C.; Santonocito, C. "Electrolyser in H2 Self-Producing Systems Connected to DC Link with Dedicated Phase Shift Converter", International Conference on Clean Electrical Power, ICCEP '2007, pp. 632-638, 21-23 May 2007.

[3] del Real, A.J.; Arce, A.; Bordons, C. "Hybrid model predictive control of a two-generator power plant integrating photovoltaic panels and a fuel cell", 46th IEEE Conference on Decision and Control, pp. 5447-5452, 12-14 Dec. 2007.

[4] Ibanez, F.; Perez-Navarro, A.; Sanchez, C.; Segura, I.; Bernal, E.; Paya, J. "Wind generation stabilization using a hydrogen buffer", European Conference on Power Electronics and Applications, pp. 1-10, 2-5 Sept. 2007.

[5] Cavallaro, C.; Cecconi, V.; Chimento, F.; Musumeci, S.; Santonocito, C.; Sapuppo, C. "A Phase-Shift Full Bridge Converter for the Energy Management of Electrolyzer Systems", IEEE International Symposium on Industrial Electronics, ISIE'2007, pp. 2649-2654, 4-7 June 2007.

[6] Ugartemendia, J.J.; Ostolaza, X.; Moreno, V.; Molina, J.J.; Zubia; I. "Wind generation stabilization of fixed speed wind turbine farms with hydrogen buffer", 11th. Spanish-Portuguese Conference on Electrical Engineering (11CHLIE), pp. 1-5, 1-4 July 2009.

[7] Andrijanovitš, A.; Egorov, M.; Lehtla, M.; Vinnikov, D. "New Method for Stabilization of Wind Power Generation Using an Energy Storage Technology". Journal on Agronomy Research, vol. 8, (S1), pp. 12-24, May 2010.

[8] Tao, H.; Kotsopoulos, A.; Duarte, J.L.; Hendrix, M.A.M. "Family of multiport bidirectional DC-DC converters", IEE Proceedings on Electric Power Applications, vol. 153, no. 3, pp. 451- 458, 1 May 2006.

[9] Tao, H.; Duarte, J.L.; Hendrix, M.A.M. "Multiport converters for hybrid power sources", IEEE Power Electronics Specialists Conference, PESC'2008, pp. 3412-3418, 15-19 June 2008.

[10] Vinnikov, D.; Andrijanovitš, A.; Roasto, I.; Lehtla, T. "New Integrated Converter for Hydrogen Buffer Interfacing in Distributed Energy Systems", International Conference on Renewable Energies and Power Quality (ICREPQ'11) – accepted for publication.

[11] Vinnikov, D.; Roasto, I. "Quasi-Z-Source-Based Isolated DC/DC Converters for Distributed Power Generation", IEEE Transactions on Industrial Electronics, vol. 58, no.1, pp. 192-201, Jan. 2011.

[PAPER-IX] **Andrijanovits, A.**; Blinov, A.; Vinnikov, D.; Martins, J. Magnetically Coupled Multiport Converter with Integrated Energy Storage. Przeglad Elektrotechniczny, Vol. 88(7b), pp. 171 – 176, 2012.

Anna ANDRIJANOVITS[1], Andrei BLINOV[1], Dmitri VINNIKOV[1], João MARTINS[2]

Tallinn University of Technology (1), Universidade Nova de Lisboa-FCT-DEE and UNINOVA-CTS (2)

Magnetically Coupled Multiport Converter with Integrated Energy Storage

Abstract. *This paper presents a new integrated DC/DC converter for hydrogen-based energy storages. As compared to traditional individual converter based solutions for interfacing of an electrolyzer and a fuel cell, the proposed topology features reduced energy conversion stages. In order to improve the response time of the hydrogen buffer a battery was integrated into the interface converter with no need for an extra charging/discharging circuit. The paper analyzes and discusses the operating principle of the new converter and provides some design guidelines. Finally, theoretical background is experimentally verified.*

Streszczenie. *W artykule przedstawiono nową zintegrowaną przetwornicę DC / DC dla magazynów energii na bazie wodoru. W porównaniu do tradycyjnych rozwiązań z oddzielnymi przetwornicami do elektrolizera i ogniwa paliwowego, proponowaną topologię cechuje zmniejszona liczba etapy konwersji energii. W celu poprawienia czasu reakcji bufora wodorowego akumulator został zintegrowany z interfejsem przetwornicy, bez konieczności stosowania dodatkowego obwodu ładowania/rozładowania. W artykule przedstawiono analizę i omówiono zasady działania nowego przekształtnika, i podano wybrane zalecenia projektowe. W końcowej części przedstawiono wyniki eksperymentalne, weryfikujące założenia teoretyczne (**Wieloterminalowa przetwornica o sprzężeniu magnetycznym z zintegrowanym zasobnikiem energii)***

Keywords: electrolyzer, fuel cell, hydrogen buffer, multiport converter.
Słowa kluczowe: elektrolizer, ogniwo paliwowe, bufor wodoru, przekształtnik wieloportowy.

Introduction

In recent years, hydrogen-based long-term energy storages implemented in a renewable energy system (RES) have attracted much attention [1-4]. Essential elements of such a hydrogen buffer (HB) are an electrolyzer (EL), a hydrogen storage system and a fuel cell (FC). To achieve proper voltage matching the main components of the HB should be connected to the DC-bus of the RES via different power electronic converters: the EL is interfaced by help of a step-down DC/DC converter, while the FC is connected by help of a step-up DC/DC converter. Moreover, the battery should have a special charger circuit that integrates it to the DC-bus of a DES. It finally leads to complex multiconverter systems with a high number of energy conversion stages, complex control and reduced efficiency. The main trend in technology development here is to reduce the power losses in the interface converters to obtain the highest possible energy efficiency of the HB.

Recently a new integrated (multiport) DC/DC converter for HB interfacing in the RES was proposed [5]. Thanks to the implemented multiport converter concept (Fig. 1) the number of energy conversion stages was significantly reduced.

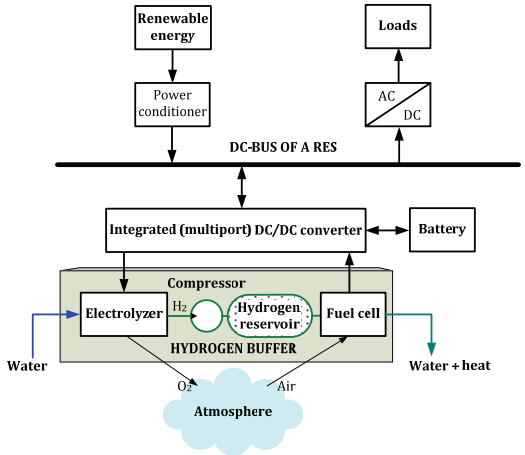

Fig. 1. Typical structure of the distributed energy system with the hydrogen buffer interfaced via multiport DC/DC converter

The resulting advantages of the proposed solution include reduced component count, lower cost, and control simplicity. Furthermore, the multiport converter technology may best satisfy integrated power conversion, efficient thermal management, compact packaging, and centralized control requirements [6, 7]. These advantages can potentially improve the overall cost, efficiency and flexibility of the hydrogen buffers used in the RES.

This paper discusses a possibility for further improvement of the hydrogen buffer with multiport DC/DC converter proposed in [5] by integrating the battery into the fuel cell side port. To decrease switching losses and improve the overall performance of the converter the half-bridge RES-side inverter was replaced with a three-level neutral point clamped (3L-NPC) voltage source inverter.

Basics of hydrogen buffers

Hydrogen is one of the promising alternatives that can be used as an energy carrier. The universality of hydrogen implies that it can replace other fuels for stationary generating units for power generation in various industries. Having all the advantages of fossil fuels, hydrogen is free of harmful emissions when used with dosed amount of oxygen, thus reducing the greenhouse effect [8].

Hydrogen based energy storage system or HB includes the following main stages: hydrogen production, hydrogen storage and electricity production [15]. In the excess energy periods the hydrogen generation system is connected to the DC-bus of the RES. In this stage electrical energy from the RES is converted into chemical energy by using water electrolysis and this energy is stored in a tank. In order to stabilize energy production during the absence of the renewable energy when more power is needed, stored hydrogen could be re-used. In this stage, hydrogen is converted into electrical energy by using a FC. The FC takes the hydrogen from the tanks to generate electricity, plus water and heat as by-products. Combination of an energy storage system and an RES allows controllable power production.

Water to hydrogen conversion efficiency is averaged at 65 % and FC conversion efficiency is 65-70 %, which yields an overall efficiency of the HB at 20-40% [9-11]. Since the FC has a slow response time and prefers to be operated under constant power, a battery is often used as an additional energy storage.

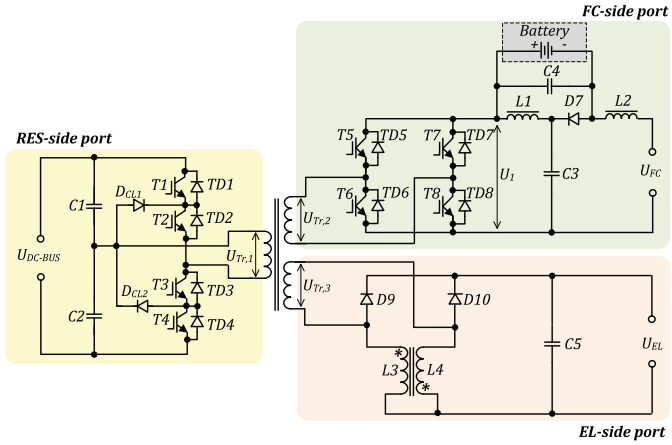

Fig. 2. Power circuit layout of the multiport converter with integrated energy storage

Generalized operation principle of the multiport converter with integrated energy storage

In the proposed multiport structure (Fig. 2) the EL and the FC are magnetically coupled with the RES-side converter by help of a multiwinding voltage matching transformer. Thus, all the ports of the converter are galvanically isolated, which could be a compulsory requirement for safety reasons in RES applications. The proposed converter consists of three ports: two unidirectional low-voltage ports for the interconnection of the EL and the FC and one high-voltage bidirectional port for the interconnection of the hydrogen buffer with the main DC-bus of a RES. There are two main operation modes of the integrated converter:

a) The EL operation mode. In this mode the surplus power from the DC-bus of a RES is supplying the electrolyzer and the multiport converter acts as a step-down converter.

b) The FC operation mode. In this mode electricity is generated by the fuel cell to cover the power deficiency in the DC-bus of the RES and the multiport converter acts as a step-up converter. In the FC operation mode several submodes could also be distinguished:

1) Battery assisted mode: the FC and the battery provide both the power to the DC-bus to manage the peak power demand.
2) Battery charging mode: FC power is higher than the load demanded power, the battery being charged from the FC.
3) Battery stand-by mode: the battery is fully charged and the fuel cell provides full power only to the DC-bus.
4)

A. EL operation mode

In the EL operation mode the converter acts as a traditional step-down isolated DC/DC converter with a 3L-NPC voltage-source inverter (VSI), a step-down isolation transformer and a current-doubler rectifier (Fig. 3). Implementation of a three-level half-bridge inverter with the PWM control algorithm presented in [12] allows all transistors of the inverter to be operated under the ZVS without additional components merely utilizing parasitic elements of the circuit, such as junction and freewheeling diode capacitances across each IGBT, and leakage inductance of the isolation transformer. In addition, the current doubler rectifier introduced with coupled inductors offers loss reduction in the secondary side of the converter in contrast to the traditional full-bridge rectifier due to the twice reduced operation current of the rectifier diodes and the secondary winding of the transformer.

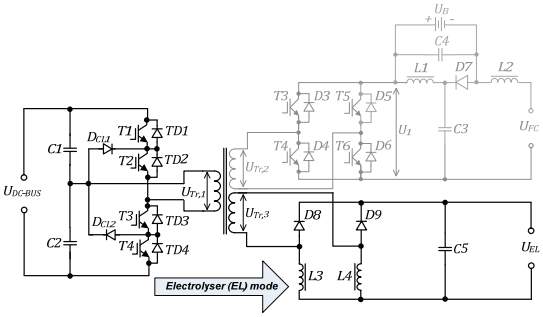

Fig.3. Power circuit configuration in the electrolyser (EL) mode

The EL voltage could be controlled by the duty cycle variation of the transistors *T1…T4*. Neglecting losses in the components, the voltage U_{EL} during the EL mode is

$$U_{EL} = \frac{U_{DC-BUS}}{2 \cdot n_1} \cdot D, \quad (1)$$

where $U_{DC\text{-}BUS}$ is the DC-bus voltage of the main system (input voltage of the converter), D is the duty cycle of the inverter switches (*T1…T4*) and n_1 is the turns ratio of the isolation transformer windings 1 and 3:

$$n_1 = \frac{U_{Tr,1}}{U_{Tr,3}}, \quad (2)$$

where $U_{Tr,1}$ and $U_{Tr,3}$ are the amplitude voltages of the primary (high-voltage, DC-bus side) and tertiary (low-voltage, EL side) windings of the isolation transformer, respectively.

B. FC operation mode

In the FC operation mode the converter acts as a step-up isolated DC/DC converter and the power flows from the FC to the high-voltage DC-bus, thus performing the power back-up function. The configuration of the power circuit in FC mode is presented in Fig. 4.

The power flow from the FC to the DC-bus is controlled by the quasi-impedance-source inverter (qZSI). This inverter is operated with continuous input current [13], which is a very important property since FC systems are limited power sources and cannot handle rapid changes in the current they produce. The integrated freewheeling diodes *TD1…TD4* of transistor modules *T1…T4* together

with capacitors *C1* and *C2* act as the voltage-doubler rectifier. In the conditions of changing FC voltage the amplitude voltage $U_{Tr,2}$ of the secondary winding of the isolation transformer is kept constant by the variation of the duration of a shoot-through switching state of the qZSI. The shoot-through switching state is the simultaneous conduction of both switches of the same phase leg of the qZSI. This switching state is forbidden for the traditional voltage source converters because it could destroy the inverter. In the qZSI, the shoot-through states are used to store the magnetic energy in the DC-side inductors *L1* and *L2* without short-circuiting the DC-capacitors *C3* and *C4*. This magnetic energy in turn provides the boost of the voltage $U_{Tr,2}$ seen on the transformer secondary winding during the active states of the qZSI [14].

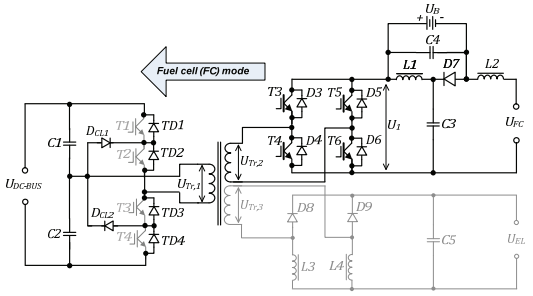

Fig.4. Power circuit configuration in the fuel cell (FC) mode

Neglecting losses in the components, the voltage $U_{DC\text{-}BUS}$ during the FC mode could be regulated by the variation of a shoot-through duty cycle D_S:

$$U_{DC-BUS} = \frac{2 \cdot U_{FC}}{n_2 \cdot (1 - 2 \cdot D_S)}, \tag{3}$$

where U_{FC} is the fuel cell voltage, D_S is the shoot-through duty cycle of the qZSI switches (*T3*… *T6*). FC-side and RES-side ports of the converter are magnetically coupled through the isolation transformer's secondary and primary windings, respectively (Fig. 4) and the desired turns ratio of the isolation transformer n_2 is

$$n_2 = \frac{U_{Tr,2}}{U_{Tr,1}}, \tag{4}$$

where $U_{Tr,1}$ and $U_{Tr,2}$ are the amplitude voltages of the primary (high-voltage, DC-bus side) and secondary (low-voltage, FC side) windings of the isolation transformer, respectively.

To compensate the short-term peak power demands of the DC-bus during the FC operation mode the power from an additional energy storage device may be required. A battery might be used in this case. Generally, to apply a battery an additional charging circuit is required, leading to increased complexity of the converter. However, by utilizing the property of the qZSI, the battery could be connected without any additional circuits, as shown in Fig. 1. The average voltage across the battery terminals equals the average capacitor *C4* voltage:

$$U_B = U_{C4} = \frac{D_S}{1 - 2 \cdot D_S} \cdot U_{FC}. \tag{5}$$

Hence, the state-of-charge (SOC) of the battery is controlled by varying the shoot-through duty cycle D_S of the qZSI switches. The battery current depends on the voltages U_{C4} and U_B as well as on its internal resistance r_B (Fig. 5):

$$i_B = \frac{U_B - U_{C4}}{r_B}, \tag{6}$$

where U_B is the voltage rating of the battery. Hence, the state of charge of the battery depends on the voltage:

$$U_{SOC} = U_B - U_{C4}. \tag{7}$$

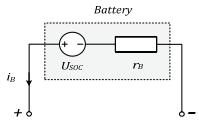

Fig. 5. Simplified equivalent circuit of a battery

In order to keep the system in continuous conduction mode (CCM) the current of the diode *D7* should never reach zero during the non-shoot-through state and the following expression should be satisfied:

$$i_B < i_{Tr,2}, \tag{8}$$

where $i_{Tr,2}$ is the current of the transformer secondary winding.

Next, the power equations for particular submodes of the FC operation mode are justified:

1. Battery assisted mode: $P_{FC} < P_{DC\text{-}bus}$

The FC and the battery provide the power to the DC-bus; the power equation is

$$P_{FC} - P_{DC-bus} + P_B = 0, \tag{9}$$

where P_{FC} is the power of the fuel cell, $P_{DC\text{-}BUS}$ is the power flowing into the DC-bus and P_B is the power provided by the battery. In this case $i_{L1} > i_{L2}$

2. Battery charging mode: $P_{FC} > P_{DC\text{-}bus}$

The FC supplies both the battery and the DC-bus in this case $i_{L1} > i_{L2}$ and the power equation is

$$P_{FC} - P_{DC-bus} - P_B = 0. \tag{10}$$

3. Battery stand-by mode: $P_{FC} = P_{DC\text{-}bus}$

The fuel cell provides full power to the DC-bus and the battery is fully charged. In this case $i_{L1} = i_{L2}$ and the power equation is

$$P_{FC} - P_{DC-bus} = 0. \tag{11}$$

Experimental verification

To validate the proposed topology the experimental setup with the power rating of 1.2 kW was assembled (Fig. 6). Operating parameters and component values of the experimental setup are listed in Table I.

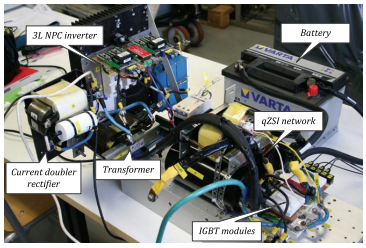

Fig. 6. Experimental 1.2 kW setup of the proposed multiport converter

Table 1. Desired operating parameters of the experimental converter

Parameter	Value
General	
DC-link voltage of the main system, $U_{DC\text{-}BUS}$	560 V
Rated voltage of the electrolyzer, U_{EL}	80 V
Light-load FC voltage, $U_{FC,max}$	70 V
Full-load FC voltage, $U_{FC,min}$	46 V
Operating frequency of the isolation transformer, f	15 kHz
Number of turns of the voltage matching transformer, $N_{Tr,1} / N_{Tr,2} / N_{Tr,3}$	24 / 6 / 15
Capacitance of C1 and C2	60 uF
Capacitance of C3 and C4	180 uF
Inductance of L1 and L2	65 uH
Inductance of L3 and L4	1.2 mH
EL mode	
Duty cycle of VSI switches, D	0.45
FC mode	
Desired voltage amplitude of the intermediate DC-link, U_1	70 V
Duty cycle of active states, D_A	0.4
Duty cycle variation of shoot-through states, D_S	0...0.17
Battery (VARTA E9)	70 Ah/12 V

A. EL operation mode

First, the system was studied in the electrolyzer mode. During the experiment no control of the output voltage was performed and 3L-NPC VSI operated with the constant duty cycle. The experimental voltage and current waveforms of the RES- and EL-side ports are presented in Fig 7. The 3L-NPC half-bridge inverter had the zero-voltage switching of all transistors without any additional components (Figs. 8 and 9).

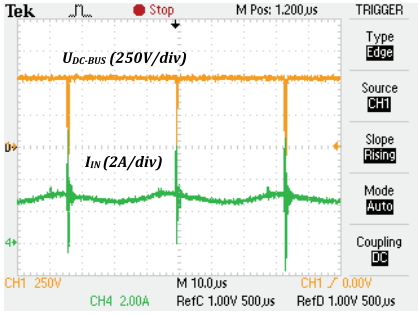

(a)

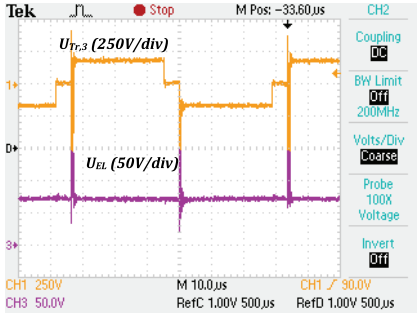

(b)

Fig. 7. Experimental waveforms of the proposed converter in the EL mode: input voltage and current of the RES-side port (a) and output voltage of the EL-side port (b)

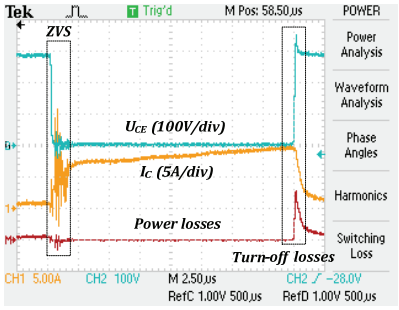

Fig. 8. ZVS operation of outer transistors (T1 and T4) of the proposed converter in the EL mode (duty cycle D=0.4)

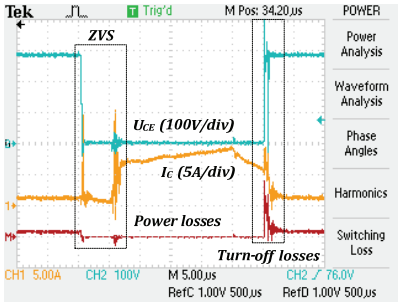

Fig. 9. ZVS operation of inner transistors (T2 and T3) of the proposed converter in the EL mode (duty cycle D=0.4)

It was found that a sufficient condition for the ZVS is that the isolation transformer should have relatively high leakage inductance of windings and the dead time implemented should be smaller than the time needed to utilize the leakage energy. Finally, it was found that by help of the proposed configuration the total losses in semiconductors in the RES-side port could be decreased by at least 25% in comparison with the topology presented in [5].

B. FC operation mode

During the fuel cell mode the converter was tested with the minimal FC voltage, thus having terminal voltage of 46 V. To boost the FC voltage to the desired voltage level of the intermediate DC-link (70 V) the shoot-through duty cycle DS was set to 0.175. In active states the isolation transformer was supplied with voltage pulses with a duty cycle of 0.35. As is seen from Fig. 10, the qZSI ensures the demanded gain of the FC voltage ($U_{FC,min} = 46$ V and $U_1 = 70$ V, as expected).

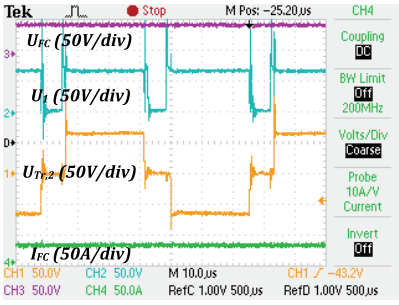

Fig. 10. Experimental waveforms of the proposed converter in the FC mode at the minimal FC voltage: intermediate DC-link voltage, voltage of the secondary winding of the voltage matching transformer and fuel cell current

Further, different possibilities of the FC operation mode were tested. It was assumed that the available FC power cannot meet the increase in the load. The system without the battery (Fig. 11a) had an appreciable voltage drop at the DC-bus, while the system with the battery was able to correspond to the increased load current and provided considerably more stable output voltage (Fig. 11b).

Assuming an initial output power P of 1 kW, the transformer current during this test can be calculated by

$$i_{Tr,2} = \frac{P \cdot (1 - 2 \cdot D_S)}{U_{FC}} = 14.1(A) \cdot \quad (12)$$

Hence, the battery current should not exceed this value in order to keep the system in CCM. Using Eq. (5) we can obtain the initial voltage across the battery (U_{C4}=12.4 V). Since the battery was fully charged, its initial current was close to zero.

After the load change to 1.2 kW, the battery current increased to 10 A. Having the battery internal resistance of 40 mΩ, we obtain:

$$U_{C4} = U_B - (i_B \cdot r_B) = 11.6(V) . \quad (13)$$

Assuming the intermediate DC-link voltage variation due to the battery within 1 V, the output voltage variation is

$$\Delta U_{DC-BUS} = 2 \cdot \Delta U_{DC-link} \cdot \frac{N_{Tr,1}}{N_{Tr,2}} = 8(V) , \quad (14)$$

which is acceptable within the required range of 5%.

The 3L-NPC half-bridge topology operating in the rectifier mode provided the demanded voltage doubling effect of the peak voltage of the secondary winding of the isolation transformer, thus ensuring the ripple-free voltage of 560 V DC at the DC-bus of a RES (Fig. 11b), while the maximal voltage across IGBT modules was approximately one-half of the output voltage (Fig. 12).

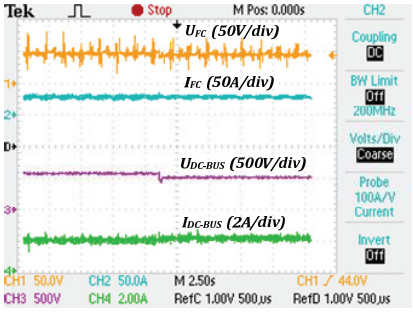

(a)

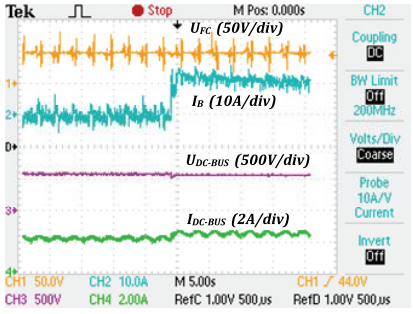

(b)

Fig. 11. Experimental waveforms of the proposed converter in the FC mode at the minimal FC voltage and limited current when the load increases: without the battery (a); with the battery (b)

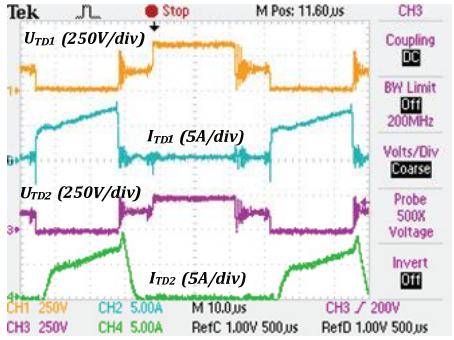

Fig. 12. Experimental waveforms of the proposed converter in the FC operating mode at the minimal FC voltage: freewheeling diode *TD1* and *TD2* voltage and current

Fig. 13 shows the battery state changing from charging to discharging during the operation with limited FC current when the load suddenly increases. As estimated, during charging $i_{L1}>i_{L2}$ and when the battery supplies the load $i_{L1}>i_{L2}$. Since the battery voltage remains relatively constant during the operation, the intermediate DC-link voltage of the qZSI is stable.

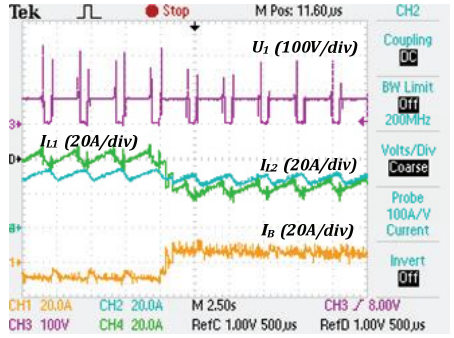

Fig. 13. Intermediate DC-link voltage, current of the inductors *L1* and *L2* and battery current during the operation with limited current when the load increases

Conclusions

The proposed novel integrated multiport DC/DC converter for hydrogen-based energy storages is capable of ensuring stabilized supply voltage for the electrolyzer as well as providing the regulated voltage on the DC-bus despite the variation of the fuel cell voltage with the load. During the hydrogen production mode (electrolyzer mode) the converter acts as a VSI-based step-down DC/DC converter while in the power back-up (fuel cell) mode the converter operates as a qZSI-based step-up DC/DC converter. The battery integrated to the FC-side port will help to balance the power difference between the FC and the load and finally improve the dynamic response of the hydrogen buffer.

In the research it was found that a 3L-NPC topology with a dedicated control algorithm in a RES-side port allows losses in the semiconductors to be reduced by at least 25%. The integration of a battery in a FC-side port require no additional charging circuit. At the same time stabilized output voltage during short-term high power demands is provided when the available FC power cannot meet the increase in the load.

Acknowledgment

This research work has been supported by Estonian Ministry of Education and Research (Project SF0140016s11), Estonian Science Foundation (Grants ETF8538) and European Social Fund (project "Doctoral School of Energy and Geotechnology II").

REFERENCES

[1] Zobaa, A.F.; Cecati, C., "A comprehensive review on distributed power generation", International Symposium on Power Electronics, Electrical Drives, Automation and Motion, SPEEDAM'2006, pp. 514-518, 23-26 May 2006.

[2] Cavallaro, C.; Chimento, F.; Musumeci, S.; Sapuppo, C.; Santonocito, C. "Electrolyser in H2 Self-Producing Systems Connected to DC Link with Dedicated Phase Shift Converter", International Conference on Clean Electrical Power, ICCEP '2007, pp. 632-638, 21-23 May 2007.

[3] del Real, A.J.; Arce, A.; Bordons, C. "Hybrid model predictive control of a two-generator power plant integrating photovoltaic panels and a fuel cell", 46th IEEE Conference on Decision and Control, pp. 5447-5452, 12-14 Dec. 2007.

[4] Ibanez, F.; Perez-Navarro, A.; Sanchez, C.; Segura, I.; Bernal, E.; Paya, J. "Wind generation stabilization using a hydrogen buffer", European Conference on Power Electronics and Applications, pp. 1-10, 2-5 Sept. 2007.

[5] Vinnikov, D.; Andrijanovits, A.; Roasto, I.; Jalakas, T.; "Experimental study of new integrated DC/DC converter for hydrogen-based energy storage," 2011 10th International Conference on Environment and Electrical Engineering (EEEIC), pp. 1-4, 8-11 May 2011

[6] Tao, H.; Kotsopoulos, A.; Duarte, J.L.; Hendrix, M.A.M. "Family of multiport bidirectional DC-DC converters", IEE Proceedings on Electric Power Applications, vol. 153, no. 3, pp. 451- 458, 1 May 2006.

[7] Tao, H.; Duarte, J.L.; Hendrix, M.A.M. "Multiport converters for hybrid power sources", IEEE Power Electronics Specialists Conference, PESC'2008, pp. 3412-3418, 15-19 June 2008.

[8] Andrijanovitš, A; Egorov, M; Lehtla, M; Vinnikov, D. "A Hydrogen Technology as Buffer for Stabilization of Wind Power Generation", 8th International Symposium "Topical Problems in the Field of Electrical and Power Engineering", Doctoral School of Energy and Geotechnology, pp. 62-70, 2010.

[9] Cavallaro, C.; Cecconi, V.; Chimento, F.; Musumeci, S.; Santonocito, C.; Sapuppo, C. "A Phase-Shift Full Bridge Converter for the Energy Management of Electrolyzer Systems", IEEE International Symposium on Industrial Electronics, ISIE'2007, pp. 2649-2654, 4-7 June 2007.

[10] Ugartemendia, J.J.; Ostolaza, X.; Moreno,V.; Molina, J.J.; Zubia; I. "Wind generation stabilization of fixed speed wind turbine farms with hydrogen buffer", 11th. Spanish-Portuguese Conference on Electrical Engineering (11CHLIE), pp. 1-5, 1-4 July 2009.

[11] Andrijanovitš, A.; Egorov, M.; Lehtla, M.; Vinnikov, D. "New Method for Stabilization of Wind Power Generation Using an Energy Storage Technology". Journal on Agronomy Research, vol. 8, (S1), pp. 12-24, May 2010.

[12] Andrijanovits, A.; Vinnikov, D.; Roasto, I.; Blinov, A.; , "Three-level half-bridge ZVS DC/DC converter for electrolyzer integration with renewable energy systems," 2011 10th International Conference on Environment and Electrical Engineering (EEEIC), pp. 1-4, 8-11 May 2011.

[13] Cintron-Rivera, J.G.; Yuan Li; Shuai Jiang; Peng, F.Z.; "Quasi-Z-Source inverter with energy storage for Photovoltaic power generation systems," 2011 Twenty-Sixth Annual IEEE Applied Power Electronics Conference and Exposition (APEC), pp.401-406, 6-11 March 2011.

[14] Vinnikov, D.; Roasto, I. "Quasi-Z-Source-Based Isolated DC/DC Converters for Distributed Power Generation", IEEE Transactions on Industrial Electronics, vol. 58, no.1, pp. 192-201, Jan. 2011.

[15] Martins, J. F.; Joyce, A.; Rangel, C.; Sotomayor, J.; Castro, R.; Pires, A.; Carvalheiro, J.; Silva, R. A.; Viana, S.; "RenH2 – Stand-Alone Energy System Supported by Totally Renewable Hydrogen Production"; Proc. of POWERENG 2007, April 12-14, 2007, Setúbal, Portugal.

***Authors**: M.Sc. Anna Andrijanovits, Tallinn University of Technology, Dep. of Electrical Drives and Power Electronics, Ehitajate tee 5, 19086 Tallinn, Estonia, E-mail: anna.andrijanovits@ieee.org; M. Sc. Andrei Blinov, Tallinn University of Technology, Dep. of Electrical Drives and Power Electronics, Ehitajate tee 5, 19086 Tallinn, Estonia, E-mail: andrei.blinov@ieee.org; Dr. Dmitri Vinnikov, Tallinn University of Technology, Dep. of Electrical Drives and Power Electronics, Ehitajate tee 5, 19086 Tallinn, Estonia, E-mail: dmitri.vinnikov@ieee.org; Dr. João Martins, Universidade Nova de Lisboa-FCT-DEE and UNINOVA-CTS, P-2829-516 Monte de Caparica, Portugal, E-mail: jf.martins@fct.unl.pt*

DISSERTATIONS DEFENDED AT TALLINN UNIVERSITY OF TECHNOLOGY ON *POWER ENGINEERING, ELECTRICAL ENGINEERING, MINING ENGINEERING*

1. **Jaan Tehver**. Boiling on Porous Surface. 1992.
2. Salastatud.
3. **Endel Risthein.** Electricity Supply of Industrial Plants. 1993.
4. **Tõnu Trump**. Some New Aspects of Digital Filtering. 1993.
5. **Vello Sarv.** Synthesis and Design of Power Converters with Reduced Distortions Using Optimal Energy Exchange Control. 1994.
6. **Ivan Klevtsov**. Strained Condition Diagnosis and Fatigue Life Prediction for Metals under Cyclic Temperature Oscillations. 1994.
7. **Ants Meister**. Some Phase-Sensitive and Spectral Methods in Biomedical Engineering. 1994.
8. **Mati Meldorf**. Steady-State Monitoring of Power System. 1995.
9. **Jüri-Rivaldo Pastarus**. Large Cavern Stability in the Maardu Granite Deposit. 1996.
10. **Enn Velmre**. Modeling and Simulation of Bipolar Semiconductor Devices. 1996.
11. **Kalju Meigas**. Coherent Photodetection with a Laser. 1997.
12. **Andres Udal**. Development of Numerical Semiconductor Device Models and Their Application in Device Theory and Design. 1998.
13. **Kuno Janson**. Paralleel- ja järjestikresonantsi parameetrilise vaheldumisega võrgusageduslik resonantsmuundur ja tema rakendamine. 2001.
14. **Jüri Joller**. Research and Development of Energy Saving Traction Drives for Trams. 2001.
15. **Ingo Valgma**. Geographical Information System for Oil Shale Mining – MGIS. 2002.
16. **Raik Jansikene**. Research, Design and Application of Magnetohydrodynamical (MHD) Devices for Automation of Casting Industry. 2003.
17. **Oleg Nikitin**. Optimization of the Room-and-Pillar Mining Technology for Oil-Shale Mines. 2003.
18. **Viktor Bolgov**. Load Current Stabilization and Suppression of Flicker in AC Arc Furnace Power Supply by Series-Connected Saturable Reactor. 2004.
19. **Raine Pajo**. Power System Stability Monitoring – an Approach of Electrical Load Modelling. 2004.
20. **Jelena Shuvalova**. Optimal Approximation of Input-Output Characteristics of Power Units and Plants. 2004.
21. **Nikolai Dorovatovski**. Thermographic Diagnostics of Electrical Equipment of Eesti Energia Ltd. 2004.
22. **Katrin Erg**. Groundwater Sulphate Content Changes in Estonian Underground Oil Shale Mines. 2005.

23. **Argo Rosin**. Control, Supervision and Operation Diagnostics of Light Rail Electric Transport. 2005.
24. **Dmitri Vinnikov**. Research, Design and Implementation of Auxiliary Power Supplies for the Light Rail Vehicles. 2005.
25. **Madis Lehtla**. Microprocessor Control Systems of Light Rail Vehicle Traction Drives. 2006.
26. **Jevgeni Šklovski**. LC Circuit with Parallel and Series Resonance Alternation in Switch-Mode Converters. 2007.
27. **Sten Suuroja**. Comparative Morphological Analysis of the Early Paleozoic Marine Impact Structures Kärdla and Neugrund, Estonia. 2007.
28. **Sergei Sabanov**. Risk Assessment Methods in Estonian Oil Shale Mining Industry. 2008.
29. **Vitali Boiko**. Development and Research of the Traction Asynchronous Multimotor Drive. 2008.
30. **Tauno Tammeoja**. Economic Model of Oil Shale Flows and Cost. 2008.
31. **Jelena Armas**. Quality Criterion of road Lighting Measurement and Exploring. 2008.
32. **Olavi Tammemäe**. Basics for Geotechnical Engineering Explorations Considering Needed Legal Changes. 2008.
33. **Mart Landsberg**. Long-Term Capacity Planning and Feasibility of Nuclear Power in Estonia under Certain Conditions. 2008.
34. **Hardi Torn**. Engineering-Geological Modelling of the Sillamäe Radioactive Tailings Pond Area. 2008.
35. **Aleksander Kilk**. Paljupooluseline püsimagnetitega sünkroongeneraator tuuleagregaatidele. 2008.
36. **Olga Ruban**. Analysis and Development of the PLC Control System with the Distributed I/Os. 2008.
37. **Jako Kilter**. Monitoring of Electrical Distribution Network Operation. 2009.
38. **Ivo Palu**. Impact of Wind Parks on Power System Containing Thermal Power Plants. 2009.
39. **Hannes Agabus**. Large-Scale Integration of Wind Energy into the Power System Considering the Uncertainty Information. 2009.
40. **Kalle Kilk**. Variations of Power Demand and Wind Power Generation and Their Influence to the Operation of Power Systems. 2009.
41. **Indrek Roasto**. Research and Development of Digital Control Systems and Algorithms for High Power, High Voltage Isolated DC/DC Converters. 2009.
42. **Hardi Hõimoja**. Energiatõhususe hindamise ja energiasalvestite arvutuse metoodika linna elektertranspordile. 2009.
43. **Tanel Jalakas**. Research and Development of High-Power High-Voltage DC/DC Converters. 2010.
44. **Helena Lind**. Groundwater Flow Model of the Western Part of the Estonian Oil Shale Deposit. 2010.
45. **Arvi Hamburg**. Analysis of Energy Development Perspectives. 2010.

46. **Mall Orru**. Dependence of Estonian Peat Deposit Properties on Landscape Types and Feeding Conditions. 2010.
47. **Erik Väli**. Best Available Technology for the Environmentally Friendly Mining with Surface Miner. 2011.
48. **Tarmo Tohver**. Utilization of Waste Rock from Oil Shale Mining. 2011.
49. **Mikhail Egorov**. Research and Development of Control Methods for Low-Loss IGBT Inverter-Fed Induction Motor Drives. 2011.
50. **Toomas Vinnal**. Eesti ettevõtete elektritarbimise uurimine ja soovituste väljatöötamine tarbimise optimeerimiseks. 2011.
51. **Veiko Karu**. Potential Usage of Underground Mined Areas in Estonian Oil Shale Deposit. 2012.
52. **Zoja Raud**. Research and Development of an Active Learning Technology for University-Level Education in the Field of Electronics and Power Electronics. 2012.
53. **Andrei Blinov**. Research of Switching Properties and Performance Improvement Methods of High-Voltage IGBT based DC/DC Converters. 2012.
54. **Paul Taklaja**. 110 kV õhuliinide isolatsiooni töökindluse analüüs ja töökindluse tõstmise meetodid. 2012.
55. **Lauri Kütt**. Analysis and Development of Inductive Current Sensor for Power Line On-Line Measurements of Fast Transients. 2012.
56. **Heigo Mõlder**. Vedelmetalli juhitava segamisvõimaluse uurimine alalisvoolu kaarleekahjus. 2012.
57. **Reeli Kuhi-Thalfeldt**. Distributed Electricity Generation and its Possibilities for Meeting the Targets of Energy and Climate Policies. 2012.
58. **Irena Milaševski**. Research and Development of Electronic Ballasts for Smart Lighting Systems with Light Emitting Diodes. 2012.